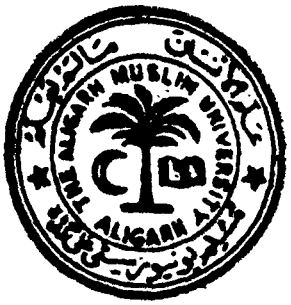

THE STUDY OF FORBUSH DECREASES

DISSERTATION

Submitted in Partial Fulfilment of the Requirements
for the Award of the Degree of

Master of Philosophy

IN

PHYSICS

HEMAGHANDRAN PILLAI. G. P

Under the Supervision of

PROF. R. S. YADAV

DEPARTMENT OF PHYSICS
ALIGARH MUSLIM UNIVERSITY
ALIGARH (INDIA)

1992

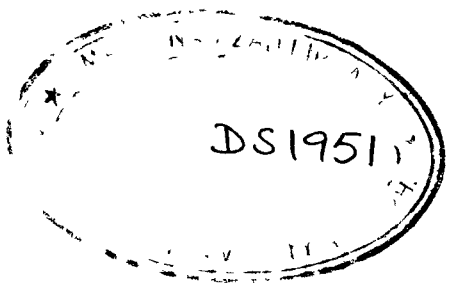

DEDICATED

TO MY

FATHER and MOTHER

PROFESSOR R.S. YADAV.

DEPARTMENT OF PHYSICS
ALIGARH MUSLIM UNIVERSITY
ALIGARH-202002 (India)
Tele No. : 9001
Tel. No. : 564 230 *AMU IN*

CERTIFICATE

Certified that **Mr. Hemachandran Pillai. C.P.,** has carried out the work on **The Study of Forbush Decreases** under my supervision and this work is suitable for submission for the award of the degree of Master of Philosophy.

[PROF. R.S. YADAV]

ACKNOWLEDGEMENTS

I take this opportunity to record my sincere and profound gratitude for **Prof. R.S. Yadav,** under whose guidance and overall supervision the investigation reported in this dissertation have been carried out. I am grateful to him for his keen interest in the work, constant encouragement and generous support throughout this period.

I express my sincere thanks to **Prof. Israr Ahmad,** (former chairman), **Prof. B.N. Khanna,** chairman, Department of Physics and the co-ordinator, DSA/COSIST for having provided all the facilities in the Department.

I am thankful to **Dr. N.K. Sharma,** senior research colleague for his valuable suggestions in completing this work. Thanks are also due to my colleague **Mr. H.A. Bakshi** and all my friends for their co-operation and helps.

I also record my appreciation to the technical staff of the Department for their helps during the course of my work.

I am also thankful to **Mr. Mohd. Owais Khan** for neat and clean typing of this dissertation.

I express my gratitude to all, who remembered me and wished success in my endeavour.

Finally, I feel deeply obliged to my father, mother, brothers, sisters and brother-in-law, who have given me moral support and continuing encouragement.

Hemachandran Pillai
1-8-1992

HEMACHANDRAN PILLAI. C.P.

CONTENTS

****

CHAPTER 1

INTRODUCTION

(1) DISCOVERY OF COSMIC RAYS

Cosmic rays were discovered in the beginning of this century. During those days it was believed that these rays were γ-rays of ultra-high frequency. The credit of the discovery goes to the certain experiments undertaken, independently by Elster and Geitel (1900) and Wilson (1900). The observed a slow discharge in the effectively insulated electrometers. Later on Vector. F. Hess (1913) proposed the existence of very high penetrating and ionizing radiation entering the earth's atmosphere from outer space. R.A. Millikan (1927) established that the radiation discovered by Hess did come from beyond the earth's atmosphere and gave them the name **Cosmic Rays.**

From coincidence counter arrangements, Bothe and Kolhorster (1928), detected the presence of charged particles in Cosmic rays. The latitude effect observed by Compton (1933) supported the presence of charge particles in the primary cosmic radiation. The large amount of intensity from west compared to east led Rossi (1930) and Johnson (1938) to predict the dominating presence of positively charged particles. The protonic nature of cosmic radiation was confirmed by Schein et al. (1941).

The existance of nuclei heavier than proton was investigated by Freier (1948) through the measurements in nuclear emulsion exposed at high altitude in balloons. The use of nuclear emulsions of various sensitivities has shown the existence of nuclei with charges ranging from two to twenty seven. The use of the ingenious combination of Cerenkov and Scintillator detectors and spark chambers led the discovery of electron and positron in cosmic rays. The use of earth's satellite and deep space probes, reaching beyond the earth's magnetic field influence, made it possible to explore the composition of cosmic rays of very low kinetic energy. The recent use of nuclear photographic emulsion of large dimensions has dramatically produced the visual evidence that cosmic rays contain various nuclei up to uranium and even perhaps transuranic elements. (Fowler et al. 1967). The use of special plastics together with nuclear emulsions exposed at great heights revealed the detailed charge composition in the high energy region.

By observing the so called extensive air showers cosmic radiation at very high energy (10^{14} eV) has been studied. These showers due to the particles of high energy contain several million prticles and extend over several square kilometers. At present continuous measurements of various components are being carried out

on a world wide scale. The nucleonic component at sea level and mountain altitude is being recorded by 1 G Y and NM 64 neutron monitors. The hard and soft component and with different azimuths is being recorded by means of standard cubical telescopes consisting of GM and Scintillation counters. These have made possible the study of reliably seperate specific variations and their relationship with terrestrial, geomagnetic as well as solar atmospheric phenomena and contributed a more profound understanding about the various features and the mechanism of cosmic ray time variations.

Thus the cosmic ray researches have served as a unique tool for investigating a large variety of problem in High energy physics, Elementary Particle Physics, Astronomy, Astrophysics, Cosmology, Geophysics and Heliosphere.

The earth's atmosphere is being continuously bombarded by high energy particles, arriving from outer space. These paricles are known as **primary cosmic rays.** As these prticles penetrate in the atmosphere, they lose their energy and gradually disappear on colliding against the oxygen and nitrogen atoms of air. At the same time they give rise to secondary particles, of low energy known as **Secondary cosmic rays.** They are very much different in

nature and energy. Thus at each point within atmosphere, the total cosmic radiation consists partly of primary particles and partly of secondary particles.

Absorption measurements of the intensity of cosmic rays in lead have shown that the intensity of cosmic rays is reduced by about 30 percent in the first 10 cm of lead. Half of the beam which is capable of penetrating 10 cm of lead can also penetrate one metre of lead [Rossi 1933]. These results suggests, that cosmic ray beam consist, of a soft component and a penetrating hard component.

The soft component consists of mostly the γ-rays. (gamma rays) and positive and negative electrons ($e^{\pm}$). It is very much effective in producing showers and is rapidly absorbed. The absorption of soft component is being proportional to Z^2/A per gram. It is strongly absorbed in heavy elements than in light elements.

The portion of cosmic rays which penetrate the large thickness [greater than 10 cm of lead] of the absorber and excites the detecting system is known as the hard component. It mainly consists of μ-mesons and a minor portion of fast protons and fast electrons. Its absorption is proportional to the mass of the particles.

(2) COMPOSITION OF PRIMARY COSMIC RAYS AND ENERGY SPECTRUM

The intensity of cosmic rays recorded at the earth is controlled by the solar activity, particularly the low energy cosmic ray particles (i.e. $E<10^{10}$ eV), by the process known as solar modulation. In fact, it is not absolutely clear whether at any time during the solar activity cycle, the full intensity of cosmic rays is recorded. The composition of cosmic rays, as measured on the earth, depends on the composition of the source (or origin), acceleration process at the source and what happens to the cosmic ray particles during their propagation through the galaxy.

It is almost established that the primary cosmic rays consists of exclusively of stripped nuclei. Approximately 95% of the particles are protons, about 4.5% are α-particles, and all the heavier nuclei constitute in total less than 0.5% of the flux. Recent rsults are given in table 1.1.

Proton component: Singly charged nuclei in the primary cosmic radiation are mainly protons, deutrons ($_1H^2$), and tritons ($_1H^3$) have also been discovered but the abundance of deutrons and tritons are not yet well known. Proton measurements are difficult to make due to corrections necessary for albedo.

α-particle: In doubly charged nuclei ($_2He^3$ and $_2He^4$) the

Table 1.1
Composition of cosmic ray Intensity

Groups	Elements	Atomic Number Z	Cosimc Ray Abundance CR in %	Cosmical Abundance CA in %	Ratio CR/CA
Proton	H	1	93	91	1
Alpha	He	2	6.3	9.1	0.7
L	Li,Be,B	3-5	0.10	4×10^{-7}	3×10^{5}
M	C,N,O,F	6-9	0.42	0.11	3
H	Ne - K	10-19	0.14	0.014	10
VH	Ca -Zn	20-30	0.04	2×10^{-3}	20
VVH	Ga - U	31-92	2×10^{-6}	10^{-6}	2
SH	> U	~110	?	?	?

[Here L= Light, M=Medium, H=Heavy, VH=Very heavy & SH=Superheavy]

universal abundance of $_2He^3$ nuclei is small compared to $_2He^4$. Out of all components, the α-particle component is measured very accurately. This is because of their good intensity, easier indentification (by counter or photographic plates) and no albedo problem. This component has been measured over a various latitudes (from λ=0° to 55°).

Table 1.2

Latitude λ	L_α = no. of particles / m^2/ sec/ steradian
0°	17
4°	18±1.9
41°	90±5
55°	300±25

L-Nuclei group: Nuclei Li, Be and B constitute the L-nuclei, statistically it is shown that the flux of these light nuclei in the cosmic ray beam is very poor compared to other groups. In 1950 Bradt measured the flux of L-nuclei at λ=30°. He gave the upper limit for the value of flux $J_L \sim 0.4$ particles/ (m^2 sec ster) which implies almost complete absence of this group in the primary cosmic rays. The presence of Li, Be and B in cosmic rays is assumed to be due to the break up of the M-nuclei and heavier nuclei in collisions with interstellar matter.

M-Nuclei group: The M-nuclei are made up of C, N, O and F. Most of the measurements on this group have been performed at geomagnetic latitude λ=41° using emulsion plates. Other technique, were also used occasionally. On the basis of the measurements of Bristol, Bombay and Rochestor groups, the best value of the flux J_M at λ=41° is

$$J_M = 5.5 \text{ to } 7.5 \text{ particles } /(m^2 \text{ sec. sterad.})$$

At relativistic energies the abundance ratio C:N:O:F is approximately as 1.15:0.32:1.0:0.02. The relative abundance of F is not yet known very accurately.

Heavy Nuclei group: The flux of heavy nuclei has been measured mostly at geomagnetic latitude λ=30°, 41°, 55°. The flux at 41° ranges from 2.1 to 2.8.

In order to have better understanding of H-nuclei, we can divide this group in to the following sub groups.

H_1 nuclei $10 \leq Z \leq 15$

H_2 nuclei $16 \leq Z \leq 19$

H_3 nuclei $20 \leq Z \leq 28$

H_4 nuclei $29 \leq Z \leq 80$

H_5 nuclei $Z > 80$

at relativistic energies the ratio of abundance of H_1:H_2: H_3 is about to 70:9:21.

H_1-Nuclei: H_1 group constitutes about 70% of the H-nuclei. In H_1 group neon, magnesium and silicon are most abundant. In this group the nuclei Na, Al and P with odd Z have very small abundance and the nuclei with even charge are on the average 10 times more abundant than nuclei with odd charge.

H_2-Nuclei: The H_2 group constitute less than 10% of the H-group and these nuclei in primary cosmic rays are produced due to breaking up of nuclei of H_3-group in their journey through interstellar space, therefore, it seems that these nuclei may be entirely absent in sources of cosmic rays.

H_3-Nuclei: The element of H_3 group i.e. (Fe, Ca, Ti, Mn, Ve, Sc) constitutes about 20% of the H-nuclei. In this group element Fe is more abundant. Next to Fe, Ca and Ti are prominent.

H_4 and H_5 group: The abundance of H_4 and H_5 nuclei is very low. A combined experiments using both plastics and emulsions (Blanford et al. 1970) and (Price et al. 1971) have provided the evidence of the nuclei upto charges Z = 90. The existance of transuranic elements was claimed by several workers. The observation of transuranic element in cosmic rays is of high significance, because they provide information about the age of cosmic rays and the 'source' of cosmic rays.

ENERGY SPECTRUM

The intensity distribution of cosmic ray particles can be expressed either by an energy spectrum or by a rigidity spectrum. Instead of later a momentum spectrum is sometimes presented. The energy spectrum is referred as either kinetic energy or total energy. For individual charge component, energy per nucleon is considered. There are two types of energy spectra:

1. The integral energy spectrum
2. The differential energy spectrum

The differential energy spectrum for proton, has the form of power law i.e.

$$N(E)dE = K\, E^{-\gamma}\, dE$$

where N(E) is the number of nuclei with kinetic energy between E and E + dE per unit area per unit solid angle. K and γ are constants. The exponent γ-for the proton is about 2.6 and $K = 6.3 \times 10^{6}$.

The intensity of protons N(>E) with an energy greater than E is also expressed in the form of the power law (integral energy spectrum)

$$N(>E) = K'\, E^{-\gamma'}.$$

The intensity of cosmic ray particles in wide range of energy from 1 Bev to 10^{20} eV per nucleon has been

measured by different techniques.In the lower energy range upto 10 BeV/nucleon, the energy of primary particle is measured directly by scattering measurements in nuclear emulsion exposed at high altitudes.

From 10 BeV/nucleon to 15 BeV/nucleon the energy spectra of different primary cosmic ray particle can be measured by geomagnetic latitude effect. At higher energies beyond 15 BeV per nucleon the energy spectrum is determined by making use of the reactions produced by the primary cosmic ray particles in the atmosphere or in nuclear emusion.

At very high energies $\geq 10^{14}$ eV/nucleon, the estimate of the flux of primary particle is made from the study of extensive air showers (E.A.S) produced by such a high energy particles. At present, at higher energies, the knowledge about the energy spectrum as well as about chemical composition of individual component of cosmic ray is not available in detail. All techniques regarding the measurements of energy spectrum for various energy is shown in the table 1.3.

Table 1.3

Energy of P.C.R.	Measuring Techniques
1 BeV-10 BeV per nucleon	Scattering measurements.
1 BeV-15 BeV per nucleon	geomagnetic effect.
10^{11} eV > E > 15 BeV	Reaction produced by PCR. in the earth atmosphere.
10^{11} - 10^{13} eV/nucleon	Measuring production of JETS in nuclear emulsion
$\geq 10^{14}$ eV	E.A.S.

Techniques regarding the measurements of energy spectrum for various energy.

(3) PROPAGATION THROUGH EARTH'S ATMOSPHERE

When primary cosmic ray nuclei traverses the atmosphere, they make nuclear collision with air nuclei of the atmosphere (Nitrogen and oxygen). The collision probability is proportional to the exp $(-x/\lambda_z)$. Where x is the atmospheric matter traversed in gm cm^{-2} and λ_z is the main free path of the nuclei of charge z. The mean free path does not only depend on the charge z but also on the energy E of the nuclei

$$\lambda_z = f(z, E_z)$$

For relativistic energy, mean free path is 70 gm cm^{-2}. For protons, alpha particles and heavy nuclei it is still smaller.

The main result of the action of the primary rays on the top layers of the atmosphere is the production of meson. Much of the energy of primary particle goes into the creation of new short lived particles such as π-meson ($\pi^{\pm}, \pi^{0}$), heavy meson ($K^{\pm}$, K^{0}) and hyperons. If the energy is great enough pairs of protons and anti-protons, neutrons and anti-neutrons are also produced. Among all of these secondaries, π-mesons are most abundant. Measons (charged and neutral) are as effective as protons and neutrons in producing nuclear interaction.

Charged pions ($\pi^{\pm}$) are unstable particle (life time 2×10^{-8} sec) and will decay into $\mu^{\pm}$mesons.

$$\pi^{+} \longrightarrow \mu^{+} + \nu_{\mu}$$
$$\pi^{-} \longrightarrow \mu^{-} + \bar{\nu}_{\mu}$$

Since charged pions are of short life time also the interaction cross section with nuclei is large, the number of particles reaching the lower atmosphere (or at sea level) is quite negligible. mesons, on the other hand, are relatively long lived (life time $\sim 10^{-6}$ sec) and therefore, reach the sea level.

A considerable fraction, however, mesons ($\mu^{\pm}$) decay into electrons ($e^{\pm}$) and two neutrinos (ν , $\bar{\nu}$) according to the reaction

$$\mu^{+} \longrightarrow e^{+} + \nu_{e} + \bar{\nu}_{\mu}$$
$$\mu^{-} \longrightarrow e^{-} + \bar{\nu}_{e} + \nu_{\mu}$$

Neutral pions (π^{o}) have very small life time ($\sim 10^{-14}$ sec). The neutral pions has two decay modes

$$\pi^{o} \longrightarrow \gamma + \gamma \quad \text{(gamma rays)}$$

This gamma ray materialise in to electron-positron pairs

$$\gamma \longrightarrow e^{+} + e^{-}$$

Because of their very short mean life, neither $\pi^{\pm}$, π^{o}nor any heavy mesons or hyperons can constitute a component of marked intensity any where in the atmosphere. Thus the secondary cosmic rays mainly consists of

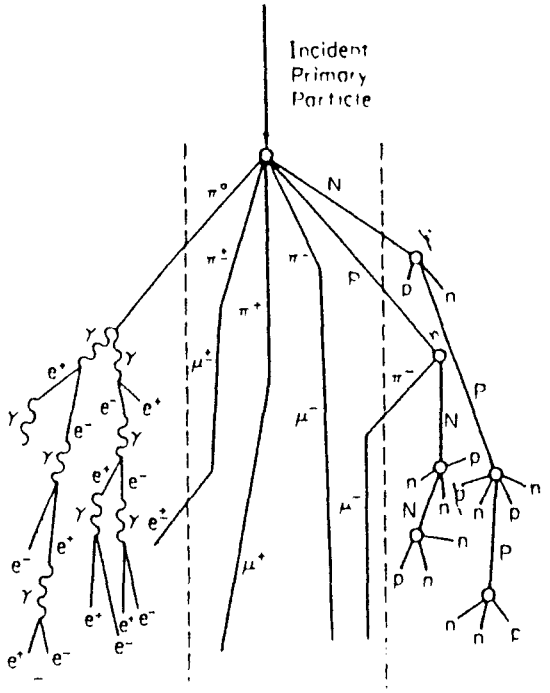

electromagnetic or softcomponent.

Meson or Hard component.

Nucleonic component.

Fig.1.1 Diagramatical representation of production of the secondary Cosmic ray components.
N,P- High energy nucleons.
n.p- Disintegration product nucleons.

(a) Meson component or Hard component ($\mu^{\pm}$mesons)

(b) Electromagnetic component or soft component (e^+, e^- and photon)

(c) Nucleon component (Neutron and protons)

At sea level the secondary radiation consists of about 75% hard component, 25% soft component and 0.1% nucleonic component.

(4) EFFECTS OF GEOMAGNETIC FIELD ON COSMIC RAY PARTICLES

The external magnetic field of the earth can be represented by a magnetic dipole-field that would be produced by a bar magnet short in comparison with the radius of the earth, located near earth's centre with its north pole towards the geographic south and south pole towards geographic north (fig.1.2). More precisely geographic axis lies at an angle of about 11.5° from geomagnetic axis. This is the centred dipole model of the terrestrial magnetic field. The field itself extends far beyond the reaches of earth's atmosphere. At an altitude of 1000 miles, its strength is still about one-half the field strength at the earth's surface.

The primary cosmic rays encounter the magnetic field well before they have a chance to collide with the molecules of the earth's atmosphere. If the primary cosmic rays are electrically charged, they will be

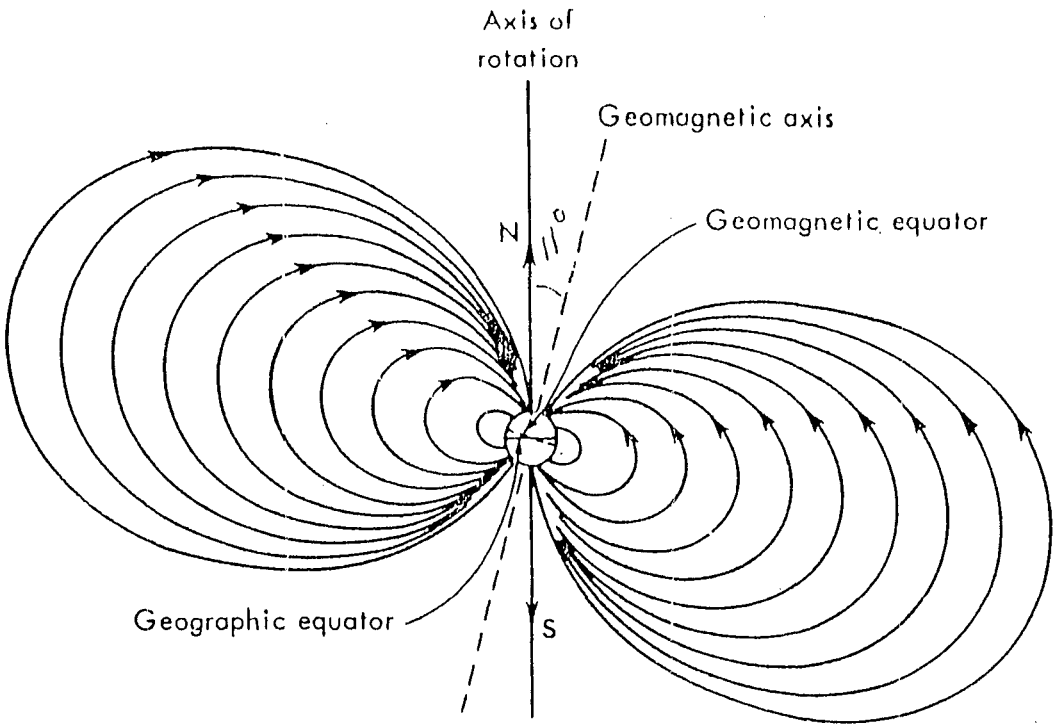

Fig. 1.2 Earth's magnetic field.

deflected by earth's field in one direction or other depending whether their charge is positive or negative.

The deflecting force experienced by a positively charged particle moving through a uniform magnetic field causes the particle to travel in a circle. The direction of the force is given by the following right-hand rule. If the fingers of the right hand, point in the direction of the field B and thumb points in the direction of the particle motion V, the force F points out of the palm. Since the deflecting force must be directed towards the centre of the circle, to counter act the centrifugel force, a positively charged particle must move clockwise (fig.1.3 a) with respect to an observer lined with the magnetic fields. For the same direction of B, the deflecting force experienced by a negatively charged particle is directed towards the centre when the particle moves counter clockwise (fig.1.3 b). For any given set of conditions reversal of the field, charge or direction of motion reverses the direction of the force. Also radius of the circle describing the motion of particle decrease as the momentum of the particle decreases and as the strength of magnetic field increases.

Stormer's theory: A moving charged particle in a magnetic field experience a deflecing force that act as right angles to both magnetic field and direction motion, cause

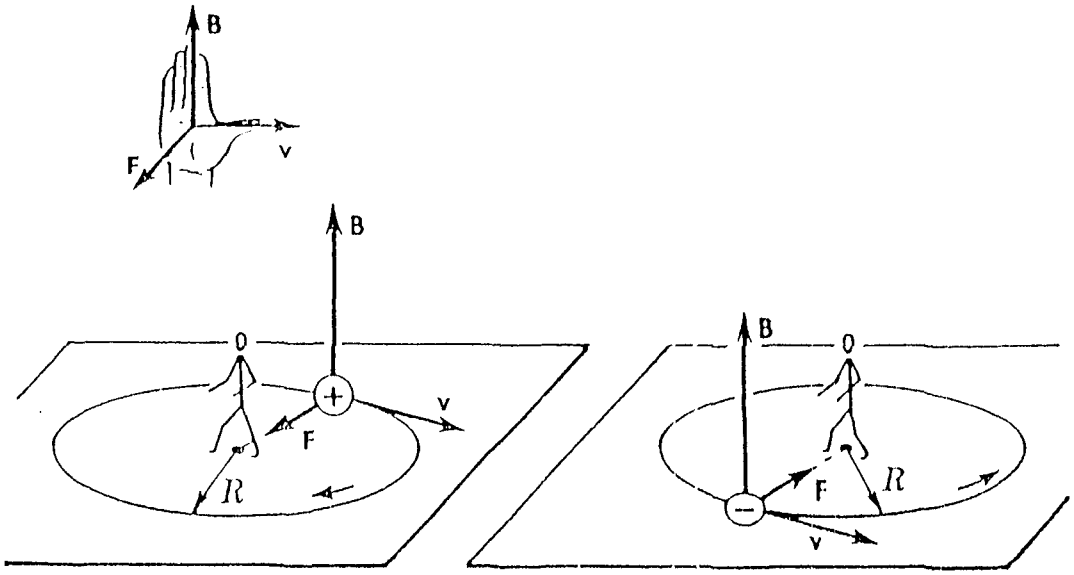

(a) (b)

Fig. 1.3 The deflecting force experienced by a charged perticle moving through a uniform magnetic field.

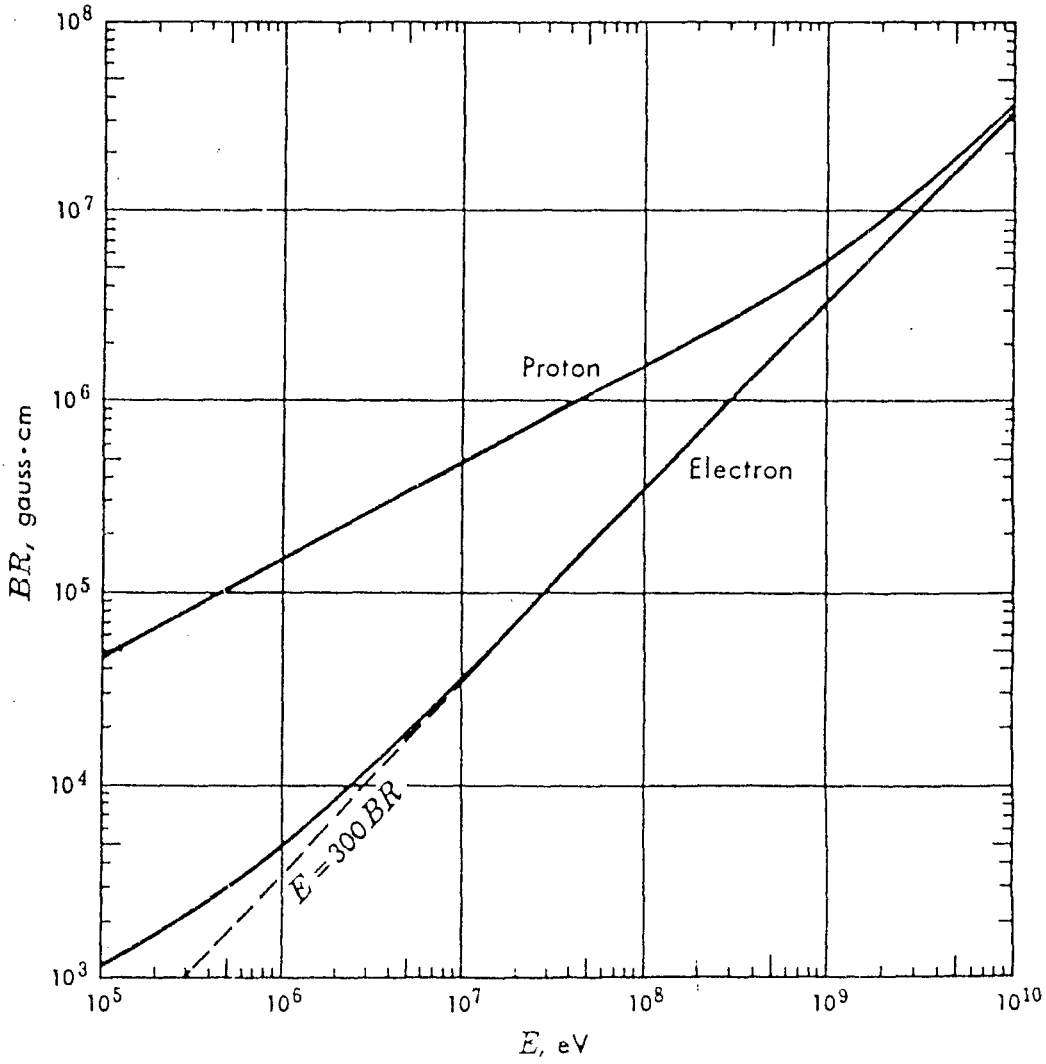

Fig. 1.4 Magnetic rigidity BR as a function of kinetic energy E for protons and electrons.

the particle to move in a circle (fig.1.3).

This is represented by $BeV = mV^2/R$

$$BR = mV/e$$

BR is known as magnetic rigidity measured in gauss-cm applying relativistic correction

$BR = m_o/\sqrt{1-\beta^2} \times V/e$, $\beta = V/e$

B is measured in gauss and R in cm.

$$BR = 3 \times 10^{10} \times m_o/e \times V/\sqrt{1-\beta^2}$$

$$BR = m_o/e \times Vc/\sqrt{1-\beta^2}$$

As $V \longrightarrow c$

$$BR = m_o/e \times c^2/\sqrt{1-\beta^2} \qquad .....(1)$$

According to the theory of relativity, total energy

$$E = mc^2 = m_o/\sqrt{1-\beta^2} \times c^2$$

Since 1 erg = 300/c eV

$$E = 300 \times m_o/e \times c^2/\sqrt{1-\beta^2} \text{ eV} \qquad .....(2)$$

Comparing E = 300 BR

From the figure (1.4), for sufficiently large energies, both curves approaches the straight line representing the equation E = 300 BR.

For high energy particles with Z elementary charge, the magnetic rigidity is Z time, smaller than for a singly charged particle of same energy.

In this case E/Z = 300 BR

For a moving particle in a magnetic field the radius R of the circle

$$R \propto 1/B$$

Where B the magnetic field.

We have $Bz\ eV = m V^2/R$

$$BR = mV/ze, \quad mV = p$$

$$BR = p/ze$$

$R \propto 1/B$ for a given charge

$R \propto P$ i.e. $R \propto P/B$

$$BR \propto P$$

For multi charged particle

$$BR \propto P/ze.$$

A multicharged particle experience a stronger side thrust than a singly chraged and its trajectory is deflected in to a circle of smaller radius.

Let us see how earth's magnetic field effects the motion of charged particles. Consider a particle under the action of this field that circles the earth at geomagnetic equator.

To keep the particle in a particular orbit the two condition must be satisfied:

(i) The force exerted by the magnetic field must point towards the centre of the earth and the particle must move from east to west if it is positive and from west to east if it is negative.

(ii) The second condition is that the magnetic rigidity of the particle must be equal to the product earth's radius (R = 6.38 x 10^8 cm) and field strength at the equator (B = 0.32 gauss)

$$BR = 0.32 \times 6.38 \times 10^8$$
$$= 2 \times 10^8 \text{ guass - cm.}$$

From the graph above a magnetic rigidity of 2 x 10^8 gauss- cm corresponds to KE in the neighbourhood of 60 BeV, consequently charged particles with energy of this order or less must strongly deflected by earth's magnetic field.

Rossi concludes that for each point on the earth and positive particles of any given magnetic rigidity there exists a cone (Stormer cone), with the axis pointing towards east such that all direction fig.1.5 a, within the cone corresponds to bounded trajectors and therefore forbidden direction.

Since in the case of positive particles forbidden stormer cone point towards east, so positively charged particles from eastern region is smaller than wastern region of sky. In the case of negative particles situation is opposite. This predicted asymmetry which is known as **east-west effect.**

The character of allowed and forbidden regions of the sky at an intermediate latitude, 30° N, for positive

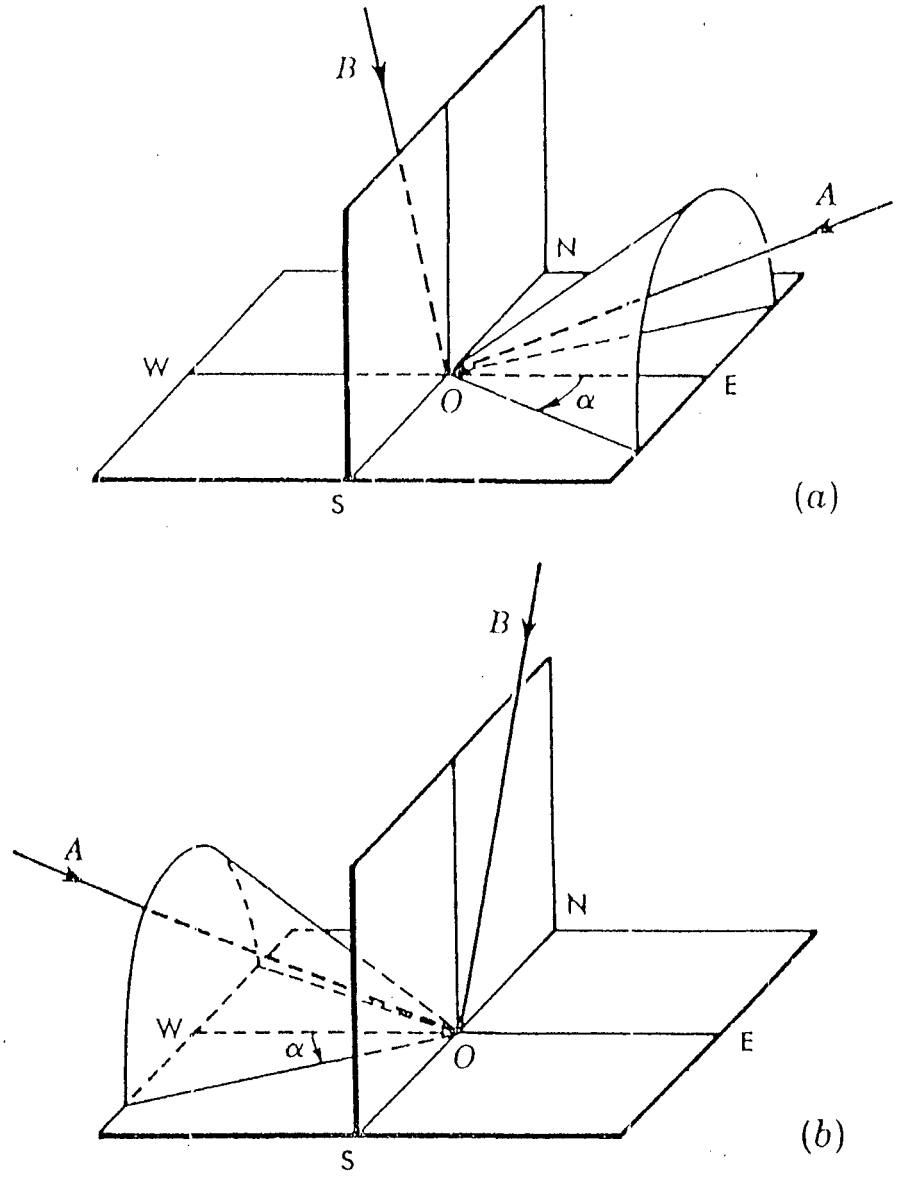

Fig.1.5 : (a) Stormer cone for positive particles
(b) Stormer cone for negative particles

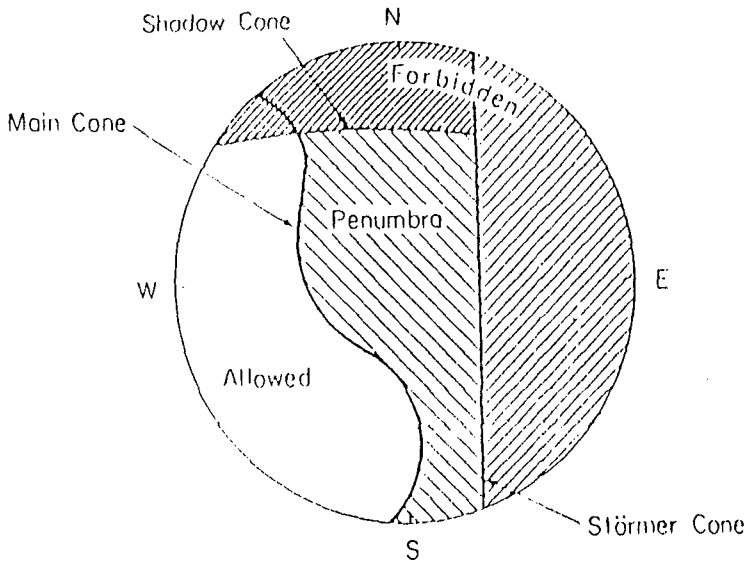

Fig.1.6 The allowed and forbidden directions of particles for a given latitude and rigidity.

particles of a given rigidity (10 GV) is depicted in the fig. 1.6. The stormer allowed cone includes the entire portion of the hemisphere west of the arc that is so labelled. Absolutely no 10 Gv particle, can reach the regions lying outside this cone. Part of the allowed cone lies in the earth's shadow. All of the main cone, west of the indicated arc, is accessible to 10 Gv particles. between the boundaries of the main cone and the stormer cone lies the penumbral region, characterized by alternate light and dark bands.

An important concept in the application of the theory of geomagnetic effects to the interpretation of cosmic ray measurements was introduced by W.F.G. Swann. He showed that as a consequence of Liouville's theorem the particle flux is the same at all allowed places, and zero elsewhere.

(5) COSMIC RAY SOURCE AND ORIGIN

(a) Origin of Cosmic Rays

Cosmic rays have been discovered in 1911, even then it is not very well known, where they originate and how they acquire their tremendous amount of energy per nucleon. Further it is not certain whether the whole primary spectrum can be ascribed to particles of one and the same origin. However, various theories concerning

the origin of cosmic rays have revealed that the cosmic rays are partly of solar origin and partly of galactic origin and a part of cosmic rays having very high energy per nucleon, have their origin even beyond our galaxy (i.e. Extra galactic origin).

1. Solar Origin

The term solar origin signifies that the origin of the cosmic rays exists somewhere on the sun. In fact, during solar flare the sun produces large number of particles of energies varying from several hundred MeV to several BeV. This acceleration occur during the high solar activity when a large erruption takes place and large masses of ionized gases shoot-out from the surface of the sun in the interplanetary place. The magnetic disturbance accompanying these erruptions are strongly suspected as the agency through which some of the protons in solar atmosphere acquire high energies. However, the isotropy of quiescent cosmic rays and the presence of high energy particles (protons of energy $\geq 10^{15}$ eV) demands the origin outside the solar system. If the cosmic ray particles have energy of the order of 10 BeV which form the major portion of cosmic rays then neither the earth's magnetic field (0.5 gauss) nor the interplanetary field ($\backsim 3 \times 10^{-5}$ gauss) can maintain their isotropy. For a

proton of energy 10^{15} eV, the radius of curvature of IMF will be nearly 10^{17} cm, which is 6500 times the earth-sun distance, while the radius of curvature in the vicinity of earth will be 6×10^{12} cm which is 10,000 times the radius of the earth. Thus proton of energy of 10^{15} eV or more do not go under appreciable deflection, neither in IMF nor in earth's magnetic field, so if they are produced by sun, they would come from the direction of the sun. But the shower experiment have shown that there is no preferential direction of arrival of high energy particles.

2.3 Galactic Origin

It is natural to assume that cosmic rays are produced in galaxies rather than in the nearly empty space between the galaxies. The main question is whether cosmic rays seen near the earth originate in our galaxy (Milky way) or outside our galaxy. If the cosmic rays are from outside our galaxy, they might be pervading the whole universe or restricted to our local cluster of galaxies. The general argument for galactic origin is given below:

The energy needed for maintaining the cosmic rays in our galaxy is available.

The cosmic ray energy density is about 10^{-12} ergs/cm^3 and the galactic volume including the halo is about 10^{68} cm^3, and the life time of the cosmic rays in

the galaxy is about 10^8 years. The energy needed to maintain the cosmic rays at its present intensity is

$$E_{C_R} = 10^{-12} \times 10^{68} / 3 \times 10^7 \times 10^8 = 3 \times 10^{40} \text{ ergs/sec.}$$

3. Extragalactic Origin

Until few years ago it was generally belived that all cosmic rays arriving at earth are produced in our galaxy. However, the occurance of primary cosmic rays of energy at least as great as 6×10^{19} eV has established that these particles, having large radius of curvature 4×10^{22} cm, cannot remain trapped in the galactic disk (thickness 10^{21} cm) or even galactic halo (radius 5×10^{22} cm).

If so they are to be found in the space beyond our galaxy. On the other hand the cosmic ray spectrum does not break-off at 6×10^{19} eV, it continues well beyond this energy and if the particles having energy greater than 6×10^{19} eV are protons they will lead the only conclusion that these particles are of extra galactic origin.

(b) Sources of Cosmic Rays

Possible sources of cosmic rays are

1. Supernova
2. Pulsar
3. Rapid X-ray burster

The energy given in the above equation can be supplied either from supernova explosion, pulsars and from rapid X-ray burster (Singh, L.M. and Duorah 1983). With the observation in recent years of ultra-high energy gamma rays from specific astrophysical sources, it has become possible to state with some confidence that the sources of the high energy cosmic rays are now known. It is not known whether or not such sources contribute the whole of the observed cosmic ray beam or whether they are capable of producing the highest energy cosmic rays. The authors Kilikove et al. (1969) and Syrovatski et al. (1971) paid great attention to possibility of galactic origin of ultra high energy (UHE) cosmic rays, $E>10^{17}$ eV.

1. Supernova: The Basic Source of Cosmic rays in Galaxy.

In order to explain the possible role of supernova as sources of cosmic rays in the Galaxy it is important to know the cosmic ray energy in the shells at some stage of their evolution as to know the total energy of the cosmic rays formed as a result of an explosion and all subsequent process of acceleration and breaking. Since the departure of particles from the shells is probably fairly significant, this total energy may far exceed the energy of cosmic rays retained in the shell. From this point of view the total amount of energy generated by a number of supernova reaches 10^{50} ergs.

If T_{sn} = 50 years, the average time between supernova explosion. The mean power of supernova

$$U_{sn} \sim W_{sn}/T_{sn} \sim 10^{50}/(50x3x10^{7}) = 10^{41} \text{ ergs/sec}$$

Since the requirement of a source to produce cosmic rays is $U_{source} \sim 3x10^{40}$ ergs/sec, supernova acts as a cosmic ray source.

2. Pulsar as a source of cosmic radiation

In case of pulsars the central bodyis responsible for the pulsation is thought to be rotating neutron star having a rotational energy of 10^{52} ergs. If again a pulsar is born every 50 years (a pulsar is expected to originate in a supernovae explosion) and if say ten percent of the pulsar energy loss goes to particle radiation then the energy supply to cosmic ray is

$$E_P = 10^{51}/(50x3x10^{7}) = 10^{41} \text{ ergs/sec}$$

which is enough to maintain the intensity of cosmic rays in Pulsars. So pulsars in Galaxy act as a possible source of cosmic ray.

3. Rapid X-ray burster as a source of cosmic rays

Primary cosmic rays particlesconsists of mostly protons and nuclie of light and heavy elements. The origin and acceleration of high energy cosmic rays have always been a problem. Even before the discovery of pulsar, the origin and acceleration field of the nebulous

clouds and in the supernova shells (Ginzburg 1969). The rapidly rotating neutron star represents a plausible glactic site for the production of energetic particles. Gunn and Ostriker (1969) proposed that the pulsars were the sites for acceleration of cosmic rays. Singh and Duorah (1983) have found that a rapid burster M X B - 1730-335 may be constant source of high energy cosmic ray particles. In what follows, we consider this burster as the model cosmic ray generator. This burster is known to be a rapidly rotating neutron star accreting matter from a companion. Electrons can be pulled out from the stellar surface much more rapidly than the positive ions. The electron work function for matter in supper strong magnetic field is at least an order of magnitude less than positive ion binding energy (Ruderman and Southerland 1975). Hence the neutron star surface is a copious supplier of electrons. These electrons moving in magnetic field lines emit curvature radiation photons which are energetic enough to produce additional $e^{\pm}$ pairs. The positron escape from the polar cap upward while the electrons strike the surface of the polar cap area and may throughout C,O,Ne etc. nuclei, which were produced. On the accreted matter being converted into heavier nuclei by thermonuclear reactions over a long period of time. These nuclei will then be accelerated to very high energies. A

neutron star which produce X-ray burst for six months will be not enough to produce the required cosmic ray composition of heavy nuclei. When a particle of charge Z traverse a distancel in uniform magnetic field of strength B, the highest energy attained by the particle is given by 300 ZB1 eV Rose (1973). Modifying this expression suitably for our purpose, a particle moving inside the accretion funnel with angular width 1/ (Rose 1973) the maximum energy gained by the charge Z while travelling for a distance of 10^2 cm is found to be

$$E_{max} \sim 2 \times 10^2 \ (z/\gamma) \ eV$$

$$\text{Where} \quad = 1/\sqrt{1-v^2/c^2}$$

For a nuclei of charge Z = 50 and = 10-100, the maximum energy attainable is around 10^{21}-10^{22} eV. A highly magnetised neutron star whose polar cap is sufficiently hot (10^7-10^8°K) in general is a constant source of high energy cosmic rays. The physical condition available in a long period transient like MxB 1730-335 are suitable enough to produce the composition and energy of cosmic rays.

****

References

1. Berenzinsky, V.S. (1977) Proc: 15th ICRC **10** 84.
2. Blanford, G.E., Fleischer, R.L., Klarmann, J., Walker, R.M., Price, P.B., Wefel, J.P. and Well, W.C. (1970) Acta phys. Sc. Hung 29 Suppli. **1** 423.
3. Bothe, W. and Kohlhorster, W. (1928) Naturewise **16** 1044.
4. Carmichael, H. (1962) Space Sci. Rev. **1** 28.
5. Compton, A.H. (1923) Phys. Rev. **43** 387.
6. Duggal, S.P. (1979) Rev. Geophys. Space Phys. **17** 1021.
7. Elester, J. and Geital, H. (1900) Phys Z **2** 560.
8. Forbush, S.E. (1946) Phys. Rev. **70** 771.
9. Fowler, P.H. , Adams, R.A., Cowen, V.G. and Kidd, J.M. (1967) Proc. Roy. Soc. **A-301** 39.
10. Freier, P.S. and Webber, W.R. (1963) J. Geophys. Res. **68** 1605.
11. Ginzburg, V.L. (1969) The Astro Physics of Cosmic rays.
12. Gunn, J.E. and Ostriker, J.P. (1969) Phys. Rev. Lett. **22** 728.
13. Johnson, T.H. (1938) Rev. Med. Phys. **10** 193.
14. Kiraly, P. et. al (1981) Nature **293** 120.
15. Mc Crackken, K.G. and Rao, U.R. (1970) Space Sci. Rev. **11** 155.

16. Millikan, R.A. and Bowen, I.S. (1936) Phys. Rev. **43** 695.

17. Price, T.A. (1979) Ap. J. **227** 676.

18. Protheroe, R.J. and Clay, R.W. (1985) Nature **315** 205.

19. Rossi, B. (1930) Phy. Rev. **36** 606.

20. Ruderman, M.A. and Sutherland, P.G. (1975) Ap. J. **196** 51.

21. Rose, W.K. (1973) Astrophysics.

22. Rao, U.R (1972) Spac. Sci. Rev. **12** 719.

23. Sakurai, K. (1974) Astrophysic Space Sci. **28** 375.

24. Schein, M. and Jessew, P. (1941) Phy. Rev. **59** 515.

25. Singh, L.M. and Duorah, H.L. (1983) 18th ICRC **2** 329.

26. Simpson, J.A. (1983) Ann. Rev. Nucl. Part. Sc. **33** 323.

27. Steecker, F.W. and Wolfendale, A.W. (1985) Proc. 19th ICRC **2** 354.

28. Stecker, F.W., Walsh, T. and Rudaz, S. (1985) Proc: 19th ICRC **2** 358.

29. Wilson, T.C.R. (1900) Proc: Camb. Soc. **I-1** 32.

30. Wolfendale, A.W. (1979) Pramana **12** 631.

CHAPTER 2

THE SUN AND THE INTERPLANETARY MEDIUM

THE SUN

The sun is one of the normal stars in the main sequence in our galaxy, which contains 10^{11} stars. Although the sun is a small star, but it is the only star whose surface is directly observable from the earth by the naked eye and it produces a disk image in the telescope. This fact is very important for studying the various phenomena occuring on the sun's surface as well as in other stellar objects similar to the sun. By studying the detailed structure of the atmosphere and interior of the sun, we are able to understand physical characteristics of stars similar to the sun. The sun is our nearest star and it is the star of average size, mass and brightness. It is much closer to us than the other much bigger and brighter stars. The distance of the sun from earth is 1.5×10^{11} meters which is called the astronomical unit (A.U). In our planetary system the sun is the main source of energy. It is the only star which presents its surface details. The distance of the sun from the centre of our Milky way galaxy is $\sim$30,000 light years (Fig. 2.1). Its mass and density are 2×10^{33} gm and $\sim$100 gm x cm^{-3} respectively. The acceleration due to gravity at the sun has been estimated to be $\sim 2.74 \times 10^{4}$ cm sec^{-2}. All parameters of sun are given in table 2.1.

(1) THE CORE OF THE SUN

In the central part of the sun, the solar material is

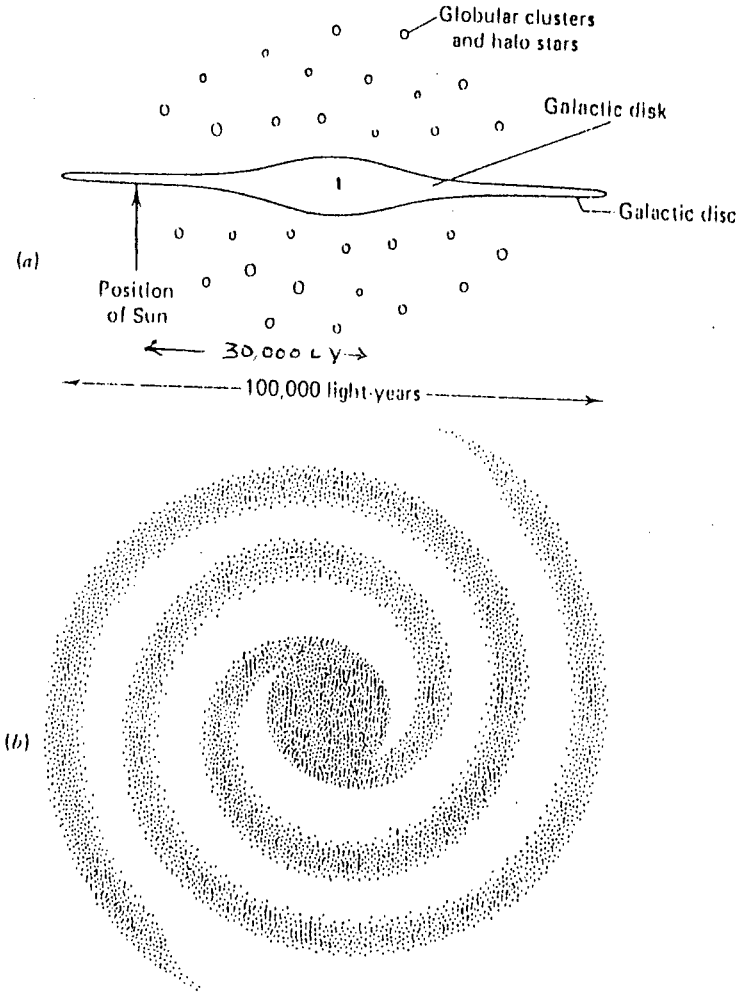

Fig. 2.1:(a) Position of the sun from the centre of our Milky Way Galaxy.

(b) Spiral arms showing the position of the sun.

Table 2.1

Parameters of sun	
1. Earth-Sun distance	1.5×10^{11} meters (A.U)
2. Distance of the sun from centre of our Milky way galaxy	30,000 light years
3. Diameter of sun	139×10^{4} Km.
4. Mass of the sun	$\sim 2 \times 10^{33}$ gram.
5. Density	~ 100 gm cm^{-3}
6. Radius of its visible disk (Photosphere)	$\sim 7 \times 10^{5}$ Km (109 times the radius of earth)
7. Accleration due to gravity	$\sim 2.74 \times 10^{4}$ cm sec^{-2}
8. Power out put of the sun	$\sim 4 \times 10^{26}$ watts
9. Life time	$\sim$ 10 billion years
10. Temperature	$\sim 15 \times 10^{6}$ °K

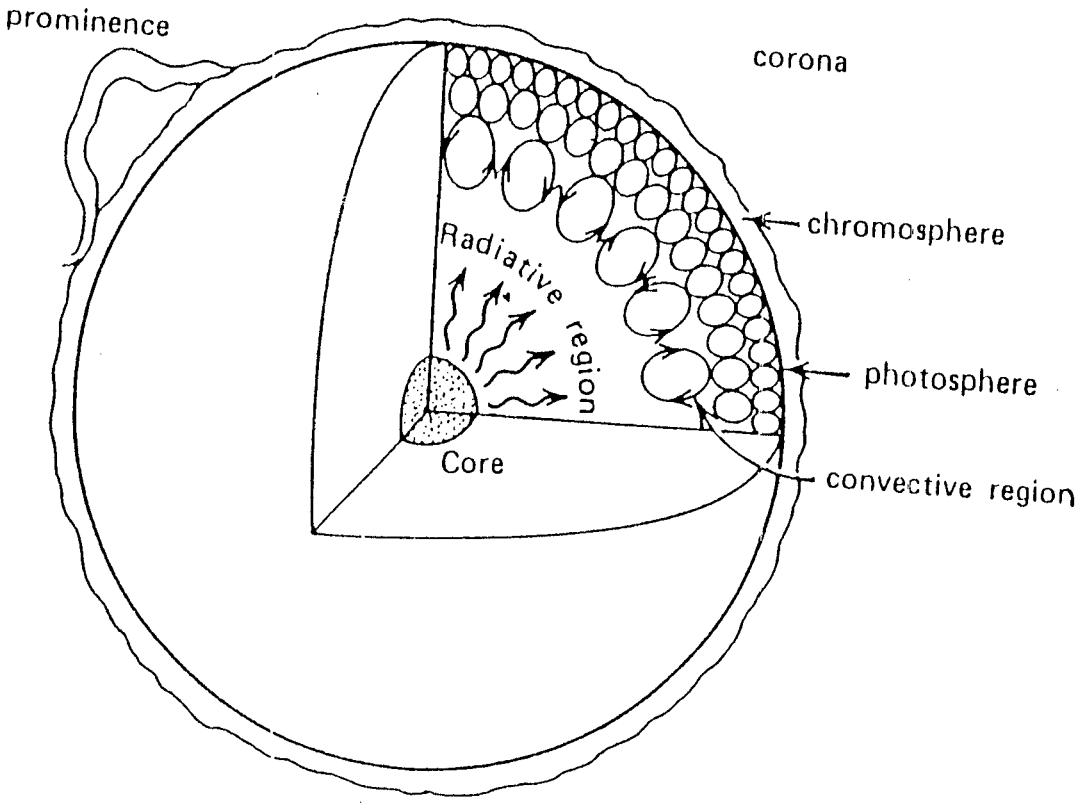

Fig. 2.2 Schematic view of the core of the sun.

highly compressed under its own gravitational attraction. The mean central density is about 100 gmxcm^{-3} and the temperature has been estimated to be 15×10^6°K. Due to such a high central density and temperature, thermonuclear reaction takes place in the core of the sun. The process by which the energy is liberated in the core of the sun are discussed below:

(a) **Proton-Proton Cycle**

Energy is released by the P-P cycle in the core of the sun. The P-P cycle, is the main source of the energy generated in the sun and the other stars with an abundance of hydrogen. Most of the energy production takes place in the core of the sun, where the temperature is about 15×10^6°K and density is about 150 times that of water. It would be possible for two hydrogen nuclei to collide and form a nucleus of deuterium (or heavy hydrogen) and two other particles, a positron and a neutrino are produced. The reaction can be written in Table 2.2.

Table 2.2

(A)	$_1H^1 + {}_1H^1 \rightarrow {}_1H^2 + e^+ + \nu_e$
	$_1H^2 + {}_1H^1 \rightarrow {}_2He^3 + \gamma$ (high energy)
(B)	$_1H^1 + {}_1H^1 \rightarrow {}_1H^2 + e^+ + \nu_e$
	$_1H^2 + {}_1H^1 \rightarrow {}_2He^3 + \gamma$
(C)	$_2He^3 + {}_2He^3 \rightarrow {}_2He^4 + 2\ {}_1H^1$
	or $4\ {}_1H^1 \rightarrow {}_2He^4$ + Energy

(b) **The CNO Cycle**

P-P cycle is believed to be main source of energy generated by sun and it is also the power source for stars less massive than the sun. But CNO cycle is main source of energy generated in more massive stars. The P-P cycle generate energy per gram that depends on the fourth power of the central temperature of the star on the other hand CNO cycle is much more sensitive to temperature, its energy generation rate depends on the twentieth power of temperature since more massive stars will in general have higher central temperature, it is apparent why the CNO cycle will dominant in their energy generation. In CNO cycle hydrogen is also converted in to helium, however, nuclei of the elements carbon, nitrogen and oxygen are also involved, although they are continuously renewed in the cycle and are not used up permanently. The sequence of the nuclear reaction in the CNO cycle is shown in Table 2.3.

During this cycle, four hydrogen nuclei are converted in to one helium nucleus and the original carbon atom reappears. Here the function of carbon is as a catalyst, if a star had no carbon atom in the core, it would not be able to generate energy by using this cycle. The enormous amount of heat so produced in the core is transferred out word by radiative transfer and convective process.

Table 2.3

A	$_6C^{12} + {}_1H^1 \rightarrow {}_7N^{13} +$ (gamma ray)
	$_7N^{13} \rightarrow {}_6C^{13} + e^+ +$ neutrino
	$_6C^{13} + {}_1H^1 \rightarrow {}_7N^{14} +$ (gamma ray)
B	$_7N^{14} + {}_1H^1 \rightarrow {}_8O^{15} +$ (gamma ray)
	$_8O^{15} \rightarrow {}_7N15 + e^+ +$ neutrino
	$_7N^{14} + {}_1H^1 \rightarrow {}_6C^{12} + {}_2He^4$
C	$4\,{}_1H^1 \rightarrow {}_2He^4 +$ Energy

(2) THE ATMOSPHERE OF THE SUN

The atmosphere of the sun or the solar atmosphere has three distinct layers (i) Photosphere (ii) chromosphere and (iii) Corona. The physical conditions of these layers are very much different. The relatively dense opaque lower layer is known as the photosphere. The increasingly rarified transparent and extended regions are called the chromosphere and the corona. The relative positions and various characteristics of these layers are presented in the fig. 2.3 and are discussed in the succeeding subsections.

(a) The Photosphere

The photosphere is defined as that layer of the solar atmosphere, which produce, all visible radiations of the sun and produces a continuous spectrum. The emission coefficient is very high for this layer. Thickness of this layer is about 300 Km. The temperature of the photosphere is not excatly known, however, it is generally accepted that at its top where the photosphere is almost transparent, the temperature is about 6000°K. At the lower depth, the photosphere converts in to an opaque region known as 'convective zone' of the sun, which extend by 1/10 of the solar radius. Hydrogen is the most abundant element in the photosphere and helium is five to ten times less abundant than hydrogen.

The most prominent feature on the solar photosphere are

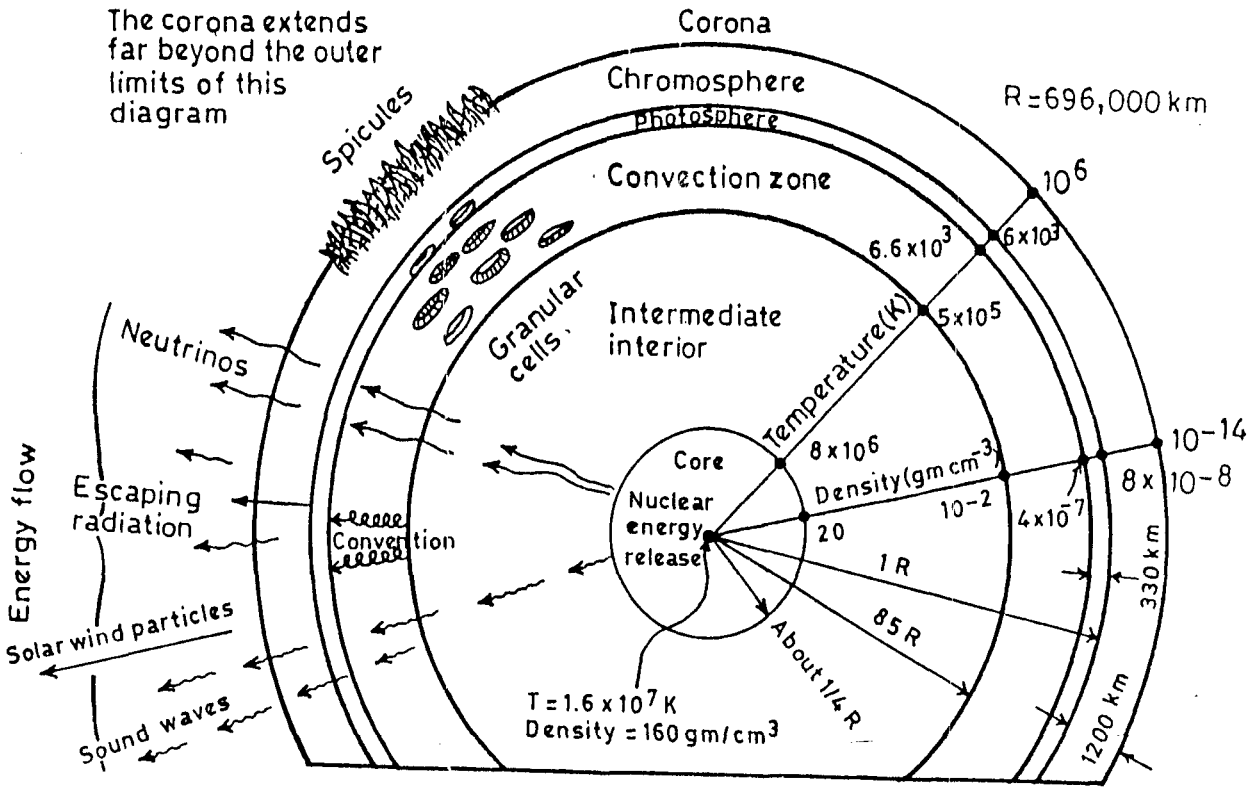

Fig. 2.3 The general features of solar properties, structure and models of outward energy flow, providing qualitative picture of the sun.

sunspots. The photosphere is not uniformly bright hut consists of a large number of granules on a some what darker background. The size of these granule, varies from 200 to 1800 km and have an average size ~700 km. The average life time is 8.6 mts, it varies from 8 to 10 minutes. The temperature of the granule, is about 100°K or less, above that of photosphere. The granule, occur every where on the surface of the sun and sometimes even in the umbra of large sunspot.

The gas in solar photosphere tends to move collectively in a large scale horizontal motion. This motion is defined as supergranulation. At the central portion of the cell, material appears to rise and then goes down in to the photosphere. Besides these large velocity cells of $(15\text{-}20)\times10^3$ km diameter, on the photosphere, small regions of 2" to 3" of arc show velocity oscillations with a period of about 5 minutes. The photosphere disc shows the decrease in brightness from the centre towards the edge. This effect is known as **Limb darkening.**

Faculae: Besides the granules some other bright regions are also observed in white light on the photosphere, these are called faculae. Faculae are regions of great brightness, usually greater than that of the photosphere, Faculae are usually found in association with sunspots, but sometimes occur in regions devoid of sopts. In general they appear long before the formation of a spot and survive long after it has disappeared. Photospheric faculae and chromospheric faculae

or plages are closely associated and infact, they are different manifestation of the same phenomena, at different heights of the solar atmosphere Faculae contain granules which combine to form coarse mottles having diameter of 5000 km. These mottles in turn tend to string together in to chain and the net work of these composes the faculae.

(b) The Chromosphere

During the total solar eclipses when the moon completely covers the photospheric disk, a luminous layer is seen just above the photosphere which emits bright monochromatic lines. This layer is known as chromosphere or sphere of colour.

The whole chromosphere is divided in to three regions, the lower, middle and upper chromosphere. The heights of these regions above the photosphere are approximately 8 to 1000 km, 1000 to 4000 km and 4000 to 12,000 km respectively. These layers represent temperature stratifications as shown in fig.2.4. The rise in temperature is slow in the lower chromosphere, but it rises rapidly in the middle and upper chromosphere. The chromosphere is the most spectacular region of the sun, where flares, prominences and a large variety of interesting phenomena takes place.

A chromospheric flare is short lived sudden increase of intensity in the neighbourhood of the sunspots. It is best

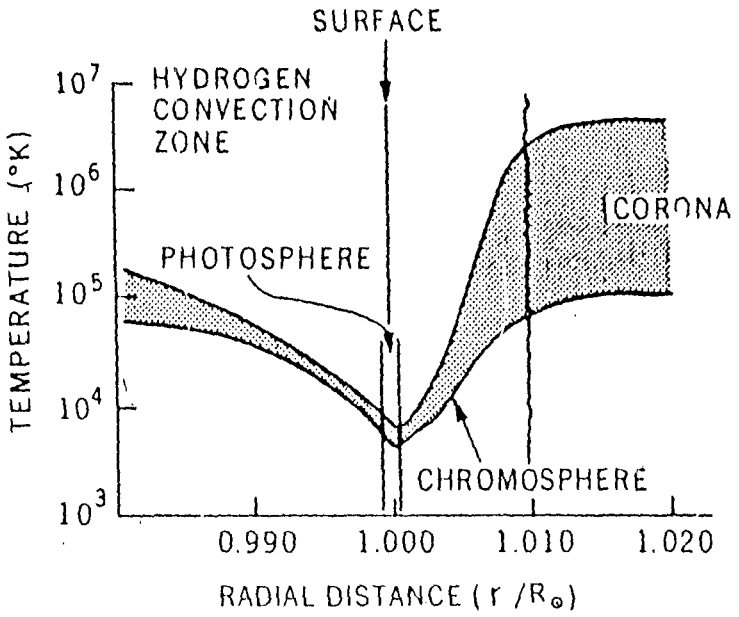

Fig. 2.4 The distribution of temperature with respect to the distance from the centre of the sun.

observed by using monochromatic filters such as H_{α} . In some rare cases flare have been seen even in white light.

Prominence: Beautiful large prominence are shown in figures 2.5, 2.6 & 2.7. Prominence may assume a great variety of shapes, resembling clouds, Jets of smoke or vapour, trees, fountains, as can be seen from modern photograph. The following classification of prominence has been suggested by Pettit.

1. Active prominence:- which appear to be under the influence of an area of attraction or of a nearly spot.
2. Eruptive prominence:- which shoot up rapidly in a direction more or less vertical to the solar surface.
3. Spot prominence:- in the form of closed rings or jets.
4. Vortical prominence:- In the form of spirals.
5. Quiescent prominence:- whose shapes change more slowly than any of the foregoing.

Spicules: When chromosphere is viewed at the limb by using monochromatic filters such as H_{α} , the irregularity of the chromosphere becomes apparent. This view shows that the upper chromosphere appear to have a spicular structure (Fig.2.8). Many individual spicule rise from the lower chromosphere at a radial speed of about 25 km/sec up to heights of about 10,000 km and disappear in a few minutes. Each spicule has a thickness of 500 to 2000 km. They appear all around the sun

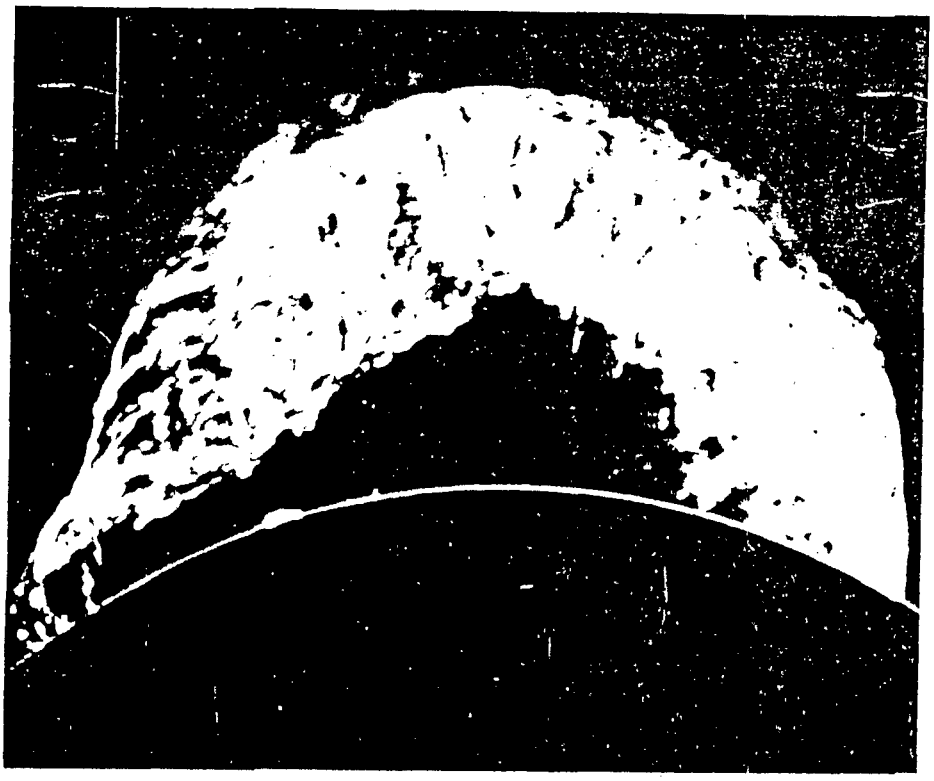

Fig. 2.5 Different types of prominence:
a large solar prominence.

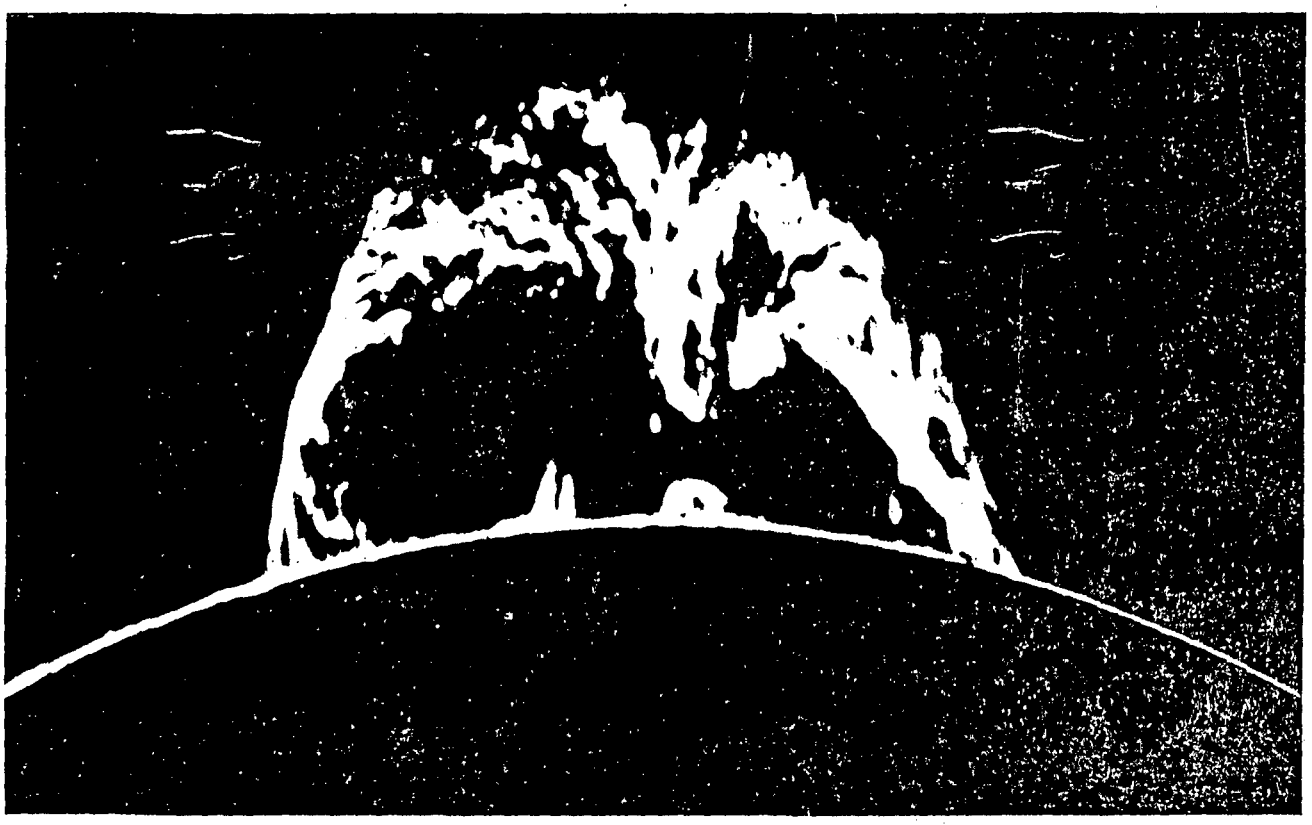

Fig. 2.6 Different types of prominence:
a beautiful prominence observed.

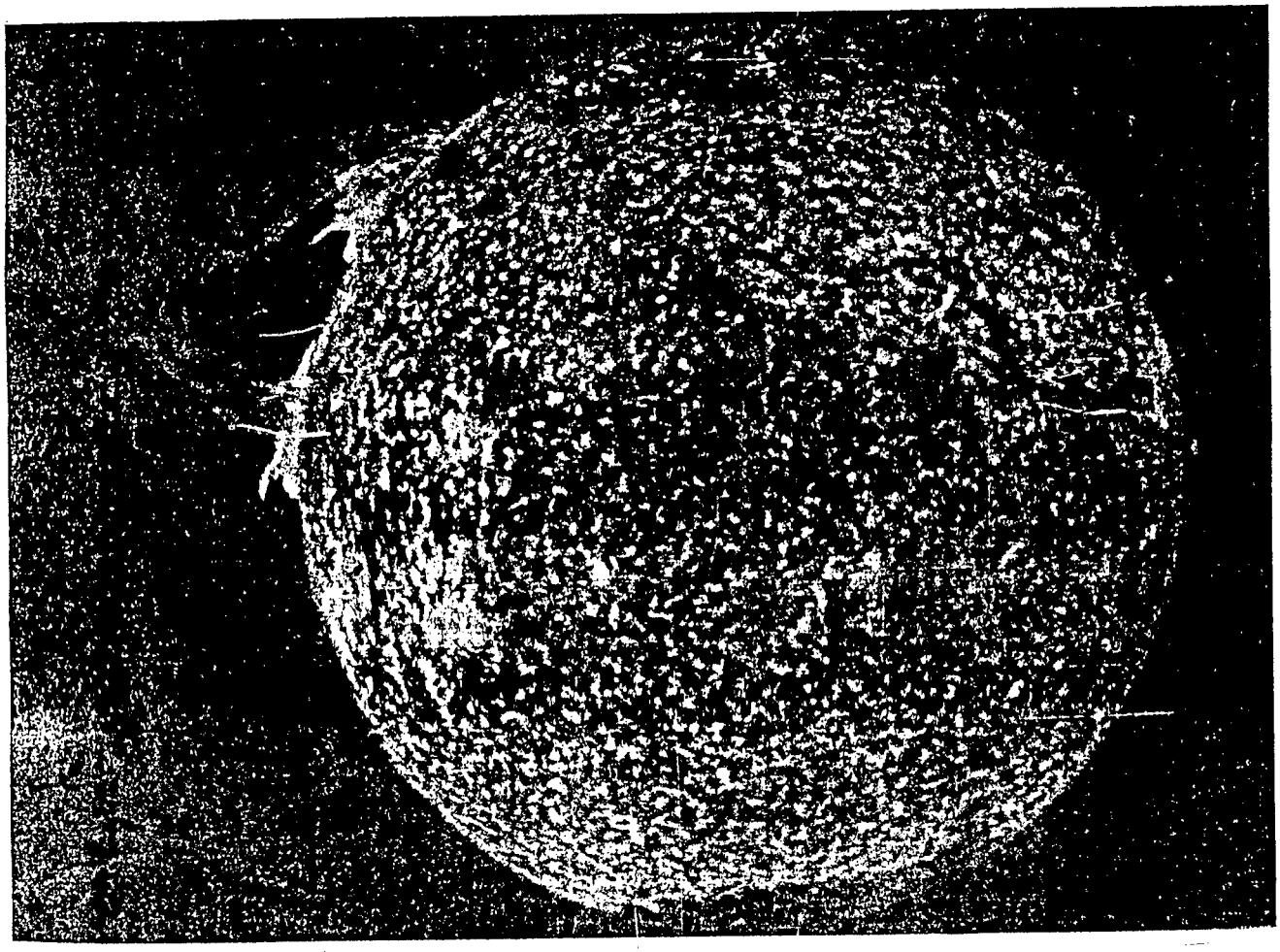

Fig. 2.7 Different types of prominence:
a prominence observed in ultra-violet light.

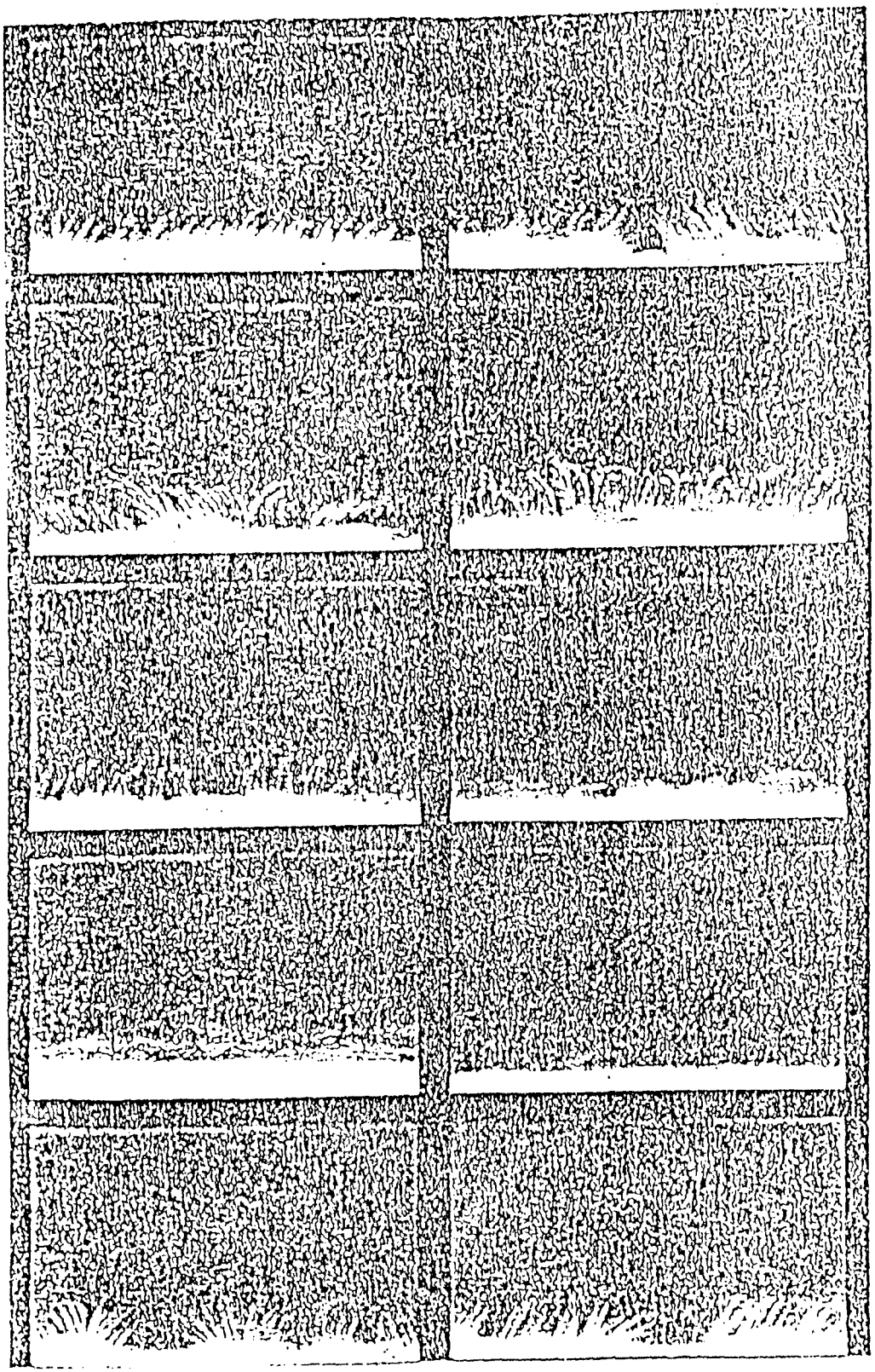

Fig. 2.8 A simple view of spicules.

and show systematic inclinations mostly towards the solar equator. From their spectra it appears that the spicules are cool formation (T$\sim$10,000°K to 40,000°K) embeded in the corona (T$\sim 10^6$°K).

When seen in Hα and K lines near limb of the chromosphere some bright regions are also observed, these are known as **chromospheric faculae or Plages**, their life time is longer than that of the photospheric faculae. In Hα , the faculae appear bright dots of diameter between 1000 to 2000 km, scattered all over the regions. When the seeing is good and spectroheliograph have sufficient resolution, the chromospheric hydrogen and calcium faculae show a granular structure.

(C) The Corona

The corona is the third and highest layer of the solar atmosphere which is only visible during total solar eclipses, but now with the development of coronograph it has been possible to observe the corona at times other than solar eclipse. It exists in the form of an extended gaseous mantle like structure around the sun and consists chiefly of very highly ionized atoms and free electrons. The temperature of the corona is $\sim 10^6$°K. The corona is not static but is continuously expanding under its own pressure gradient against the solar gravity in to the vacuum space the resultant flow,

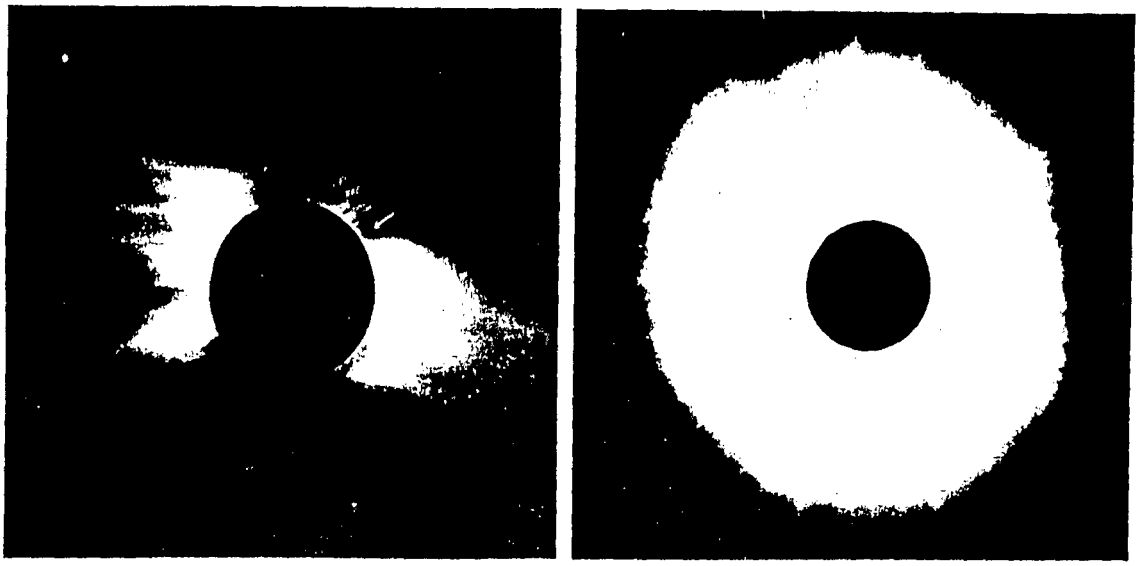

Fig. 2.9:(a) A simple view of corona near sunspot minimum
(b) A simple view of corona near sunspot maximum.

known as solar wind, reaches the earth with a supersonic velocity 400km/sec. The upper boundary of the solar corona cannot be defined, it is visible upto several solar radii during solar eclipses and there is some evidence that it reaches beyond the earth. The corona is neither uniform nor gradually fading with distance. The shape, temperature and density of the corona are functions of solar activity cycle (The density decreases from $5x10^8$ atoms/cm^3 near chromosphere to about $5x10^3$ atoms/cm^3 at a distance of about three solar radii). The minimum corona extends along the equitorial plane where as the maximum corona is symmetrical. A schematic representation of corona at sunspot maximum and sunspot minimum are shown in fig. 2.9.

The corona has three different regions designated as L,K and F which produce different types of emission. The coronal lines from highly ionized elements such as Fe Ni and Ca are emitted mostly near the limb or L- corona. This emission is 1% of total coronal emission. The K-corona produces coronal light originating from scattering by free electrons. This coronal light is polarised. By high speed of the scattering electrons the Fraunhofer lines are washed out and therefore, do not appear in the continuous spectra of K-corona. The F-corona is visible only far from the sun. It represent the sun light scattered and reflected by the interplanetary dust. The light of F-corona is slightly

polarized and contains the Fraunhofer spectrum. The F-corona consists of Fraunhofer lines. This component is not a part of the true corona, several emission lines from the corona were observed. There are several strong lines in the visible spectrum among them green line (wave length 5303 A°) and red line (wave length 6374A°) are important. The emission line component is called E-corona.

The typical features of the corona are polar rays and polar plumes which are visible during solar minimum particularly in white light. Streamers, are the formation emerging almost radially from the sun. These are observed in white light during solar eclipses and found upto 12 solar radius. The big streamers are known as **fans or helmets.** The dark regions of low temperature and low electron density are called **coronal holes.**

Heating Mechanism of Corona: The temperature of lowest corona is about one million degrees or more, inspite of the low temperature of the photosphere. With such a temperature variation, this structure is necessarily unstable. It is thought that the heat source for the maintenance of the coronal temperature is in the hydrogen convection zone. Wave generation of various mode in this zone is the source of heating the corona, they are hydromagnetic waves (fast, slow and Alfven modes) acoustic waves and gravity waves. It seems

that in hydrogen convection zone the amplitude of waves mentioned above are extremely small, propagating upward in the photosphere, the amplitude increases and so waves grow in shock waves. Thus wave energy dissipates through shock heating of chromosphere and corona.

The Solar Wind: The temperature of the corona is very high due to this high temperature, beyond a certain range, the velocity of the particles is so large that it exceeds the velocity required to escape from the solar gravitational field and consequently there is a continuous out ward flow (or expansion) of coronal gas in all directions, this flow has been termed the solar wind. The solar wind consists of about 95% protons, 4.5% alpha particles and 0.5% other positive ions with their associated electrons. The rate of expansion starts from very low velocities beneath the corona. The solar wind velocity increases steadily outward, surpassing the sonic speed at radial distance of a few solar radii. At a distance of about 50 - 100 AU, where the solar kinetic energy becomes almost comparable to that of interstellar magnetic pressure, the wind will effectively stop. The solar wind ion flux has been observed to range from $3x10^7 cm^2/sec$ to $3x10^9 cm^2/sec$ and perhaps higher. The bulk speed of the solar wind ranges from as low as 250 km/sec upto 1000km/sec, with typical quiet period wind speeds ranging between 300 to 350 km/sec. The number density ranges from about 1 cm^{-3} to 12 cm^{-3} with an

Table 2.4

Parameters	Maximum	Minimum	Average
Proton-electron density	80	0.4	5
Velocity (km/sec)	1000	200	400-500
Proton temperature	$5x10^5$ °K	$3x10^4$ °K	$4x10^5$ °K
Electron Temperature	$2x10^5$ °K	$1x10^4$ °K	$1x10^5$ °K
Ratio of He to H_2	0.20	0.01	0.05
Magnetic field	40	0.25	6
Alfven velocity	150 km/sec	30 km/sec	70 km/sec
Proton gyroradius (km)	80	75	78

The average solar wind plasma parameters.

average value of 5 cm^{-3}. The solar wind bulk speed and density are abruptly affected by the interplanetary shocks following solar flares. The solar wind measurements by Pioneer 10 and 11 at the orbit of the Jupiter ($\sim$4.0 AU) has given the velocity of solar wind $\sim$420 km/sec and density $\sim$ 0.5 particles/cm^{-3} and a proton temperature $\sim 5 \times 10^4$°K. These results are in good agreement with the steady state model of solar wind. A number of comprehensive reviews dealing with experimental and theoretical models of solar wind are available in literature (Dessler 1967, Burlaga 1971). From experimental observations it has been established that the proton and electron density and velocity in the solar wind plasma are almost equal within the errors of measurements. However, the thermal properties such as temperature and thermal anisotropy of electrons and protons are different. This indicates that collisions are much less dominent in solar wind and that it behaves as a two fluid plasma under quiet conditions.

Synder et al (1963) have established a strong correlation between geomagnetic index K_p and solar wind velocity

$$V = 8.44 \leq K_p + 330$$

Although there was no strong correlation between plasma velocity and overall activity as determined by sunspot number and 10.7cm flux. The solar wind velocity showed a strong

27-day recurrent tendency and close association with M-region stroms, indicatig that M-regions are emitters of high velocity plasma. The coronal holes have recently been shown to be associated with these M-regions on sun and the emitter of high speed solar wind streams (Krieger et al 1973, sheelay 1976). The bulk velocity of the solar wind is mostly radial in the orbital plane of the earth. Using the comet tailobservations Brandt and Heise (1970) obtained a radial velocity of 450km/sec.

There are several established variations in solar wind structure in association with the 11-year solar activity cycle (Gosling et al. 1976) Intriligator (1975) found the frequency of high speed streams and their duration vary over the solar cycle. The coronal green line intensity has been found to be better index of solar plasma emission. The asymmetric distribution of green line intensity would suggest that the emission of solar plasma is not uniform with respect to heliographic latitudes (Demison and Hewish 1967). Further observations indicate (Cole, et al. 1974) that the solar wind speed tends to be higher and more variable at high solar latitudes.

(3) SUNSPOT

Sun spots have been observed systematically for several hundred years, although they have been known to exist and have

been seen occasionally for thousands of years, particularly by Chinese and Japanese astronomers. Although they did not have telescopes, large sun spots some times appear that are visible to the naked eye, especially when the sun's glare has been dimmed near sun rise or sun set.

The sun's surface is not smooth and featureless. There are darker patches known as sun spots. The temperature of the bright surface or photosphere is about 6000°K, an average sun spot is 2000°K lower, that is why the sun spot seems dark. The sun's spot are produced on photosphere as a result of very intense magnetic field [thousands of gauss]. The birth and typical development of a spot, as discovered by observation may be described as follows.

Sunspots start out as pores, which are small regions much darker than surrounding, and offen do not develop further, but die away after hours or days.

The sun spots are generally confined to the latitudinal zones between 5° and 40° either side of the solar equator. They vary in size from approximately 50,000km in diameter down to what is barely possible to resolve by the best optical instruments .

It has long been known that sun spot generally come in pairs with a leading spot and a trailing spot, observations of their magnetic fields revealed that the two spots in a pair

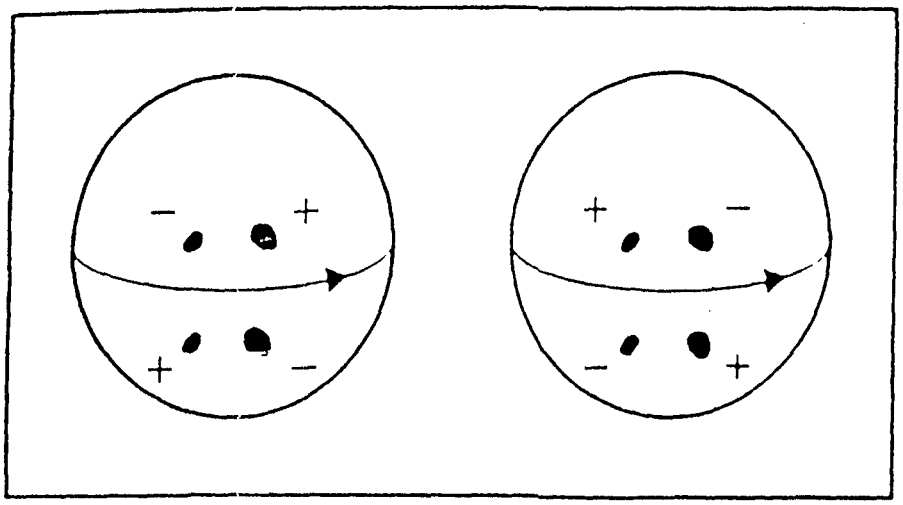

Fig. 2.10 Sunspot's polarities in the Northern and Southern hemisphere.

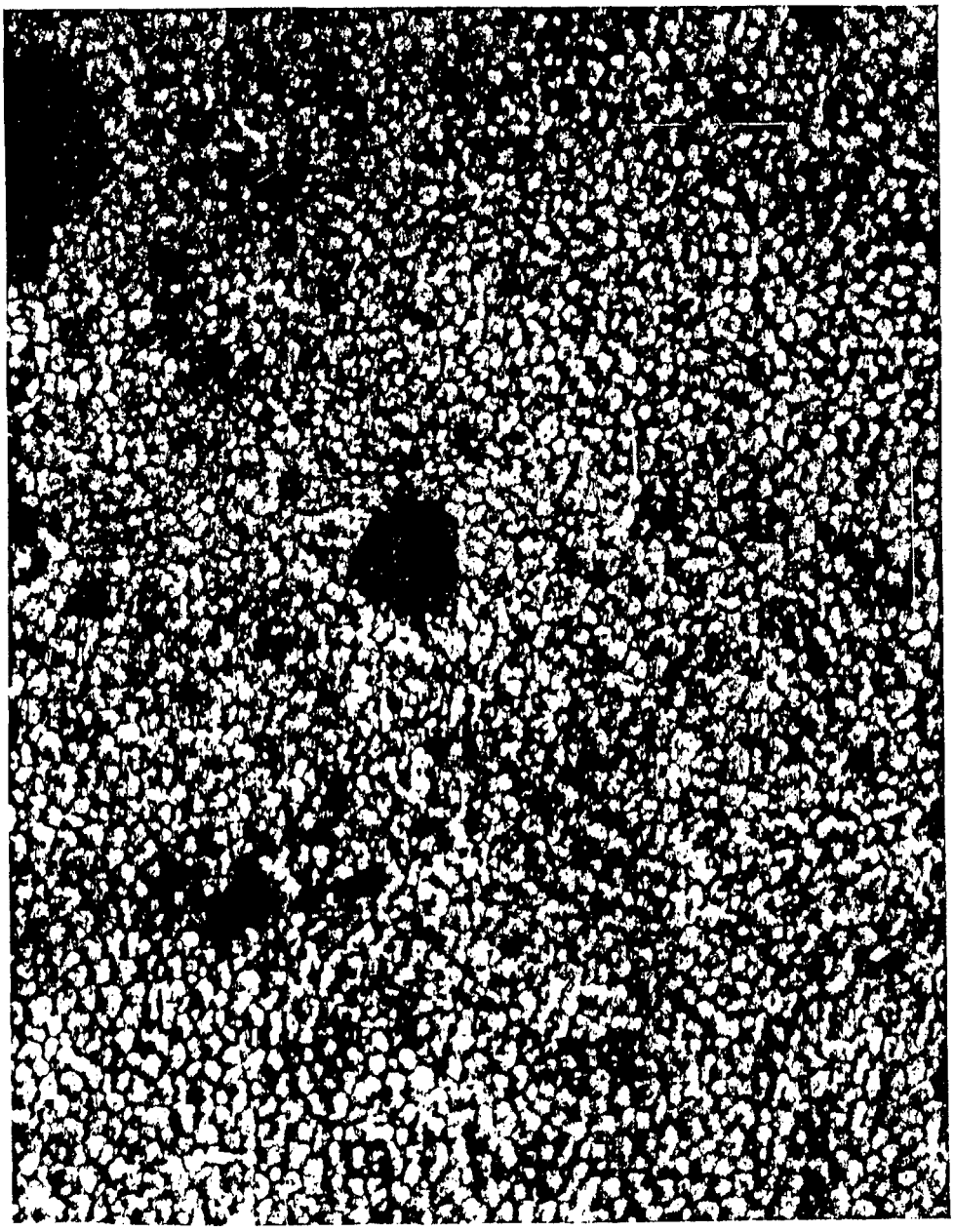

Fig. 2.11 A simple view of solar granulations. Pores and small spots.

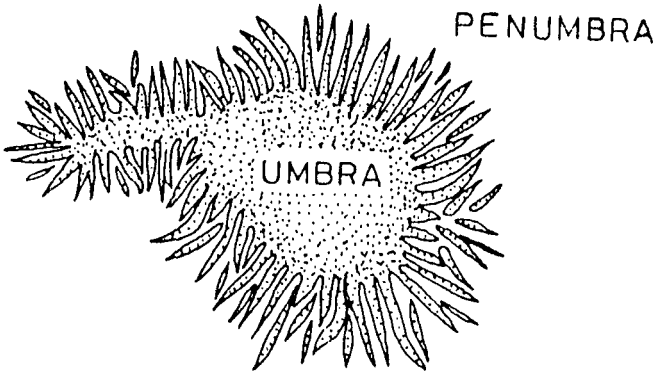

Fig. 2.12 A typical sunspot showing umbra and Penumbra.

have opposite polarities that is, if the leading sopt was a north magnetic pole, the trailing spot would be south magnetic pole and vice-versa. Further more, the polarities in the northern and southern hemisphere are reversed. After 11-year cycle new spots in each hemisphere have opposite polarities from the previous cycle (fig.2.10) If this reversal in magnetic polarities is counted, the actual sunspot cycle averages 22-year in length rather than 11-year and it is known as 22-year magnetic cycle of sun.

A simple view of solar granulation, pores and small spots is shown in fig.2.11. Sunspots are born in the growing plage regions on the sun. At first a localized magnetic field appears somewhere in the plage region and afterwards a sunspot is formed.

A full developed sunspot consists of central **umbra** through which most of the magnetic field is channeled and the less dark **Penumbra** (fig.2.12). Such darkness means that the temperatureof the sunspot umbra region is lower than that of the surrounding photospheric region (by 600°K).

The magnetic field strength has the maximum value near the centre of the sopt or where the spot is darkest i.e. in the core of the umbra. The strength of the magnetic field is about 1000-5000 gauss for well developed sunspots. The fully

developed sunspots may exists for days, weeks or months, but eventually it breaks up or decreases in size as the magnetic field decreases and diffuses. The field strength of the spot is found to be depend on its maximum area. It is of the order of 100 gauss in the smallest measurable spot, while in large spot it approches 4000 gauss.

A sunspot group is generally born in the form of a pair of two main sunspots which appear along almost the same latitude on the sun. This group is called a bipolar group. The preceeding and following sunspots are, in general called P and F spots. There are several types of sunspot groups shown in fig. 2.13.

1. Unipolar group (α -type)
2. Bipolar group (β -type)
3. Complex group (γ -type)

Unipolar group are single spots or groups of spots having the same magnetic polarity.

Bipolar group are group consists of two spots of opposite polarity.

Complex group includes spots of both polarities

A typical sunspot group known as δ -type is important in relation to the occurance of solar flares which produce such high energy particles as solar cosmic rays and electron responsible for the emission of type IV radiobursts. Another

classification of the sunspot groups, according to phases of their growth at different periods is known as Zurich classification sunspot group (A-J) which is shown in the fig.2.14.

(a) Magnetic Field of Sunspot

In 1908 the American astronomer G.E. Hale noted that the spectral lines of the spots divided in to several component each of which was distinctively polarised. The Dutch physicist P. Zeeman has proved in 1896 that this kind of splitting occurs when atoms emits light in an intense magnetic field. Thus Hale's observation clearly established that sunspots are powerful magnets since a hot gas cannot possible to form a permanent magnet like an iron bar, the existance of such magnetic fields proves that an intense electric current circulates in a ring around the sunspot. The current required to produce the field of a large spot may be as large as 10^{13} amperes.

Studies by H.Alfven in Sweeden (1954) and others have shown that such currents with their associated magnetic field would be difficult indeed to initiate in the solar atmosphere. Hence magnetic fields displayed by sun spots may be the result of electric currents that have existed from the time of sun's origin. An alternative possibility is that sun may be some kind of giant dynamo, whose rotation, internal circulation and convection produce electric current. The magnetic field

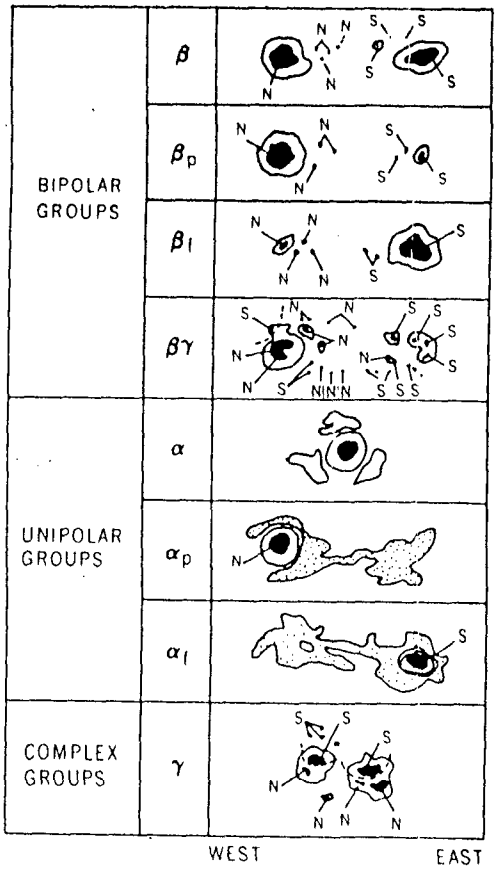

Fig. 2.13 Classification of sunspot groups.

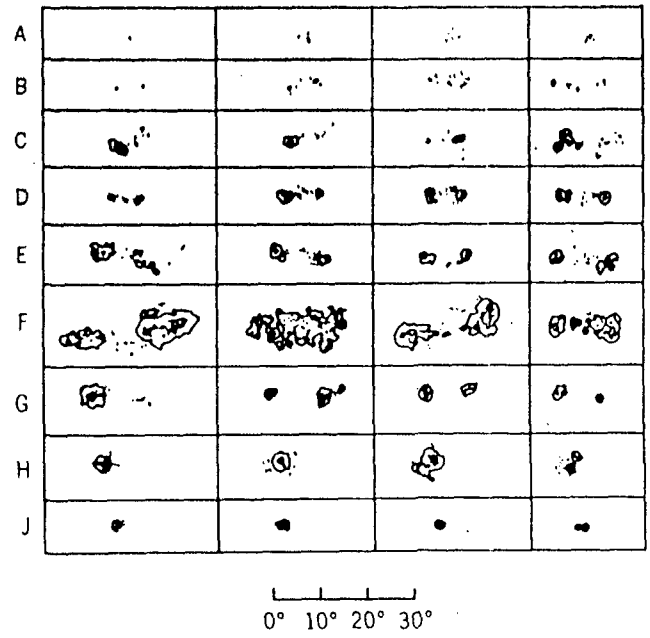

Fig.2.14 THE ZURICH CLASSIFICATION OF SUNSPOT GROUPS. FOUR EXAMPLES OF EACH CLASS ARE SHOWN. THE SCALE AT THE BOTTOM INDICATES DEGREE OF HELIOGRAPHIC LONGITUDE.

within the larger spots are about as strong as those we can readily produce with powerful electromagnet in terrestrial laboratories several thousands gauss. Smaller sunspots have weaker fields.

Hale discovered another very important property of magnetic field of sunspots. Spots tend to occur in pairs so called bipolar groups in terms of their magnetic properties. If the preceeding member of a pair (Western) is a magnetic north pole, the following (Eastern) member will be a south pole. Moreover, if this relation holds in the sun's northern hemisphere, the reverse will be true in the southern hemisphere where the preceeding spot will be a south pole and the following sopt a north pole. This type of association persists throughout one sunspot cycle. And then at the beginning of the next cycle polarities reverse in both hemisphere. Thus the length of true sunspot cycle is not eleven but 22-years (fig.2.15).

The presence of magnetic fields in sunspots raises the interesting question whether the sun itself possesses a general magnetic field. Early attempts to observe such a field gave some what inconclusive results. However the behaviour of Prominence and the structure of sun's corona so clearly suggest the presence of a magnetic field, that most astronomers believe that one must exist. But very sensitive methods were necessary for its detection.

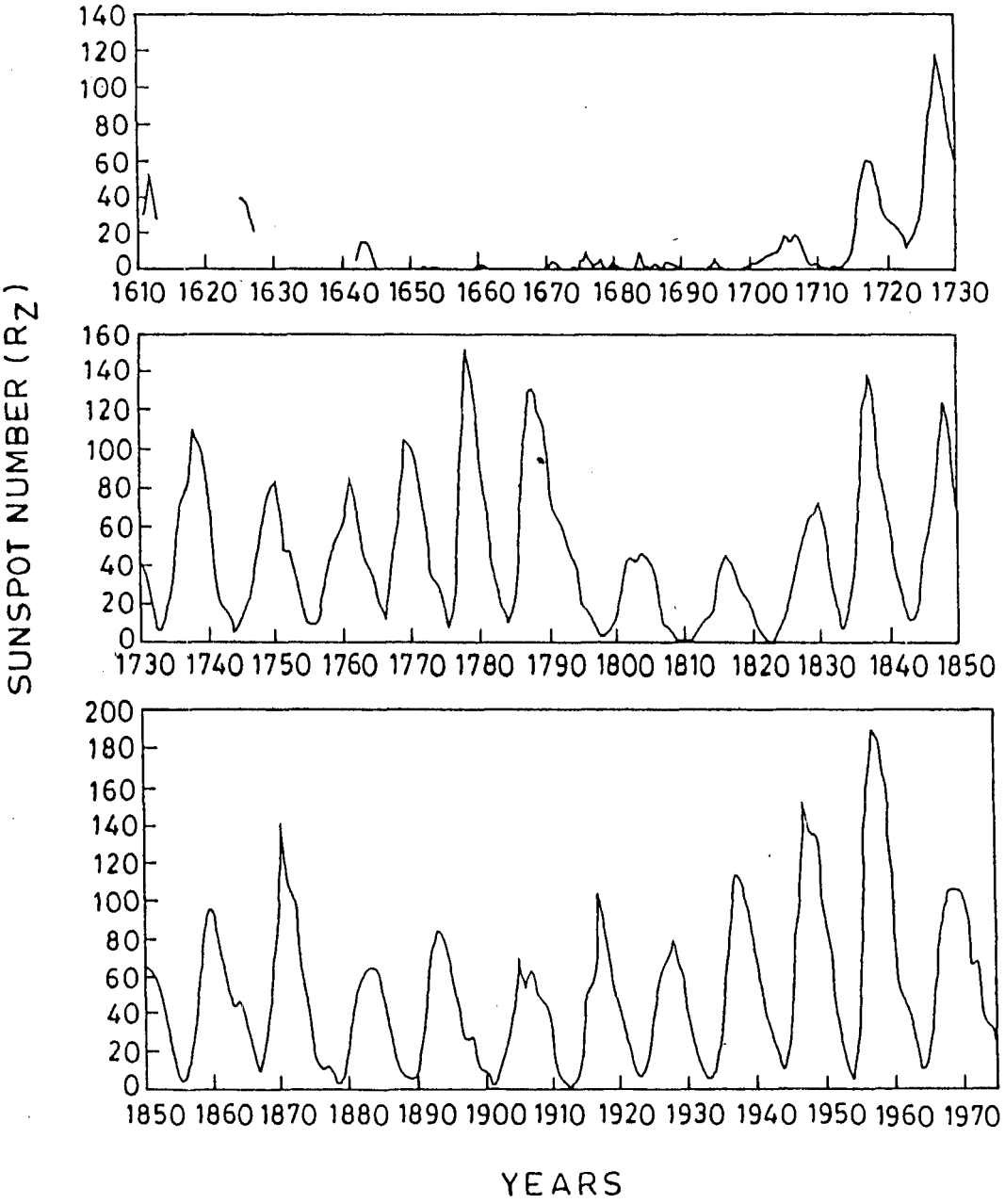

Fig. 2.15 Sunspot cycle.

The physical significance of sunspots has been a controversial topic ever since Galileo. Galileo suggested that spots were clouds in the solar atmosphere. Sir William Herschel thought that sunspots were holes in the fiery clouds through which one could see the cool, dark solid and presumably habitable surface beneath.

The most popular theory, regards the spots as great, vortical storms, like hurricanes or tornadoes. Such stroms derive their rotation from the large scale, horizontal flow of gas in to a region of low pressure.

Most distinctive features of spots result from the presence of powerful magnetic fields and associated electric currents. We can understand this in terms of an established principle of nature, that matter tends towards a position of equilibrium. Application of this principle to a sunspot shows that a static condition can occur only if both the temperature and pressure are low near the spot centre, where the magnetic field is strongest. However, it shows that a true static condition cannot persist, because heat will leak from the hot exterior in to the cool interior of the spot. As a result, gas will flow upward and outward along the magnetic lines of force. Expansion of the gas maintains the low temperature. The sunspot behaves as if it were a pump. The spot itself, apart from the gentle outward flow and occasional violent flares, is a quiet region compared with the simmering convection of the photosphere.

(b) The Sunspot Cycle

A typical sunspot comes and goes within a week, although some of the larger ones can last a month or more. It is recognized that the number of sunspot on the sun at any time did not remain the same from one year to the other but varied in some sort of cyclic pattern.

The relative sunspot number on solar disc changes from day to day and year to year. In order to express this relative number we consider the Wolf

$$R = K\ (10g + f\ )$$

Wolf number is used universally as an index of spot activity.

g = no. of sunspot groups

f = no. of individual sunspots.

R = Wolf number.

K = correction factor adjusted by Zurich observatory.

The yearly mean of the Wolf number shows a cyclic variation of about 11-year. This period is defined as solar cycle.

Sunspot cycle is not perfectly regular, successive maxima can be as close as 7.5 years and as far as 16 years apart.

At the minimum of the cycle there are only three or four spots seen on the entire solar disk sometimes none at all. At the maximum there can be 100 spots or more.

At the beginning of the cycle, the first spots start to

break out at latitudes approximately 40° from the solar equator. As these initial spots fade and die, they are replaced by newer and more numerous spots progressively lower latitudes, close to the equator. Maximum occurs about 4 year after the beginning of the cycle at which time most spots are concentrated about 15° from equator. The number of spots begins to decline there after but the equatorial migration continues. But the time that the last few spots vanishes, they have approached within 8° of the equator.

Sunspot usually appear in pairs with magnetic lines leaving one spot and entering another spot. Every one of the spots that is leading in the direction of solar rotaion in the northern hemisphere has the same polarity. A similar leading trailing pattern is also seen in the southern hemisphere but the polarity is reversed. When the spot cycle is repeated 11-years later, the same sort of pattern is exhibited, but polarity is reversed in both hemispheres. It is generally suspected that the differential rotation of the sun is responsible. Babcock Proposed a theory for solar cycle. Solar cycle is due to interaction of turbulent and highly conducting plasma in the hydrogen convection zone with force due to differential rotation of sun.

This differential rotation results a strong electrical current in the gaseous ions just below the surface, which in turn produce an intense subsurface magnetic field. As the

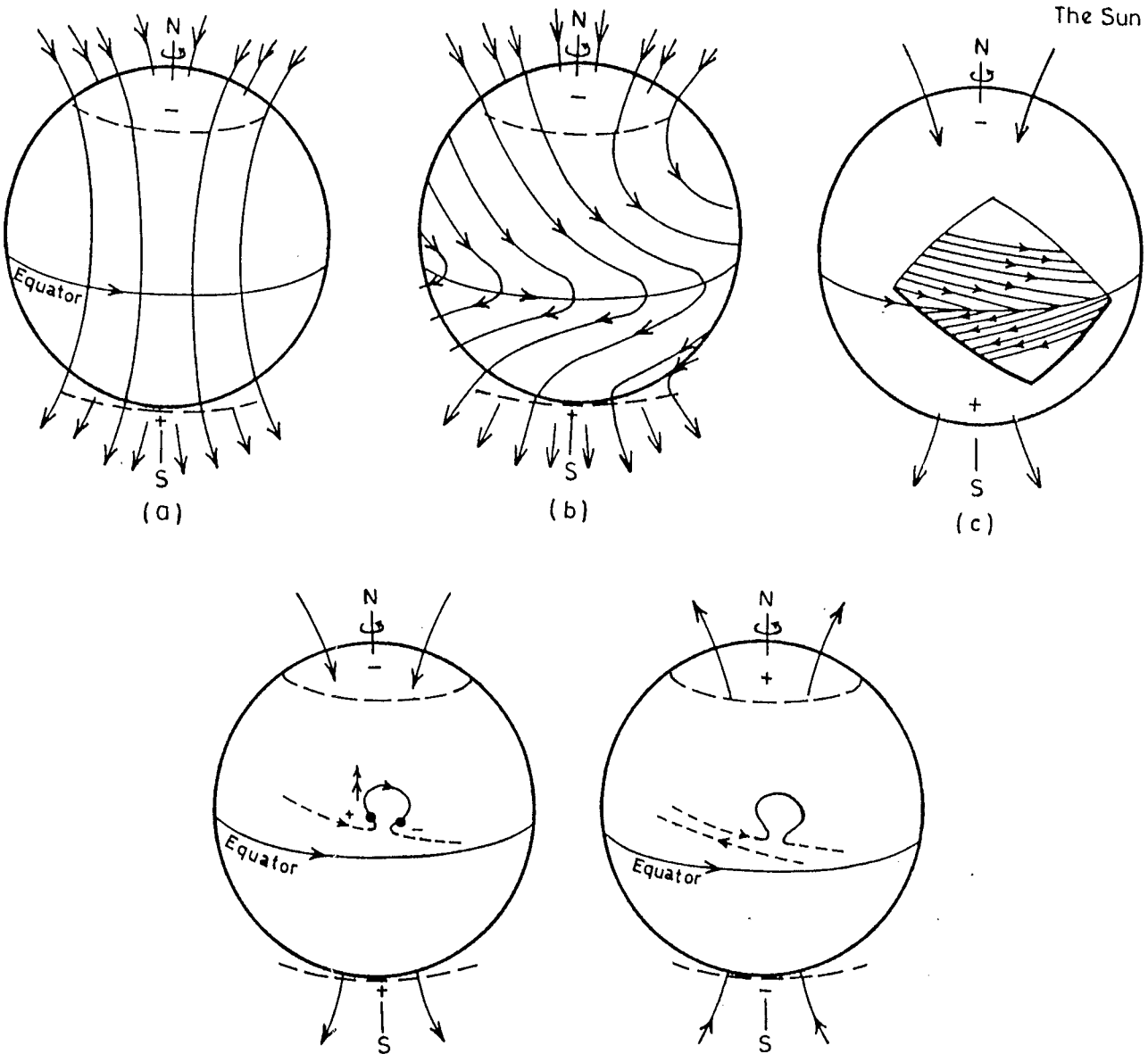

Fig. 2.16 Schematics of sunspot cycle.

differential rotation continues, the subsurface magnetic field becomes stronger and stronger and the field lines get tighter and tighter together. More and more rotational KE is converted in to magnetic energy. The build cannot continue for ever. Evantually the subsurface magnetic field become so strong that it bursts through the photosphere in isolated areas. The places where the interior solar magnetic field penetrate the photosphere seen as dark spots on the surface. The formation of sunspot releases the magnetic energy stored in the solar interior, leaving the sun free to begin another round of cycle (fig.2.16).

The sunspot cycles are associated with many cyclic phenomena occuring on the earth including the changes in our wheather and climate. A strong relationship is found between number of sunspots on sun and number of auroras. There is correlation between sunspots and occurance of violent magnetic stroms in earth's magnetic field. Variations of ozone concentration in earth's atmpsphere follows sunspot number. The state of earth's ionosphere is affected by solar activity.

The above correlations suggests that sunspot activity can be used to predict the changes in electrical, magnetic and meteorological environment to the earth.

Programmes at India: The importance of the research dealing with solar terrestrial physics has been recognized by the department of Science and Technology, Government of India.

At Indian Institute of Geomagnetism, Bombay, the research on solar terrestrial relationship forms an integral part of overall programme. At National Physical Laboratory New Delhi, the monitoring and prediction of the sunspot activity is being carried out for radio communication.

Sunspot and solar activity are being studied at Indian Institute of Astrophysics, Bengalore, solar observatery Udaipur, and in some other National Institutes and Universities in India.

Many research organizations in India are Planning to join an International Programme known as Solar Terrestial Energy Programme (STEP), which aims to study the transfer of energy from sun to the earth's atmosphere. This programme would last for five years from 1990 to 1995. At the end of the STEP we hope to have new and exciting information about sunspots and their effect on terrestrial phenomena.

(4) SOLAR FLARES

A chromospheric flare is a short lived sudden increase of intensity in the neighbourhood of sunspot. It is best observed in Hα . In some rare cases flares have been seen even in white light. A flare is a burst of light rather than a burst of matter. Flares generally tend to occur in active regions where the magnetic fields are strong complex and a highly stressed and unstable configuration. The number of

solar flare is larger during solar maximum as compared to that in solar minimum.

(a) Development of a flare

Occasionally a region near a sunspot suddenly becomes very much brighter than usual, such a region is called solar flare. During the period of high solar activity as many as 5 to 10 flares may be seen in one day. When a flare occur near the edge of a solar disc, it is a jet of gas rising upward several thousand kilometers with very high speed. The duration of the flare is very small often about an hour. In a few cases flare have been observed at a distance more than 10^5 km from a sunspot. A flare produce an emission spectrum of hydrogen, the arc spectrum of helium and the lines of singly ionized calcium and iron.

(b) Classification of flares

Flares are divided into different classes of importance $\bar{1}$, 1, 2, 3 3^+ according to area and brightness. The area is easier to measure because it does not change as rapidly as brightness. Solar flares smaller than the flare of importance 1 are often classified as importance $\bar{1}$. Since flares are not similar, we can't develop any relationship between them. The flare area is usually given in 10^{-6} parts of the solar disc. The importance of a flare being estimated by instance and from spectroscopical analysis in others. In the later case the flare size is determined through the width of the Hα line. In

case of an intense flare the line width can grow from 2A° at the start to 20A° at peak intensity. The manner of estimating importance is explained in the table 2.5.

Table 2.5

Classification of solar flares

Importance	Area in 10^{-6} of visible solar disc	Width of Hα Line in A°	Range of Duration(mts)
$\bar{1}$	<100	1.5	-
1	100-250	3	20
2	250 - 600	4.5	30
3	600 - 1200	8	60
3^+	>1200	15	180

Importance $\bar{1}$, 1 and 2 are very weak. These are small flares every day. But flares of importance 3 and 3^+ are very strong, rarely occur once in two years. Recently the importance of solar flares is further more classified into subclasses, in this classification flares of importance $\bar{1}$ and 3^+ are defined as those importance S and 4, 'S' stand for small solar flares. Importance of flares which produce solar cosmic rays of Bev energy is 3 or 3^+.

Solar falres have recently become of interest in other field than solar physics because of their dynamic effect upon earth's magnetic field, physical condition of its environment and life. The ionospheric layers of earth's atmosphere are altered by such an out burst and may fail to reflect radio

waves thereby causing communication blackout on the short wave radio waves. The blackout may last for few hours or upto few days. About a day after the occurance of a flare, the magnetic properties of earth are usually disturbed, causing the needle of a compass to react in very strange way.

(5) THE INTERPLANETARY MAGNETIC FIELD

The interplanetary magnetic field (IMF) is an integral part of solar wind and is generated out of photospheric field extended outward by the expansion of the plasma. Our knowledge of the large scale properties of IMF began with the work of Parker in 1958.

Parker (1958) showed that the conductivity of the matter in the corona is very high and heat flow is proportional to T^4, where T the temperature of the corona. From this mode he showed that the solar wind plasma freely expands continuously in the interplanetary space. Due to high conductivity IMF lines are frozen in to the solar wind plasma and they are constrained to move along with the moving plasma (Alfven 1950) and therefore they are stretched out in the form of an Archimedes Spiral by supersonic solar wind, as sun rotates. (Parker 1958, Ahluwalia and Dessler 1962). The angle Θ between the normal to the spiral field line and sun earth line, as shown in fig. 2.17 is given by

$$\Theta = \tan^{-1} (V_s/\omega r)$$

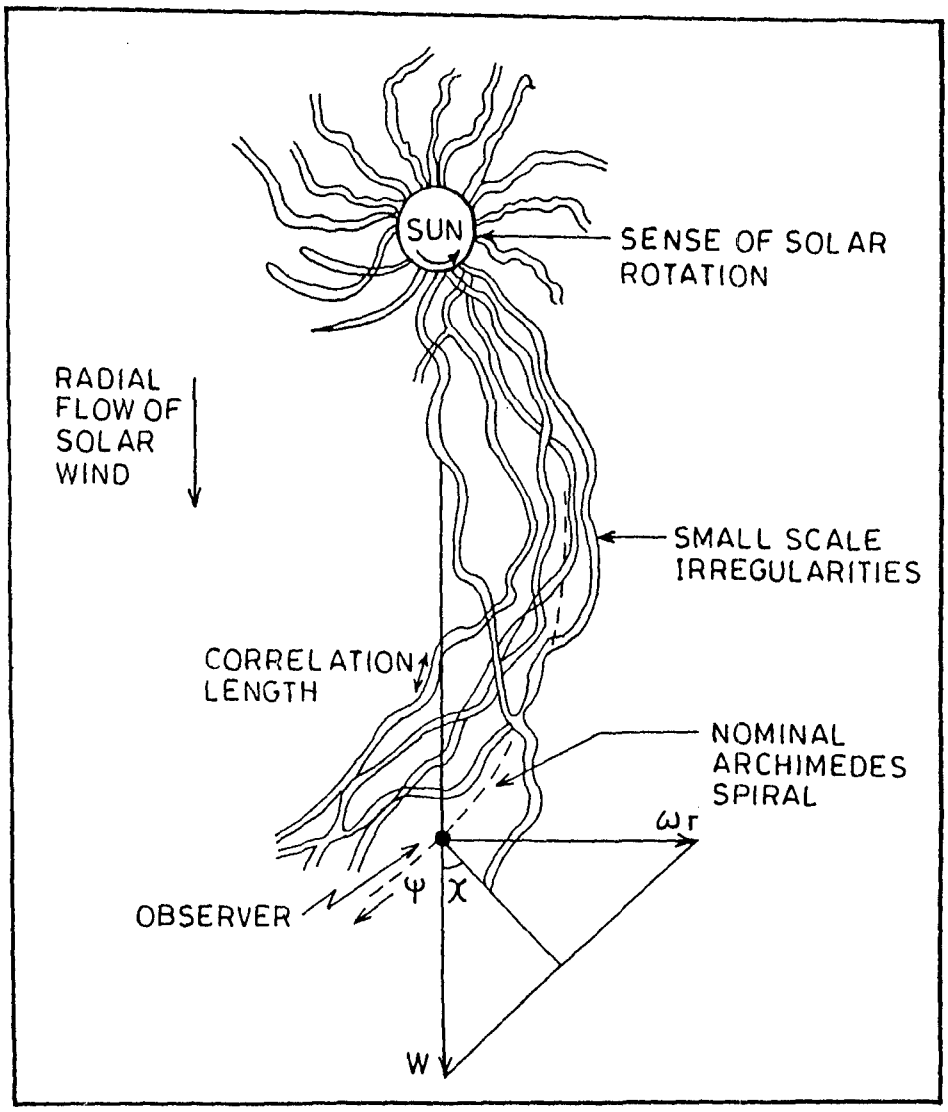

Fig. 2.17 The Archimedian spiral configuration of the interplanetary magnetic field.

V_s = Velocity of solar wind

ω = Angular velocity of rotation of sun

r = heliocentric distance from sun.
(sun-earth distance)

The angle Ψ ($i.e.\ \frac{\pi}{2} - \theta$) is referred to as the garden hose angle.

The recent measurements of IMF from a number of spacecraft have now conclusively proved that the large scale structure of the field is in very good agreement with the predicted Archimedian spiral configuration and is distributed in the form of a well defined sector structure with IMF being alternatively positive (away from sun) and negative (towards sun). This sector pattern which co-rotates with sun, is found to exist throughout the solar cycle. When solar activity is quiet the structure of interplanetary field is as shown in fig. 2.18 and consists of four sectors. This structure seems to vary with the phase of the solar activity cycle. In fact such a sector structure is clearly seen only during minimum phase of solar cycle. With the increase of solar activity the solar active regions begins to appear on the photosphere since these configuration of the solar magnetic field extending into the interplanetary space, it seems natural that a clearcut sector structure is not observable during the increasing and maximum phase of solar activity cycle. It seems that the origin of interplanetary sector structure is strongly connected with the development of active sunspot group on the sun.

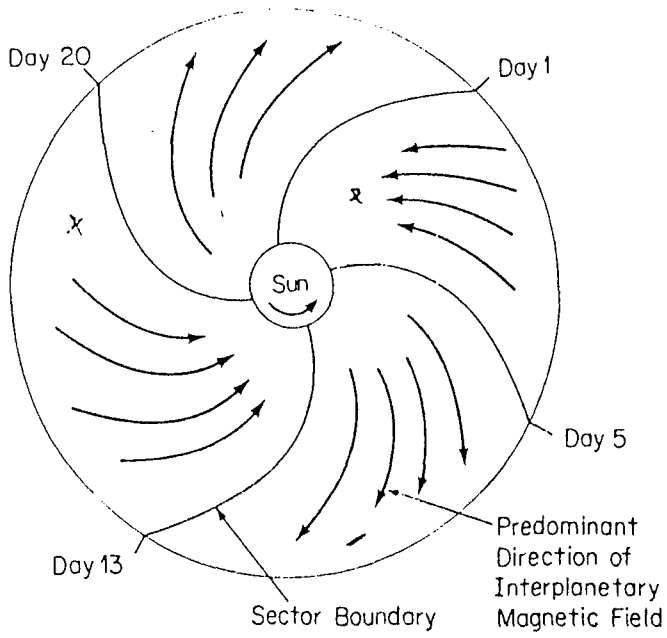

Fig. 2.18 The sector structure of interplanetary magnetic field.

An interplanetary magnetic field of an average value of 60 micro gauss was detected at 1AU with the field fluctuations between 20 and 400 micro gauss. Near the earth the magnetic field is found to be mostly in the ecliptic plane and the magnetic field spiral angle is found to be about 135° at the orbit of the earth.

The recent measurement obtained with instrument on Pioneer 10 and Pioneer 11 space crafts at the orbit of Jupiter have also confirmed the Archimedian spiral configuration of field even at a distance as large as 4.3 AU. Where the garden hose angle changes from 45° to 67°.

(6) RECENT IDEA OF HELIOSPHERE AND ITS BOUNDARY

The study of cosmicray variations in space and time has been an effective tool for probing the heliosphere. Both the ground-based as well as space craft observation of cosmic ray intensity over a long period and at varying distance have contributed to our knowledge of this region. We have now observations ranging from relatively near the sun up to $\sim$40AU and space craft V_1, V_2 and Pioneers P_{10} & P_{11} are continuously moving farther out towards the boundary of heliosphere.

The important question that require clear answer for physists is how far in to the interstellar medium does the solar influence extend?

Equivalently where does the heliospheric boundary lie? Current estimates puts this boundary at about 100-150 AU,

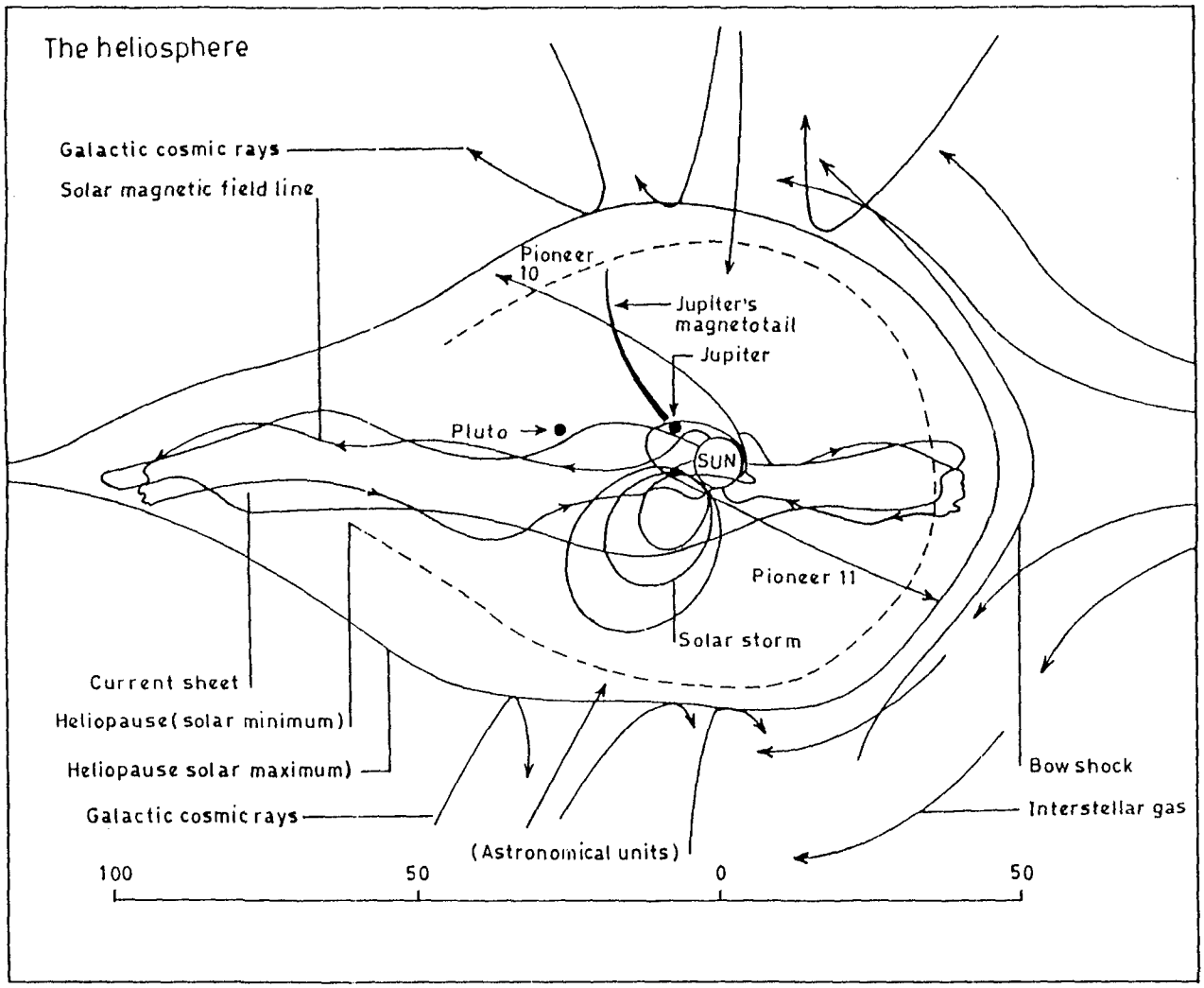

Fig. 2.19 A simple view of heliosphere.

infact, it could be much less than this.

The solar wind blows out beyond the orbit of Neptune, but evantually both the wind and interplanetary magnetic field are halted by the small pressure exerted by the interstellar gas and interstellar magnetic field. The boundary of the solar magnetic bubble is known as **helio-pause** and the region within which solar field dominates over interstellar field is the heliosphere. It is filled with fast and slow streams of solar wind, interacting violently to produce shocks and fast particles, and is swept constantly by blast waves from solar flares. Interaction of this plasma with planetary magnetospheres produces planetary magnetic storms and radiation belts and accelerate particle to high energy near the planets. The subject of intensive study through direct observations and theoretical modeling, the heliosphere also serves as a guide to the complex phenomena that must also occur near other stars, although they are too distant for their tenuous plasma envelopes to be observed.

The solar system moves through the interstellar gas at a speed of about 20 km/sec. So there is an interstellar wind apparently blowing fast the heliosphere and distorting it into a **tear-drop** shape. When the stellar wind meets the boundary of heliosphere a Bow shock is formed.

Since the heliosphere is **inflated** by the solar wind and the wind strength varies with solar cycle, the heliosphere is

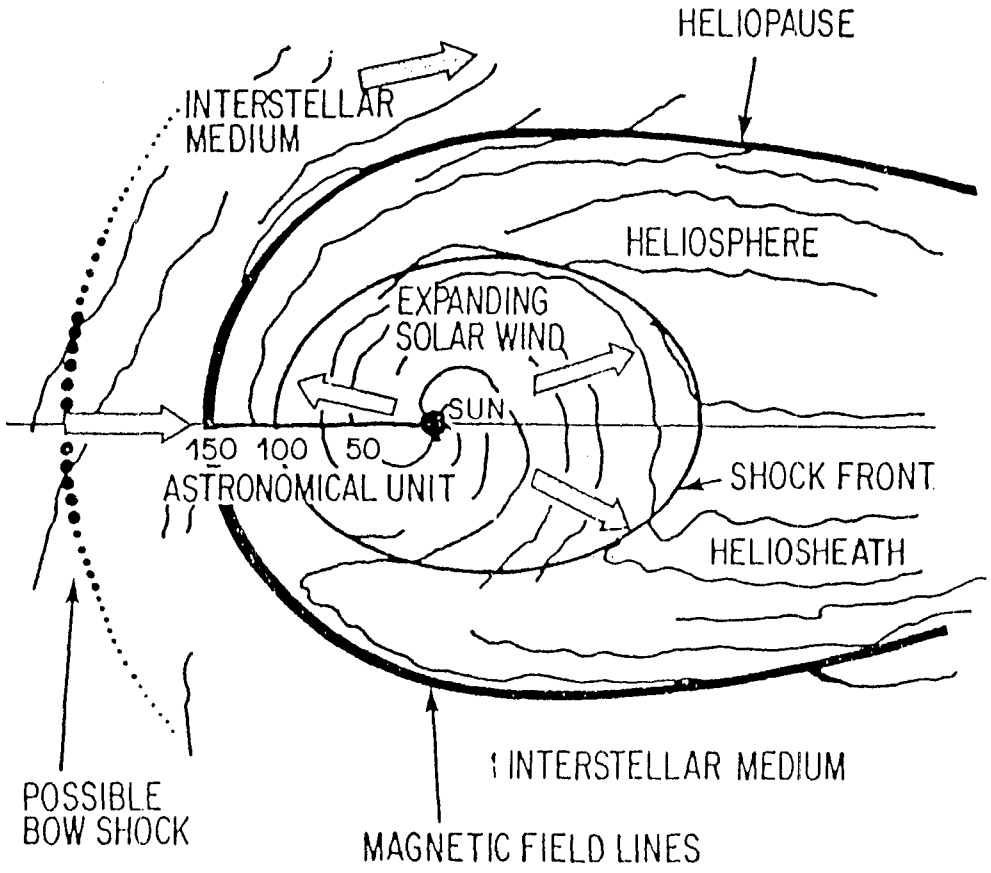

Fig. 2.20 A schematic view of heliosphere and its interaction with local interstellar medium.

believed to be expandedand contracted with solar cycle and to Wobble in extent as a result of individual major solar storms.

A schematic view of heliosphere and its interaction with local interstellar medium is shown in fig.2.20. The continuous out flow of solar wind at supersonic speed becomes subsonic outside the heliosphere. Within the region of shock front, the magnetic field is spiral and plasma flow is radial, while out side the shock front the magnetic field is likely to be disordered and plasma flow turbulent. Some features, such as the bow shock, shock front, heliosheath and heliopause, are reminiscent of the terrestrial magnetosphere, with which we are familiar. The spiral magneic field, (the so called Archimedean spiral), the continuously expanding supersonic solar wind, and subsequent turbulent flow are all features that have come to be identified with the region.

****

References

1. Axford, W.I. (1968) Space Science Revs. **8** 331.
2. Burlaga, L.F. (1971 a) Space Science Rev. **12** 600.
3. Alfven, H. (1954) Tellus **6** 232.
4. Coles, W.A., Rickett, B.J. and Rumsey, V.H. (1974) Solar wind Three, Ed. C.T. Russel, Unive of Califor.
5. Demison, P.A. and Hewish, A. (1967) Nature **213** 343.
6. Dessler, A.J. (1967) Rev. Geophy **5** 1.
7. Gosling, J. T., Hundhaussen, A.J. and Bame, S.J. (1976) J. Geophy Res. **81** 5061.
8. Handhaussen, A.J. (1970) Rev. Geophy. Space Phys. **8** 729.
9. Intriligator, D.S. (1975) 14th ICRC **3** 1033.
10. Krieger, A.S. et. al. (1973) Solar Phys. **29** 505.
11. Newkirk, G.A. (1961) Ap. J. **133** 983.
12. Leighton, R.B., Noyes, R.W and Simon, G.W. (1962) Ap. J. **135** 474.
13. Parker, E.N. (1965) Planet Spac. Sci. **13** 9.
14. Parker, E.N. (1969) Space Sci. Rev. **9** 325.
15. Parker, E.N. (1971) Astrophy J. **164** 491.
16. Sheeley, N.R. and Bhatnagar (1971) Solar Phy **18** 195.
17. Synder, C.W. and Rao, U.R. (1963) J. Geophys. Res. **68** 6361.

CHAPTER 3

COSMIC RAY INTENSITY VARIATIONS IN THE 3-DIMENSIONAL HELIOSPHERE

(1) INTRODUCTION

The discovery of cosmic rays about 80 years ago, opened up a new window for astrophysics and added an additional dimension to our study of interplanetary space. The observations of cosmic ray using ground based instruments, over long periods of time and at several location was under taken by compton (1935) and Forbush (1957). They used the ion chambers, which detected the secondary radiation produced in the earth's atmosphere by the primary cosmic radiation incident at the top of the earth's atmosphere. It was observed by Forbush that the intensity of radiation varies with time at each location. More recently the variations of cosmic rays has been studied using Neutron monitors at sea level and at mountain altitudes (Dorman 1963). These neutron monitors again detect the secondary radiation produced in the atmosphere by primary radiation, consequently neutron monitors do not respond to primary particle, with energy of a few hundred Mev or less. Instruments borne on balloons and satellite, are therefore being used to detect directly the low energy radiation and determine their secular variation (Webber 1967). The above detectors have shown the existance of several types of variation of primary radiations.

It is generally accepted that the cosmic ray intensity is isotropic and of galactic origin, with the sun emitting cosmic ray particles only occasionally. The sun and the

interplanetary medium exert a profound influence on the cosmic radiation. It causes them to undergo deviation from isotropy and change of spectrum as well as of intensity. From the observed variations of cosmic ray secondaries using geomagnetic effect (Mc cracken et al. 1965) and of the transition effect in the atmosphere (Dorman 1957) the primary cosmic ray variations have been extensively studied.

The important variations can be broadly categorised in to two classes.

(A) Isotropic and time dependent variations.

This class includes the following types of variations:

1. The 11-year variation
2. The 27-day variation.
3. Solar flare increase
4. Forbush decrease

(B) The anisotropic (or spatial) variations

It includes:

1. Solar diurnal variation.
2. Semi-diurnal variation.
3. Large anisotropies associated with solar flare increases
4. Large anisotropies associated with Forbush decrease.

The above variations are customarily divided into two categories:

1. Periodic variations.
2. Non-periodic variations.

Diurnal and semi-diurnal, 27-day and 11-year variations are periodic variations. While solar flare increase and forbush decrease are non-periodic variations.

(2) 11-YEAR VARIATIONS

It is seen that cosmic ray flux is modulated by the 11-year solar cycle of sunspot activity reaching a maximum during the quite period of solar cycle and a minimum near the peak of solar activity, thus establishing an inverse relationship between the solar activity and the galactic cosmic ray intensity (Forbush 1954, Pomerantz 1958).

The solar events pull more and more of solar magnetic field in to the interplanetary space, during the period of solar cycle. This prevent the entrance of galactic cosmic rays. Results from a large amount of data concerning the rigidity dependance of the long term modulation, indicate that the low energy component of cosmic rays shows the highest solar cycle modulaion, while particles with rigidities higher than 15 GV seen to remain relatively unaffected.

Various theoretical models have been proposed for explanation of the 11-year variation of galactic cosmic ray intensity.

Parker (1958) suggested that the interplanetary magnetic field frozen in to solar wind will tend to convect the cosmic ray particles radially outward at solar wind

velocity and establishes a positive radial density gradient. Due to the positive density gradient, cosmic ray particles always diffuse into the solar system through interplanetary magnetic field and diffusion attains a steady state when the outward convection of the particle is balanced by inward diffusion. This concept now known as **convection-diffusion process** was first proposed by Morrison (1956). In a steady state condition assuming the spherical symmetry, this model qualitatively explains the eleven-years solar cycle variation.

Using spectrum measurement of proton, helium and electron, it has been found that the convection diffusion theory is successful in explaining the experimental observation of particles of energy $\geq$ 100 Mev.

Webber and Lockwood (1981) had studied the long term variation of cosmic ray with energies > 60 Mev during 1972-1980 and from 1AU out to 23 AU using the observations from IMP 7 and 8, Voyagers 1 and 2 and Pioneers 10 and 11. Their observations also reveal that the long term modulation effects are propagate radially outwards from the sun with a typical speed of $\sim$350-500 km/sec. Lockwood and Webber (1984) further stressed the need for time dependent solutions to transport equations describing the solar cycle cosmic ray modulation.

Fillus and Axford (1985) used P_{10}, P_{11} (E>500 Mev/nucl:)

measurements and those of Earth-based neutron monitor to study the spatial and temporal modulations of cosmic rays. They observed that in the outer heliosphere near the ecliptic plane, modulation appeared to be the sum of many events of different magnitudes propagating outward at approximately the solar wind speed. Perko and Fisk (1983) presented a time dependent model of cosmic ray modulation. The cosmic ray variation was assumed to result from changes in the number of enhanced cosmic ray scattering regions which resulted from flare generated shock waves in the solar wind. This model was later applied by Perko (1987) to demonstrate the various feature of modulation at large distance in the heliosphere.

Effects of fields and flows observed in the inner and outer heliosphere had been extensively studied by Burlaga et al. (1984, 1985, 1986 a,b, 1987) and Perko and Burlaga (1987). Near earth regions of enhanced magnetic field observed were classified by Burlaga and King (1979) as post shock flows, corotating interaction regions and cold magnetic enhancements, collectively called interaction regions. Isolated interaction regions could grow in size and amplitude with increasing distance, neighbouring interaction regions could coalesce to form large merged interaction regions (Burlaga 1983). Thus with increasing radial distance from the sun, merged interaction regions become more dominant features. The fig.3.1 shows that the innerheliosphere is dominated by

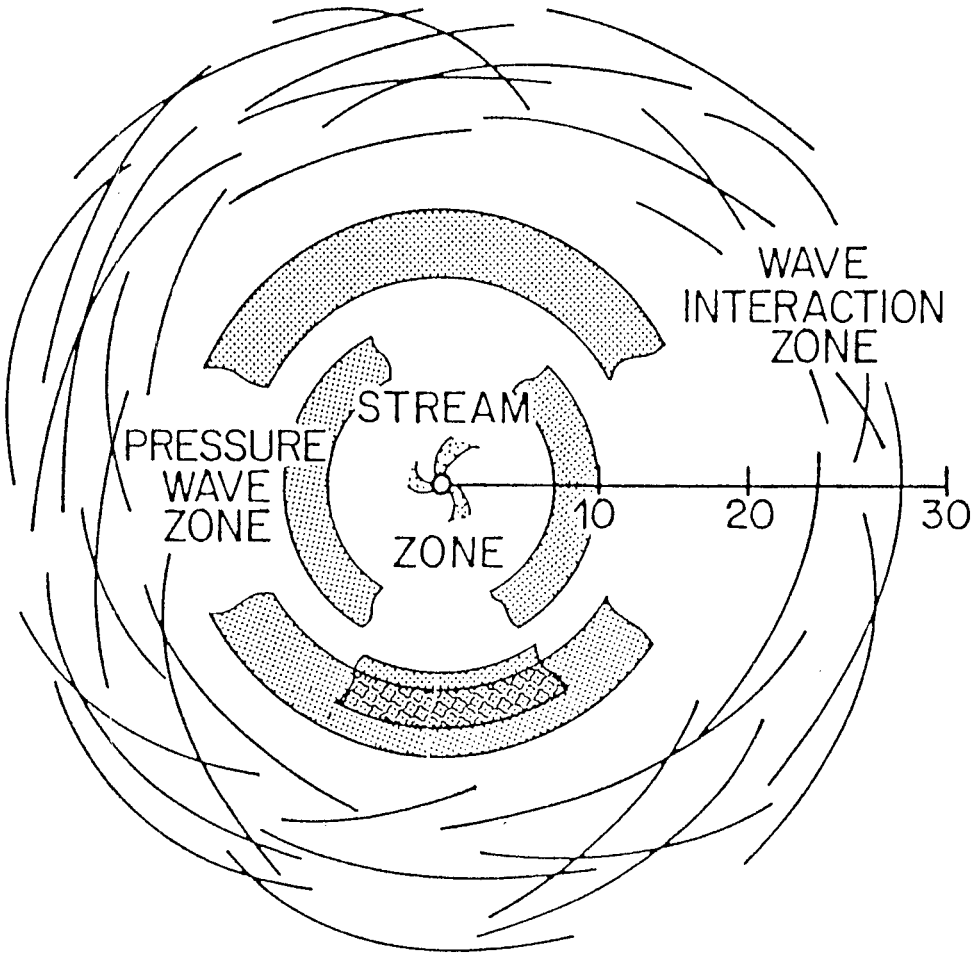

Fig. 3.1 Transition from an individual stream dominated zone close to the sun to a region of concentric shells where pressure waves dominate the structure and finally, a wave interaction region.

individual streams associated with specific solar sources. As these streams move away, they coalesce and modify the characteristics and at a large distance they appear to be radially propagating concentric shells of compressed magnetic field and enhanced fluctuations.

(a) The ~22 Year Variation

In addition to the ~11 year solar cycle periodicity in cosmic ray intensity, a ~ 22 year solar magnetic cycle periodicity has also been observed. Recent studies have specifically dealt with this modulation of cosmic rays.

Nagashima and Morishita (1980 b) using the ground based data covering four solarcycle refer to the modulation consisting of two discrete state which corresponds to the polarity of the solar polar magnetic field with respect to the galactic magnetic field when this field is aligned nearly parallel to the galactic one,the entry of cosmic rays into the heliosphere is facilitated along the magnetic lines of force in comparison to when the two fields are anti-parallel.

Jokipii and Thomas (1981), in their quantitative analysis of ~22 year cosmic ray variation the heliosphere current sheet plays an important role. Drift models predict two different paths during both halves of the 22 year solar magnetic cycle. Positive nuclei enter the heliosphere preferentially along the heliospheric current sheet when the northern solar polar magnetic field is negative and through

the polar regions during the rest of the cycle (when the northern solar polar field is positive).

The study of Webber and Lockwood (1988) with the neutron monitor data over epoch 1952-1987 illustrates the importance of the $\sim$22 year cycle in addition the well known 11 year cycle. Systematic difference in the overall shape, of successive $\sim$ 11 year cycle, and similarities on those of alternate cycles are indicative of the $\sim$22 year magnetic cycle. A sharpened peaked intensity maximum in 1987 is similar to that observed 22 years earlier in 1965 in contrast to the flatter maximum observed between 1972-1977 and 1952-1954. Also neutron monitor intensity is $\sim$1.5% higher in 1987 maximum and in 1965 in comparison to the maximum in 1972-1977 epoch. These results are consistent with the predictions of the drift model with an equatorial heliospheric current sheet.

(3) THE SOLAR DAILY VARIATIONS

Daily variations in cosmic ray intensity arises from spatial anisotropies in interplanetaryspace. These are recorded by ground-based detectors once every day as their asymptotic cones of acceptance sweep through the directions containing the spatial anisotropy. The asymptotic cone of acceptance of a detector is the solid angle that contains all the asymptotic direction of approach of particle, of various

energies which make a significant contribution to the counting rate of the detector. Comprehensive reviews on the subject has been provided by Pomerantz and Duggal (1971) Rao (1972) and Ahluwalia (1976). In addition to the prominent diurnal component, the daily variation is composed of at least two more contributions of lesser amplitudes i.e. semi-diurnal and tri-diurnal component.

Practically all the experimental studies of solar daily variation have been carried out with Earth-based detectors responding to particles of varying energies. In general two techniques have been involved: the Fourier analysis and the power spectral method. Most of the qualitative information on cosmic ray daily variation obtained through the study of diurnal (first harmonics) and semi-diurnal (second harmonic) component derived from a Fourier analysis of CR intensity observed over a period of 24 hours (i.e. 1 day).

A study of daily variation in terms of Fourier components (various harmonics) revealed the following characteristics.

1. The first harmonic is the most prominent and has an hour of maximum in the afternoon and an hour of minimum in the early morning with somewhat lesser amplitude in quiet sun period, compared to active or disturbed sun period.

2. The second harmonic is smaller in magnitude but not negligible. During high solar activity, the phase is not well defined, however, during the quiet sun period the hour of maximum lies from 0 to 3 hours local time and the hour of minimum lies at about 6 to 9 hours local time.

3. The third harmonic is still smaller but not negligible. The amplitude and phase of this harmonic component have not been yet well defined.

(a) Characteristics of Diurnal Variations

From an extensive analysis of ground based neutron monitor data, from a large number of stations during (1954-65) Rao et al. (1963) and Mc Cacken and Rao (1965) have demonstrated that the yearly average diurnal variation observed at relativistic energies (≥1 Gev) can be expressed by a spectrum of the type.

$$\delta J(R)/J(R) = AR^{-\beta} \text{ Cos } (\Psi - \Psi_o) \text{ Cos } \Lambda$$

$$\text{for } R<R_{max}$$

$$= 0, \text{ for } R>R_{max}$$

where A and Ψ_o are the amplitude and space direction of the maximum amplitude, and R and Cos Λ are the rigidity spectrum and latitude dependence of diurnal anisotropy R is rigidity in Gv. Λ is the declination and R_{max} is the upper cutoff rigidity beyond which the diurnal anisotropy does not exist and Ψ_o are space directions measured east of the sun earth line. They

summarised that the average diurnal anisotropy has following characteristics.

(a) Rigidity independent (β = 0) in the rigidity range 1-100 Gv.

(b) Varies as cosine of declination.

(c) Amplitude of the anisotropy$\sim$0.38 $\pm$ 0.2%

(d) A maximum flux is incident from 89°$\pm$1.6° east of the sun earth line.

Pomerantz and Duggal (1971) have also summarised the average characteristics of diurnal anisotropy from the results of number of investigators, that over the range from a few Gv to about 100 Gv of rigidity, the anisotropy is essentially independent of the rigidity, the direction of the maximum amplitude lies within 15° and 90° east of the sun-earth line and space amplitude varies from 0.3% to 0.5%.

From a rigorous analysis of ion chamber and meson monitor data, Forbush (1967, 1969), showed that the average diurnal variaion is composed of two distinct components W and V, the component W has its maximum or minimum in the direction 128° east of the sun-earth line, which is roughly the average IPMF direction and varies sinusoidally with a periodicity of 20 years and passes through its zero amplitude when the sun's polar magnetic field is reversed (Forbush 1973). The other component V has its maximum along 90° east of sun-earth line and varies with solar activity shows a solar cycle dependence.

Both long term and short term changes occur in the diurnal variation. The amplitude and phase of the diurnal anisotropy change with a period of one or two solar cycles (Pomerantz and Duggal 1971, Rao 1972, Agarwal and Singh 1975, Kumar 1978, Yadav 1992 and Sharma 1992).

Long-term variations of the cosmic ray diurnal anisotropy have been examined using neutron and muon monitor data for all days (Ahluwalia and Riker 1981, Pathak and Agrawal 1987) and for only geomagnetically quiet days in a year (Kumar et al. 1981, 1985, Badruddin et al. 1985 b).

It is plausible that the total diurnal anisotropy consists of two modulation component, one related to the ~22 year solar magnetic cycle and the other to an ~11 year solar activity cycle (Agrawal 1983).

Kumar Santosh studied the nature of diurnal variation of cosmic ray intensity on quiet disturbed and magnetic storm days in the period of maximum solar activity, period of minimum solar activity and transition period of solar activity. Based on his study he conclude that during the period of maximum solar activity.

1. The diurnal amplitude on magnetically disturbed days (A_d^D) as well as on days of magnetic storm (A_m^D) is larger than that of the magnetically quiet days (A_q^D) at all different latitudes.

2. During the period of minimum solar activity the amplitude

of the diurnal component is almost the same on magnetically quiet, disturbed days and of magnetic storms. Such a behaviour is observed at all the latitudes.

3. During the transition period the amplitude of diurnal variation does not show any systematic relationship on quiet and distrubed days as well as on days of magnetic storms.

The phase of the diurnal component on magnetically disturbed days and days of magnetic storms is earlier than that of the quiet days.

Yadav and Badruddin (1983) and Ahluwalia and Riker (1985) have divided the epochs of solar activity cycle 21 in to two groups corresponding to the polarity of solar polar magnetic field and obtained the average diurnal vectors: this vector during the 1970's (1972-76) was found to have shifted to earlier hours in comparison to the average vector during the 1960's (1964-68), when the northern polar field was directed inwards.

Yadav R.S. and Sharma N.K. (1992) of A.M.U., India, studied the solar diurnal variation during the periods of different polarities of the solar polar magnetic field.Using the neutron monitor data of Deep River (R_c-1.02 Gv) the behaviour of the solar diurnal anisotropy of galactic cosmic radiation, on quiet days and distrubed days has been investigated for three different periods; 1964-68 ($\pm$) when the

northern solar polar magnetic field was negative, 1972-79 (±) when it becomes positive and 1981-86 (±) when again the northern solar polar magnetic field becomes negative. It is found that the diurnal phase of the diurnal anisotropy shifts to earlier hours during the period 1972-79 (±) as compared to the period 1964-68 (±) and in 1981-86 (±) it again tends to shift towards the earlier position observed in 1964-68 (±). This shows 22 year periodicity in the phase of the diurnal anisotropy related with the 22-year solar magnetic cycle.

27-Day Variations in Diurnal Anisotropy: The 27-day variation of the cosmic ray anisotropy has been known for a long time. However, with the availability of high-resolution interplanetary plasma and field data for long periods, its relationship with these parameters have been studied. In such studies power spectral analysis has been frequently used.

Duggal et al. (1979) using neutron monitor data for the epoch 1967-74, have calculated the power spectra of the component of the solar daily vector both parallel and perpendicular to the garden - hose direction. They found significant peaks at period length of 27, 14, 9 and 7 days in the power spectrum of the component of the solar diurnal vector perpendicular to the garden-hose direction which shows in fig.3.2. Thus they observed that 27-day variation is maximum for the component of the diurnal anisotropy perpendicular to the IMF rather than that parallel to it.

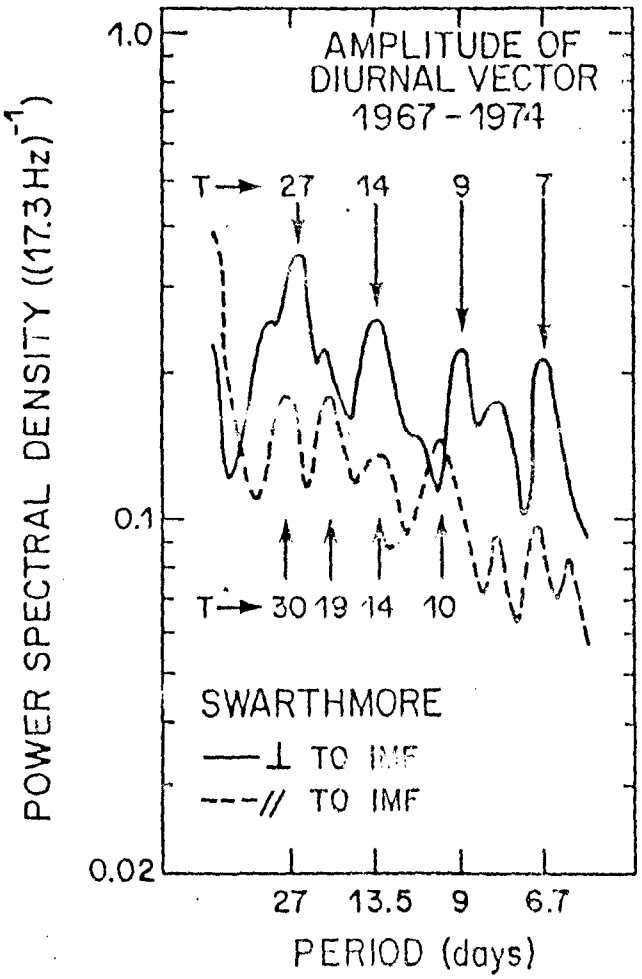

Fig. 3.2 Power spectral density of the amplitude of diurnal vector in the directions parallel and perpendicular to the IMF

Transient Variations in the Diurnal Anisotropy: Iucci et al. (1981,983) have studied the changes observed in amplitude and phase of the diurnal anisotropy during different portions of high speed solar wind streams. Amplitude was found to be larger than normal during the initial part of fast stream and less than normal during the declining phase of it, and then phase was almost constant at $\sim$18 hours.

Munakata et al. (1987) have also studied the characteristics of solar diurnal anisotropy in high speed solar wind streams originating from polar coronal holes using neutron monitor data for 17 stations and muon telescope data from 17 directions. They found that the amplitude of the diurnal anisotropy depends on the location of coronal holes (and hence IMF source) in constantly solar wind stream.

Short term variations in cosmic ray diurnal anisotropy have also been observed in association with transient disturbance from the sun e.g. interplanetary shock waves.

Yadav et al. (1987) have studied the dirunal amplitude and phase during the three classes of interplanetary magnetic clouds i.e., those stream interface and cold magnetic enhancements. It has been observed that the amplitude of the diurnal anisotropy is significantly larger during all the three types of clouds in comparison to the amplitude observed on geomagnetically quiet days. The time of

maximum has also been observed to be shifted to earlier hours during these clouds in comparison to the phase on geomagnetically quiet days. It has been further observed that among the three different types of clouds, the diurnal amplitude is larger during shock associated clouds than the interaction region and the cold magnetic enhancement associated clouds.

(b) Explanation of Diurnal Variation

Ahluwalia and Dessler (1962) gave a theory for durnal variations, according to which the spiral nature of IMF gives an electric drift resulting into a net streaming perpendicular to gardenhose angle. Stern (1964) showed that such a streaming would be exactly neutralised by an equal and opposite streaming due to the density gradients.

Parker (1964) Suggested that if there were irregularities in the IMF beyond the earth's orbit, the density gradient would be mostly wiped out and a streaming could be obtained due to corotation of cosmic rays with the sun.

Axford (1965) treated the problem by assuming general irregularities superimposed on the average pattern of IMF and showed that the streaming of cosmic ray by these modes lead to a corotation with the sun. Both these models lead to a daily variation of a amplitude $\pm$ 0.4% with an hour of maximum in the 18 hours direction. This is in agreement with the average

pattern of experimentally observed daily variation, but certainly not with its large day to day fluctuations.

Rao et al. (1972) and Hashim et al. (1972) demonstrated that average diurnal anisotropy can infact, be explained completely in terms of simple convection and diffusion. The radial convective flow will be balanced bythe inward diffusion causing net radial current to be zero and resulting a corotational anisotropy of the right magnitude. On a day to day basis, the two vectors need not necessarily balance each other resulting in varying amplitude and times of maximum for the observed diurnal anisotropy. It is seen that there are continuous days on which diurnal anisotropy is characterised by very large amplitude or by very small amplitude, some of which have recurring tendancy with 27-days periodicity.

(c) Characteristics of Semi-Diurnal Variation

The higher harmonics of daily variation with periods of 12, 8 and 6 hours (semi-diurnal, tri-diurnal and quart-diurnal) have also been investigated. The existence of at least the second and the third harmonics has been confirmed fig.3.3. The existence of semi-diurnal component has been suggested long ago and studied since then.

The long term variation in the amplitude and phase of semi-diurnal anisotropy has been studied for the epochs 1964-76 (Kumar et al. 1981), 1968-1979 (Agrawal et al. 1983)

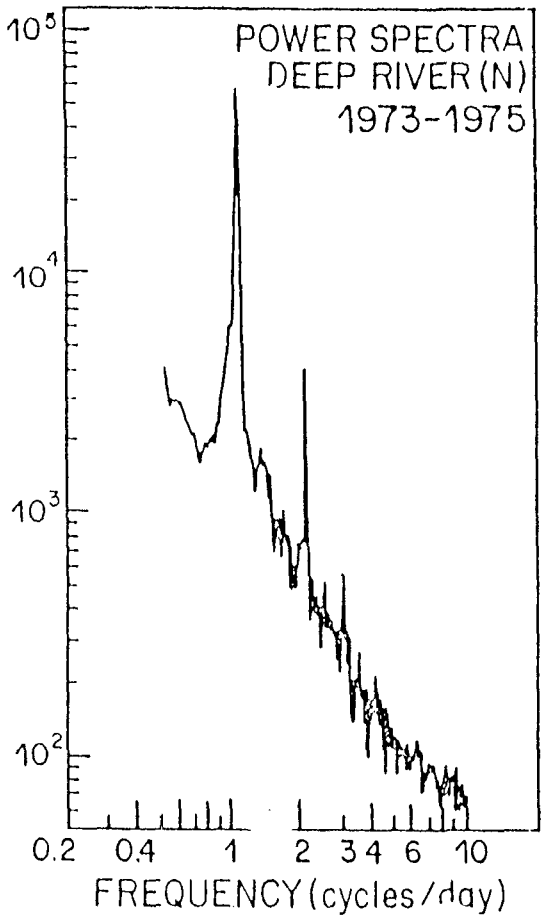

Fig. 3.3 Power spectrel results of Deep River neutron monitor. The peaks at diurnal, semi-diurnal and tri-diurnal are significant.

and 1968-1984 (Pathak and Agrawal 1987). All the three studies have found an increase in amplitude of the anisotropy during the years 1973-1974, when high speed streams were frequent, the phase remained almost constant throughout the epoch of study.

However, due to presence of large amplitude of semi-diurnal pressure wave, which can introduce a pressure induced variation and the poor statistical accuracy due to low counting rate of monitors, the existance of semi-diurnal variation of cosmic rays could not be firmly established.

The average characteristics of the semi-diurnal variation can be represented by the equation given below:

$$\delta J(R)/J(R) = A\, g(\Lambda)\, R^{\beta}, \text{ for } R<R_{max}.$$
$$= 0, \text{ for } R>R_{max}$$

Where $g(\Lambda)$ describes the dependence of anisotropy on declination and R shows the dependence of anisotropy on rigidity. The value of β for each year during 1958-1968 has been estimated $\sim 1.0\pm0.2$ and $g(\Lambda) = \mathrm{Cos}^{2}\Lambda$. The mean semi-diurnal phase for the period 1958-1968 has been observed almost constant, the maximum flux coming from the direction 132+6° west (3.2±0.04 hours) of earth sun line. The maximum cutoff rigidity upto which semi-diurnal variation exists, has not been estimated unambiguously, though R_{max} = 100 Gv may be the best choice.

(4) SOLAR FLARE INCREASES

The most striking feature of the cosmic ray intensity variations are the large transient increases of cosmic ray intensity in a few minutes ofter a visual flare on the solar disk. During solar flare sun produces large number of particles quite frequently in energy range 100-500 Mev, less frequently upto 10 Gev and on rare occasion upto 50 Gev which can be recorded by ground based detectors.

Although the flare effects display varying characteristics however, it is possible to form a rough picture of normal event in which intensity increase starts suddenly and reaches a maximum in a very short time of about 20 minutes. After maximum the intensity decreases, at first slowly, during half an hour or slightly more, then the slope becomes steep for some hours during this period. The recovery to constant level can take more than 24 hours in some prominent cases. The amplitude of increase very much depends upon the location and the type of detector. The neutron monitor located at high latitudes shows an increase of 25 to 150 times of normal intensity, whereas the meson detectors, located near equator, give an increase only a few percent of the normal intensity. The time scales of increase are different for particles of different energies, the low energy particles take longer time to attain peak of intensity.

Very little is known concerning the rigidity spectrum of solar flare effect particle. Many of the flare effects are recorded by neutron monitors but not by meson telescopes or ionization chambers, which reveals that the solar flare effect particles belong to the low rigidity part of the spectrum. The direction in which the particles arrive first is not from the direction of the sun, but from a direction west of the sun earth line making an angle of about 45°. After this initial anisotropy which persists for few minutes, isotropy is attained as the particles seem to arrive from all directions. Recent satellite measurements however, indicate that anisotropy may persists for long times for particles with energy of a few Mev. The increase in the intensity of low energy paricles in the interplanetary space has revealed that the exponent of the rigidity spectrum is higher than that for galactic particles. The event of Feb. 23, 1956 displayed an increase even at Huancayo and Kodaikanal where the cutoff rigidities are 15 and 17.5 Gv. This event was also recorded by ionization chambers and meson telescopes. It predicts that the part of particles responsible for Feb. 23, 1956 event must have rigidities of 25 Gv or more.Studies of these event, have revealed that the diffusion mechanism plays an important role in the transport of the particles from the sun to the earth, thereby providing the nature of IMF and their fluctuation in space and time.

(5) FORBUSH DECREASES

A Forbush decrease is recognized as a rapid decrease in cosmic ray intensity, followed by a more gradual recovery lasting several days. Two class of FD events which different characteristics have been indentified, recurrent (27-day period) and non-recurrent. The classical (generally non-recurrent) Forbush decreases associated with transients on the sun and the generally recurrent decreases associated with corotating solar wind high speed streams from coronal holes. Venkatesan et al. 1982, Shah et al. 1978).

Corotating Forbush decrease are similar to Forbush decrease, but they differ in that

1. The intensity drops more slowly, the time of decrease being nearly as long as recovery time.
2. Corotating Forbush decrease quasi-stationary pattern which tend to recur (Roa 1972), where as Forbush decrease are non-stationary phenomena. The 27-day variations are essentially corotating Forbush decrease which recur of 27-day intervals. Long lasting Forbush decrease resemble, Forbush decrease occurs relatively rapidly, but the depression may last for weeks or even months (Lockwood 1971). Cosmic ray storms appear to consists of a succession of closely spaced Forbush decreases and may be regarded as a type of long lasting Forbush decreases.

(a) Characteristics of Forbush Decrease

With the use of IGY and NM 64 neutron monitors as well as space probe measurements, various features of Forbush decrease have been studied by various investigators which have been summarized here

1. The rate of recovery is not clearly associated with the magnitude of the initial decrease or with the associated continuing magnetic activity.
2. The decrease in cosmic ray intensity is larger at middle and high latitude stations.
3. Forbush decreases usually occur within 1-6 hours after the onset of a typical world wide geomagnetic storm on the earth. However the presence of magnetic storm is not always necessary. Also there is no relationship between the amplitude of CR decrease and the magnitude of geomagnetic field variations.
4. The main Fd does not always initiate from a normal level. Sometimes a small decrease known as **predecrease** or a small increase known as **pre-increase** is observed in the main decrease. In many instances recovery takes place from the predecrease or preincrease level, before the onset of main decrease while in some cases the main decrease starts from the predecrease or preincrease level.
5. In some cases two or more decrease either in the decrease

phase or in recovery phase, occur closely one upon the other forming a complex structure known as **cosmic ray storm (CRS).**

6. In addition to Fd's initiated by solar flares, Fd's corotating with strong 27-day recurrence tendancy have also been detected. It has been suggested that the corotating Fd's observed at low energies ($\sim$10 Mev) can manifest themselves as the enhanced diurnal wave trains at high energies >1 Gev. (Mc Cracken et al. 1966, Rao et al. 1972).
7. A sudden large increase in cosmic ray intensity during early recovery called **post increase** of a Fd is also observed. The rate of this increase is even faster than the rate of main Fd.

(b) Theories of Forbush Decreases

An associatioon between Forbush decrease and geomagnetic storm was identified in the earliest papers (Sandstrom, 1965 and Dorman 1963). Magnetic storms were attributed to plasma cloud (compact objects composed of fully ionized plasma propagating away from the sun) by Lindeman 1919 and by Chapman and Ferraro (1929). Alfven showed (1954) that a beam of plasma moving away from the sun would carry along magnetic fields from the sun. Thus it was natural to attribute Forbush decrease to the interaction of cosmic rays with a magnetized plasma cloud. Morrison (1956) suggested

that magnetic field in a cloud is turbulent. He argued that cosmic rays would propagate in to a cloud by diffusion. Cocconi et al. (1958) and Gold (1959) suggested that the magnetic field in a cloud is ordered and rooted at the sun, forming a **magnetictongue.** They explained Forbush decreases as a consequence of scattering of cosmic rays by gradients in magnetic field (fig.3.4). The existance of shock wave, in the solar wind was suggested by Gold (1955) and Parkar (1961) showed that the ambient IMF would be compressed and distorted by a shock forming a shell of intense magnetic field. He argued that Forbush decreases could be produced by the diffusion of cosmic rays through this shell (Parker 1963) Piddington (1958) suggested that a magnetictounge could become detached from the sun by the process of magnetic, reconnection, forming a closed **bottle** or **bubble.**

Barouch and Burlaga (1975) have observed that individual cosmic ray decreases are associated with IMF enhancement over several hours and suggested that perpendicular gradient drifts in enhanced magnetic field of post-shock regions (magnetic blobs) are the mechanism responsible for producing cosmic ray decrease.

Barouch and Burlaga suggested that Fd's generally occur as a result of the passage of a region of high magnetic field intensity called magnetic blobs or simply blobs. Most of such

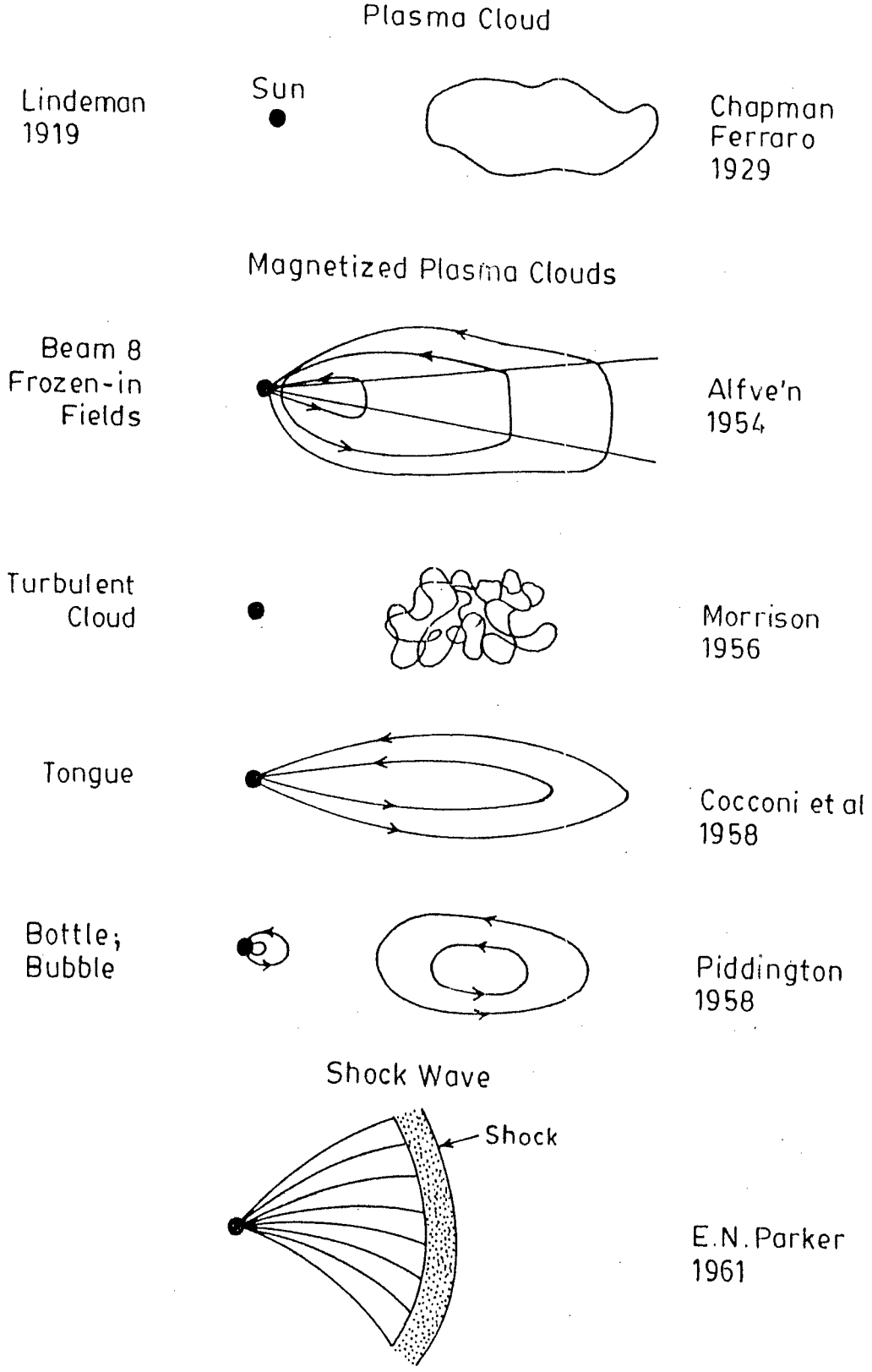

Fig. 3.4 Various possible configurations of interplanetary structure considered to be responsible for modulating cosmic rays.

regions are produced in the interplanetary medium by the steeping of streams. As the blob moves outward, it 'sweeps away' the cosmic ray particles ahead of it. It seems possible that in some instance, particles are deflected out the ecliptic plane, therefore, the enhancement before a Fd is observed occasionally. Many images of the particle diflection from the ecliptic plane can be formed. One of these is the gradient dirft. The scale length of the cross-section of a blob is $L \approx 0.25$ AU to 0.5 AU, particles with rigidity up to 100 Gv can be deflected.

Individual cosmic ray decreases originating with solar flares (associated with type IV radio bursts) studied by Iucci and collaborators (Iucci et al. 1984) led them to conclude that type IV solar flares are the origin of interplanetary perturbations associated with Forbush decrease. The perturbation front is a wide driven shock followed by magnetic blob and a high speed plasma cloud of about 0.5 AU (at 1 AU) emitted by the type IV solar flares. The radial extend of this plasma increases with distance from the sun as shown in the fig.3.5.

Thomas and Gall (1984) have found that the intensity of cosmic ray falls abruptly as the shock wave passes the Earth and recovers as the compression region moves in to the outer heliosphere. They have argued that the most important

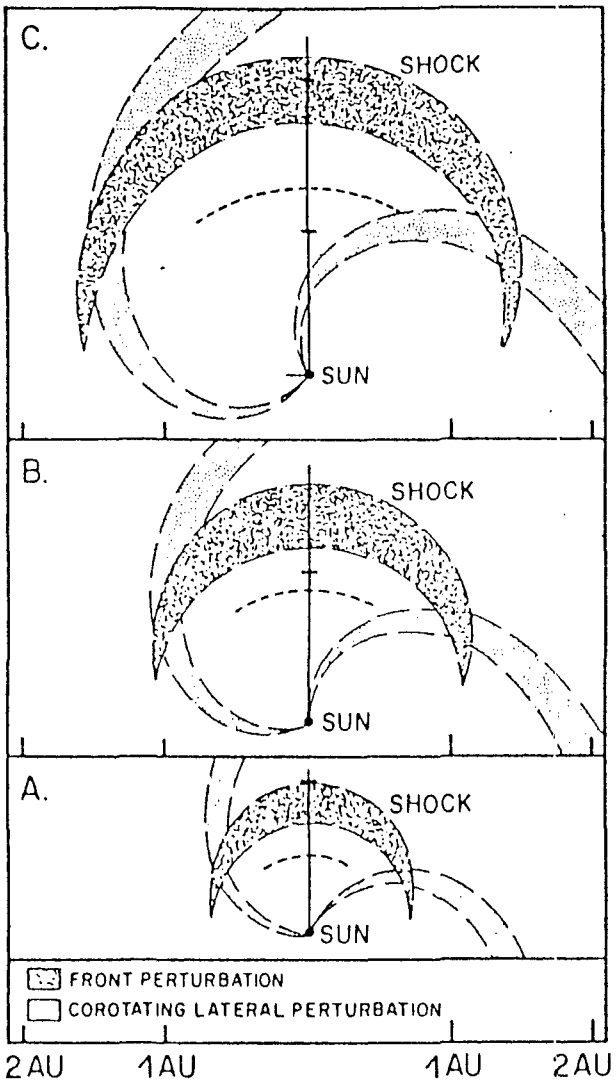

Fig. 3.5 Space-time evolution of Forbush decrease producing interplanetary perturbation.

mechanism responsible for the intensity decrease is the extra adiabatic cooling of particles trapped behind the shock as shown in the fig.3.6. This figure displays the model representing a flare generated shock responsible for Forbush decreases along with the particle trajectory. In this model extra-adiabtic cooling behind the shock front is the process responsible for Forbush decreases.

Figure 3.7 displays the radial dependence of the model fields, showing Parker spiral fields out side the shock ensemble and semi-sinusoidal dependance inside the shock.

Shah G.N. et al. (1978) studied the causes of Forbush decreases, from an analysis of the interplanetary medium plasma, shown that Fd's have different origin. They find that a non-recurrent Fd is the effect of a solar flare, a recurrent one is due to corotatingfast stream.

The effect of density gradient drift on Forbush decreases has been studied recently by Kodokura and Nishida (1986) by constructing a numerical model incorporating the effect of drifts. They have found differences in maximum density depressions and the energy spectrum of the density depressions during the two different polarity states of the heliosphere i.e. in pre and post 1980 epochs. The solar polarity reversal took place in 1980.

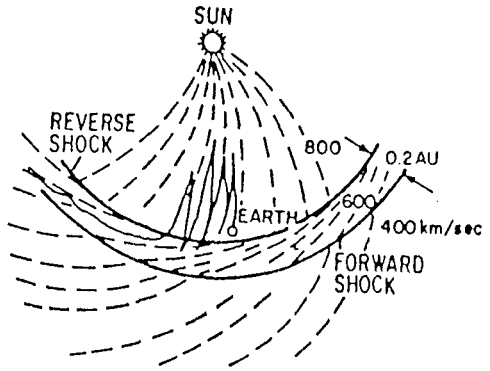

Fig. 3.6 A model representing a flare generated shock responsible for Forbush decrease along with the particle trajectory.

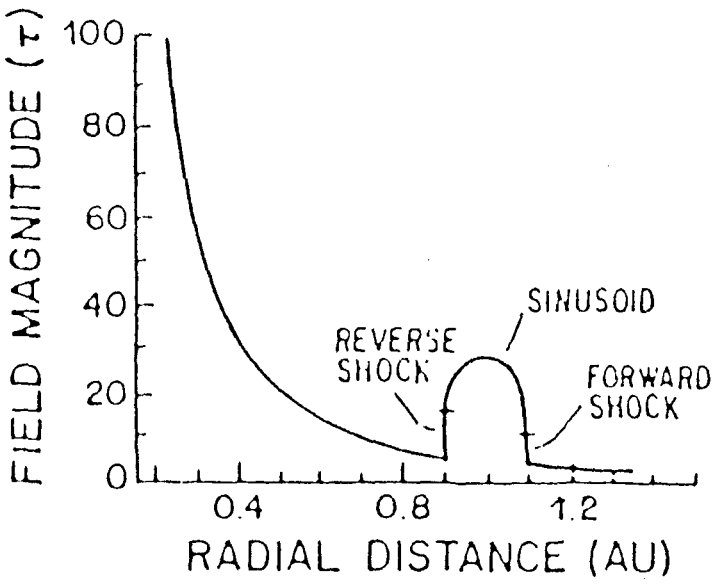

Fig. 3.7 A model for Forbush decreases.

(c) Forbush Decreases in Inner Heliosphere (~1 AU)

Ground-based neutron monitors and meson telescopes on a world wide basis have been continuously monitoring the cosmic rays entering the terrestrial environment, over the last fifty years. These observations along with interplanetary plasma and field observations by earth orbiting satellites have provided a picture of the configuration of modulating regions and the Physical process responsible for Forbsh decrease. This information in turn, has been used to test out the various models invoked to explain these decreases.

In some cases, the decreases in cosmic ray intensity are observed to take place in two distinct step Barnden 1973). These two step Forbush decreases, have been studied by Iucci et al. (1986). They showed that the first step of the decrease is symmetric with respect to flare's meridian plane and is due to a shock wave which is observed ahead of the interplanetary perturbation. On the contrary, the second step is strongly asymmetric the maximum amplitude being observed at ~30° W of the flares meridian plane and can be ascribed to be due to the magnetic perturbation following the shock. This perturbation is an irregular and compressed magnetic field: the maximum magnitude of the magnetic field is found to be placed west of the flare's meridian plane.

Yadav R.S., Rana D.s., Badruddin, Kumar Santosh of

cosmic rays and space science group Aligarh, India, have studied the latitude dependence of Forbush decrease. The pressure corrected cosmic ray intensity data, recorded by superneutron monitors, have been analysed to see the latitude dependence of the amplitude of Forbush decreases. It has been observed that the amplitude of Forbush decreases vary with geomagnetic latitude λ_m, upto $\lambda_m = 58°$ N, beyond this the amplitude is almost steady. This latitude dependence is found to be the same for events associated with magnetic storms and not associated with magnetic storms. However, the dependence is more conspicuous for the events which are associated with solar flares of importance ≥1B compared to those which are not associated with flares.

Lockwood et al. (1986) have explored the relation between Forbush decreases and long term modulation, they have studied the recovery characteristics of several Forbush decrease using the ground based neutron, monitor data and the data from IMP 7, 8 satllites at 1 AU. They have concluded that the recovery time is energy independent and that there are no apparent changes in the recovery time with solar magnetic field reversal or with the phase of the solar modulation cycle.

Recovery characteristics of Forbush decreases observed in association with shock associated magnetic cloud (Klein and Burlaga 1982) have also been studied (Badruddin et al. 1986)

in terms of interplanetary disturbance responsible for the decrease by the Earth-based observation of cosmic ray intensity and the duration for which the cloud engulfs the Earth, the recovery time increases with the duration the magneic cloud engulf the Earth, providing a simple empirical relationship. This relationship may be used for computing the recovery time of Forbush decrease in the outer heliosphere as they propagate away from the Earth, however, we need the excat expansion rate (Burlaga and Behannon 1982) of the clouds and the acceleration/deceleration of these disturbaance as they move away.

Magnetic clouds were identified (Burlaga et al. 1981) as an interplanetary structure with a dimension of $\sim$0.25 AU (at 1 AU) in which the magnetic field is higher than average, the magnetic field direction rotates monotonically through a large angle, the temperature is low.

The clouds were classified in to three groups those associated with:

(a) a shock

(b) a stream interface and

(c) a cold magnetic enhancement.

Case (a) had an interplanetary shock just ahead of the clouds, case (b) had a stream interaction region behind the cloud and case (c) had just the regions of high magnetic field strength and low temperature moving with the solar wind.

Badruddin et al. (1986) used the above three types of clouds and studied their effect on cosmic ray intensity. They observed a difference in the amplitude and time profiles of the decrease with the three types of clouds. The decrease in cosmic ray intensity associated with type (a) clouds were very large in amplitude [Forbush type] the onset of the decrease coincided with the arrival of the shock front and the recovery was almost complete within a week. The decreases associated with type (b) clods were smaller in magnitude but larger in duration and the onset were on the arrival of the cloud at the Earth. The decrease with type (c) clouds were of still smaller amplitude and duration. (fig.3.8) Thus from these results Badruddin et al. inferred that the modulation region consists of a shock front followed by a plasma sheath in which the magnetic field was high and turbulent.

Recently, Zhang and Burlaga (1988) identified two types of magnetic clouds using magnetic field and plasma data from IMP 8 and ISEE-3 during the period 1978-1982, the effect on cosmic ray intensity was consistent with the results of Badruddin et al. (1986), who adopted the superposed epoch method of analysis.

Yadav and Badruddin (1987) have attempted to distinguish between two types of shocks observed at 1 AU- the so called shocks followed by helium enhancement [a signature of driver ejecta] and those that were not(Borrini et al. 1982).

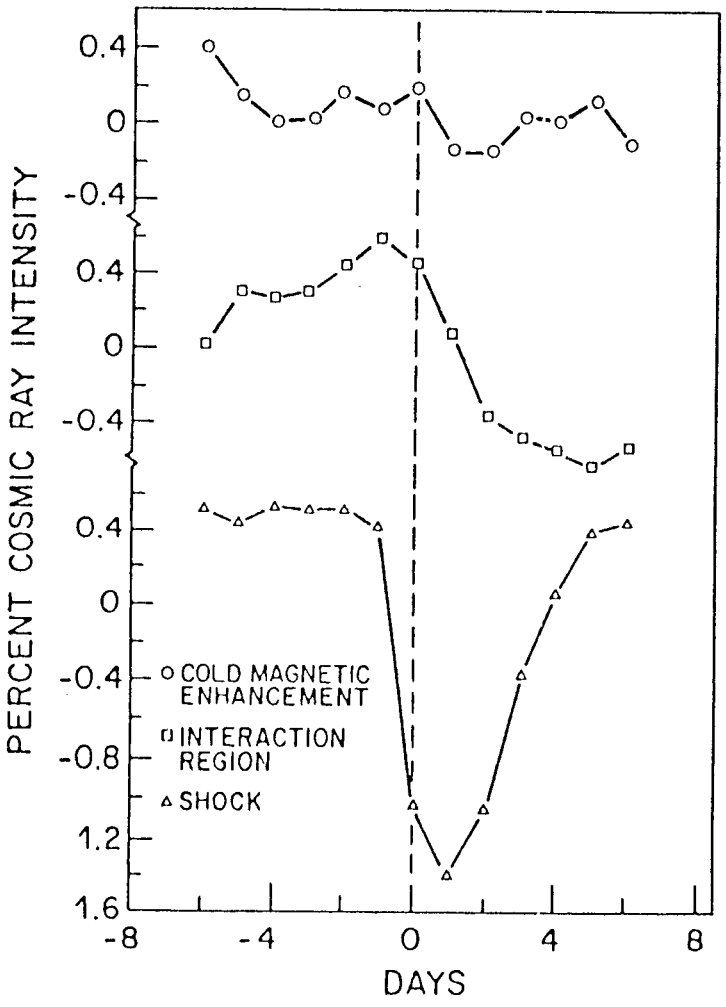

Fig. 3.8 The superposed epoch plots of cosmic ray data from Deep River neutron monitor.

The helium enhancement shocks were associated with large Forbush type decrease, wheras those not followed by helium enhancement were associated with a very small decrease. Their suggestion was that the increased turbulence between the shock front and the driver ejecta associated with the helium enhancement shocks cause this difference. This seems consistent with their earlier study and with the study Zhang and Burlaga (1988).

However, this simplistic division of He and non-He shocks irrespective of origin site is questioned by Sarris (Private Communication, 1989). The Subject is under study.

In summary, it is relevant to point out that it is necessary to explore and identify the configuration and the fundemental physical process responsible for producing forbush decreases. It is obvious that the phenomena of Forbush decrease involves a large volume of the three dimensional heliosphere and one should not be lost in small-scale parameters of localized regions at 1 AU.

(d) Forbush Decreases in Outer Heliosphere [>1 AU]

For more than five decades the cosmic ray intensity variations including Forbush decreases have been studied using ground based instruments. However, with the penetration of spacecraft into the outer heliosphere (P_{10}, P_{11} V_1 and V_2) it has become possible to detect and study the structure and

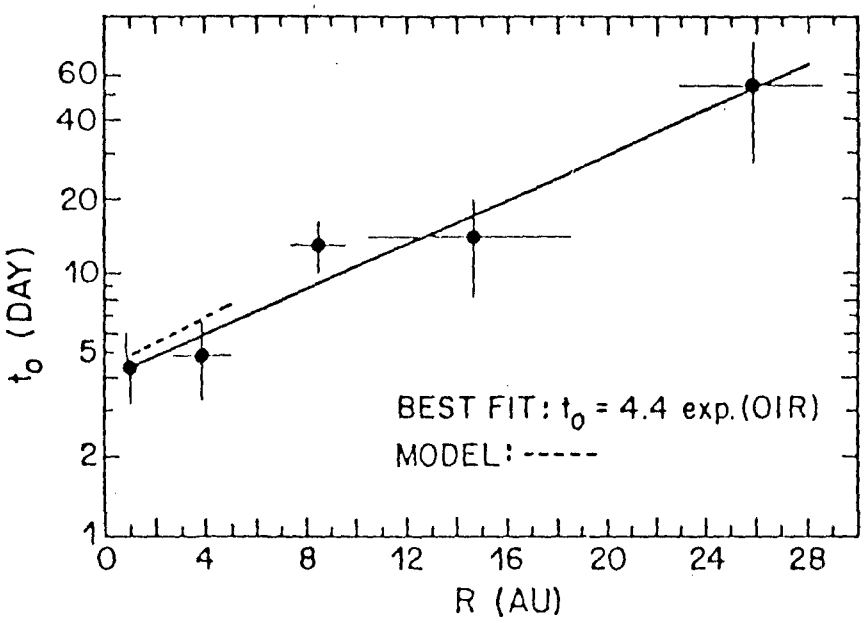

Fig. 3.9 Relationship between the recovery time of Forbush decrease and radial distance from the sun.

evolution of some individual Forbush decreases which propagate from 1 AU towards the heliospheric boundary with the solar wind or high-speed stream speed.

Lockwood and Webber (1977) detected that the modulating regions associated with Forbush decreases propagating to several AU beyond the Earth. For example, a large Forbush decrease detected at Earth by neutron monitors and space craft measurements, on April 1, 1978 was observed at 6.97 AU by Pioneer 11 and 15.91 AU by Pioneer 10 (Van Allen 1979). The decrease seen at Pioneer 10 and Pioneer 11 was comparable to that seen by the Alert Neutron monitor. The recovery times of this decrease were 6 days (at 1 AU) 22 days (at 6.97 AU) and 150 days (at 15.91 AU) the propagation speed was 960 km/sec.

A detailed study of heliocentric dependence of various characteristics (e.g. recovery time, amplitude and the time to decrease to the losest value) of 20 Forbush decreases was carried out by Webber et al. (1986), using cosmic ray data from satellite IMP 8 and space craft V_1,V_2 and Poineer 10.The average recovery time was about 5 times larger at 30 AU that at 1 AU. The magnitude of decrease was observed to decrease about 1.5% per AU on an average, thus the decrease was half as great at $\sim$30 AU than at 1 AU. The time to decrease to minimum intensity of these transient decreases were found to be about 5 times longer at 30 AU than at 1 AU.

****

References

1. Ahluwalia, H.S. (1976) Proce. Int. Cosmic Ray Symp. on High-Energy Cosmic Ray Modulation, Tokyo, 260.

2. Ahluwalia and Riker, J.F. (1981) Proce. of 17th ICRC, Paris **10** 230.

3. Ahluwalia, H.S. and Riker (1985) Proce. of 19th ICRC La Jolla **5** 116.

4. Agrawal, S.P. and Singh R.L. (1975) Proce. of 14th ICRC, Muncheo **4** 11293.

5. Agrawal, S.P. (1983) Space Scie. Rev. **34** 127.

6. Agrawal, S.P., Pathak, S.P. and Mishra, B.L. (1983) Proce. of 18th ICRC, Bangalore **3** 320.

7. Alfven, H. (1954) Tellus **6** 232.

8. Axford, W.I. (1965) Planetary Spac. Sci. **13** 115.

9. Badruddin, Yadav, R.S. and Yadav, N.R. (1985 b) Ind. J. Radio Spac. Phy. **14** 151.

10. Badruddin, Yadav, R.H. and Yadav, N.R. (1986) Solar. Phy. **105** 413.

11. Barnden, L.R. (1973) Proc. 13th ICRC Denver, **2** 1277.

12. Burlaga, L.F., Sittler, E. Mariani, F. and Schwenn, R. (1981) J. Geophy. Res. **86** 6673.

13. Burlaga, L.F. and Behannon, K.W. (1982) Solar Phy. **81** 181.

14. Burlaga, L.F. (1988) J. Geophy. Res. **93** 7217.

15. Barouch, E and Burlaga, L.F. (1975) J. Geophy. Res. **80** 449.

16. Burlaga, et. al. (1984) J. Geophys. Res. **89** 6579.

17. Burlaga, L.F., Mc Donald, F.B., Goldstein, L.L. and Lazarus, A.J. (1985) J. Geophys. Res. **90** 12027.

18. Burlaga, et. al. (1986 a) J. Geophys. Res. **91** 2917.

19. Burlaga, et. al. (1986 b) J. Geophys. Res. **91** 13331.

20. Burlaga, L.F., Ness, N.F. and Mc Donald, F.B. (1987) J. Geophys. Res. **92** 13647.

21. Burlaga, L.F. (1983) Proc. 18th ICRC, Bangalore **12** 21.

22. Borroni, G., Gosling, J.T., Bame, S.J. and Feldman (1982) J. Geophys. Res. **87** 4365.

23. Compton, A.H. (1935) Phys. Rev. **43** 387.

24. Cocooni, G., Goldn, T., Griesen, X., Hayakawa and Morrison (1958) Nuovo Cimento **8** 161.

25. Dorman, L.I. (1963) Elementary particle and cosmic ray physics **7**.

26. Dorman, L.I. (1957) Cosmic Ray Variations (Moscow).

27. Duggal, S.P., Tolba, H.F., Pomerantz, M.A. and Owens (1979) J. Geophys. Res. **84** 6653.

28. Fillus, W. and Axford, I. (1985) J. Geophys. Res. **90** 517.

29. Forbush, S.E. (1957) Proc. Nat. Acad. Sci. **43** 28.

30. Forbush, S.E. (1954) J. Geophys. Res. **59** 525.

31. Forbush, S.E. (1967) J. Geophys. Res. **72** 4937.

32. Forbush, S.E. (1969) J. Geophys. Res. **74** 3451.

33. Gold, T. (1955) Contribution to discussion in gas dynamics of Cosmic clouds, (North Holland) 103.

34. Gold, T. (1959) J. Geophys. Res. **64** 1665.

35. Hashim, A. and Bercovitch, M. (1972) Planctary Space Science **20** 791.

36. Iucci, N., Parisi, M. Storini, M. and Villoresi (1981) Proc. of 17th ICRC Paris **10** 238.

37. Iucci, N., Parisi, M., Storini, M. and Villoresi (1983) Nuovo cimento **6c** 145.

38. Iucci et. al. (1984) Nuovo cimento **7c** 467.

39. Iucci et al. (1986) Nuovo cimento **9c** 39.

40. Jokipii and Thomas, B.T. (1981) Astrophys. J. **243** 1115.

41. Kumar, S. (1978) Ph.D. Thesis A.M.U. Aligarh.

42. Kumar, S., Yadav, R.S and Agrawal, S.P. (1981 a) Proc. 17th ICRC Paris **10** 226.

43. Kumar, S., Yadav, R.S. and Agrawal, S.P. (1981 b) Proc. 17th ICRC Paris **10** 242.

44. Kumar, S., Dutt, S.C., Yadav, R.S. and Agrawal, S.P. (1985) Proc. 19th ICRC Lajolla **5** 126.

45. Kodakura, A. and Nishida, A. (1986) J. Geophys. Res. **91** 13.

46. Klein and Burlaga, L.F. (1982) J. Geophys. Res. **87** 613.

47. Lockwood, J.A. (1971) Space Sci. Rev. **12** 658.

48. Lockwood, J.A. and Webber, W.A. (1977) J. Geophys Res. **82** 1906.

49. Lindeman, F.A. (1919) Phil. Mag. **38** 669.

50. Mc Cracken, and Rao, U.R. (1965) Proc. 19th ICRC **1** 213.

51. Morrison, P. (1956) Phy. Rev. **101** 1397.

52. Munakata, Y., Moris., Ryu, J.Y., Agrawal, S.P. and Venkatesan, D. (1987) Proc. 20th ICRC Moscow **4** 39.

53. Parker, E.N. (1958 a) Astrophy. J. **128** 6621.

54. Parker, E.N. (1958 b) Phys. Rev. **110** 1445.

55. Parker, E.N. (1964) Planet Space Science **9** 195.

56. Parket, E.N. (1961) Ap. J. **133** 1014.

57. Parket, E.N. (1963) Interplanetary dynamical process (Interscience New York).

58. Pathak, S.P. and Agrawal, S.P. (1987) Proce. 20th ICRC Moscow, **4** 129.

59. Perko and Fisk, L.A. (1983) J. Geophys. Res. **88** 9033.

60. Perko, J.S. (1987) J. Geophys. Res. **92** 8502.

61. Perko, J.S. and Burlaga, L.F. (1987) J. Geophys. Res.**92** 6127.

62. Pomerantz, M.A. and Duggal, S.P. (1971) Space. Sci. Rev. **12** 75.

63. Rao, U.R. (1972) Space. Sci. Rev. **12** 719.

64. Rao, U.R., Ananth, A.G. and Agrawal, S.P. (1972) Plane. Space. Sci. **20** 1799.

65. Shah, G.N., Kaul, C.L., Razdan, H. and Bemalkhedkar (1978) J. Geophys. Res. **83** 3740.

66. Sandstrom, A.E. (1965) Cosmic Ray. Phys. (North Holland).

67. Sharma, N.K. (1992) Ph.D. Thesis, Aligarh Muslim University, Aligarh.

68. Thomas, B.T. and Gall, R. (1984) J. Geophys. Res. **89** 2991.

69. Van Allen, J.H. (1979) Geophys. Res. Letters **3** 425.

70. Venkatesan, D., Shukla, A.K. and Agrawal, S.P. (1982) Solar Phys. **81** 375.

71. Webber, W.R. (1967) J. Geophys. Res. **72** 5949.

72. Webber, W.R and Lockwood, J.A. (1981) J. Geophys. Res. **86** 11458.

73. Webber, W.R. and Lockwood, J.A. (1988) J. Geophys. Res. **93** 8735.

74. Webber, W.R. and Lockwood, J.A. (1986) Astrophy. J. **302** 511.

75. Yadav, R.S., Yadav, N.R. and Badruddin (1987) Proc. 20th ICRC Moscow **4** 83.

76. Yadav, R.S. and Badruddin (1983 a) Ind. J. Radio Space Phys. **12** 10.

77. Yadav, R.S. and Rana, D.S. (1983) Proc. 18th ICRC Bangalore **4** 227.

78. Zhang, G. and Burlaga, L.F. (1988) J. Geophys. Res. **93** 2511.

CHAPTER 4

THE LATITUDE DEPENDENCE OF FORBUSH DECREASES

(1) INTRODUCTION

Forbush decrease (Fd) is an essentially isotropic phenomenon and is the most recognisable member of many short term cosmic ray decreases. Forbush (1938) first noted the occurance of a sudden decrease of cosmic ray intensity at ground based monitors almost simultaneously with geomagnetic storm following a day or two after a large solar flare occuring on the sun. Forbush decreases are generally characterised by sudden decrease in cosmic ray intensity with total time of decrease varying between a few hours to days. Recovery of the intensity to the predecrease level can last from a few days to a week or more. Thus in general the Forbush decreases have a rapid rate of decrease and slow recovery. Simpson (1954) suggested that these world-wide decreases are caused by a sudden and drastic change in the electromagnetic condition of interplanetary medium due to the flare occuring on the sun. The intensity variation observed, which is typically $\sim$5-15% in ground based neutron monitors, is found to be energy dependent. Forbush decreases generally occur within 1-6 hours after the onset of a typical world-wide geomagnetic storm on the earth (Lockwood, 1958, Bachelet et al. 1960, Agrawal and Singh, 1976).

Different models of Fd which are explained in the chapter 3 are adequate to explain some features of some Fds.

(a) Onset time of Forbush decrease

The onset time, near the commencement of a Fd, is the first important parameter defining its characteristics as well as its relationship with other parameters on earth, interplanetary medium and the sun. Fenton et al. (1959) concluded that there are differences between onset times of Fd's and these differences are partially due to primary anisotropies. Early workers (Sandstörm 1965) analysed the cosmic ray neutron intensities recorded at a large number of stations to determine the difference in onset time for large Fd's of previous solar cycle and found that the early onset occured almost always for stations whose asymptotic direction were towards the west of the earth sun line.

(b) Magnitude of Forbush Decreases

The magnitude of Fd is the total intensity decrease upto the maximum derease value. The magnitude of Fd varies within very wide limits, from one event to another. The nature can be compared with the eleven year solar cycle variation. The Fd's are found to occur with equal probability during all the solar cycles with slightly longer tendency during sunspot maximum. However the magnitude of Fd's are found to be larger after sunspot maximum.

From the studies of dependence of Fd magnitude with geographic latitude, it has generally been noticed, that the

magnitude is approximately 2 to 2.5 times as large at a station with vertical cut-off rigidity $\sim$1 GV, than at equatorial stations with cut-off rigidity $\sim$15 GV (Lockwood 1971). Similar results have also been observed by us. (Table 4.16)

It has also been observed that the magnitude of the same Fd is different for different components of the cosmic radiation. For meson component, the decrease is usually found to be much less than of the neutron component at the same location.

(c) Recovery of Forbush Decreases

Recovery period is the duration during which the cosmic ray intensity reaches from its minimum value to some constant level for a few days, provided that no other event is seen at the recovery. The recovery phase of a Fd generally lasts for several days and in some instance in large Fds it may extent to several weeks. The recovery of Fds is usually very irregular and interrupted by many other small transient variations (Webber 1962, b). The smooth recovery phase of Fd's can be explained by an exponential function.

$$\Delta I = \Delta I_o \exp(-t/t_o) \qquad \ldots.(1)$$

where ΔI is the difference between the predecrease intensity and intensity in the recovery phase, ΔI_o is the maximum amplitude of decrease,'t' is the time interval between the

onset of the decrease and the time corresponding to intensity in recovery phase, 't_o' is the characteristic time constant during the recovery period (Webber 1962,a,b). It has been noted by several investigators (Sandstorm and Forbush, 1958, Reorderer et al. 1960, Blokh et al. 1961) that the recovery constant appears to be rigidity dependent in such a manner that monitors located at equatorial latitudes appear to recover more quickly.

Due to superposition of other small and short term variations, the recovery phase of the Fds can be very complicated, yielding different characteristics. (Reorderer et al. 1960). The recovery time of a few events was noted to be very large for about a month or more. In such events the cosmic ray intensity remained depressed to appreciable amount for many months after the initial decrease. Moreover, in some cases the complete recovery never takes place.

In this chapter an attempt has been made to study the variation of the amplitude of Fd's with geomagnetic latitude of the recording stations in the northern hemisphere, for which the adequate pressure corrected hourly cosmic ray intensity data of superneutron monitors are available.

The purpose of the present study has been approached from the phenomenological point of views by considering the latitude dependence of the amplitude of Fd's in individual events as well as in their average behaviour.

The study has become comprehensive on account of considering the following point of views.

1. In order to investigate any change in behaviour of the latitude dependence from event to event, a handsome number of events (13 events) has been analysed.
2. Some aspects of latitude dependence with Magnetic Storm (MS) have been evidentiated by considering seperately, the two classes of events, that is, the events which are associated with MS and those that are not associated with MS.
3. Sea level stations are also considered separately for analysis to establish the latitude dependence.

(2) ANALYSIS OF THE DATA

The pressure corrected hourly cosmic ray intensity obtained from World Data Centre (W.D.C-2) recorded by world wide network of superneutron monitors has been analysed for the period 1971-1973. From this period a total number of 13 most prominent Forbush decreases

recorded world wide have been selected. Out of these 13 events, eleven events are found to be associated with 'Magnetic Storm' and two events do not have any apparent association with 'Mangetic Storm'.

The geomagnetic latitudes of the cosmic ray intensity recording stations have been computed from their geographic latitude and longitude by the Chapman's formula (Chapman, 1964).

The geographic location, geomagnetic latitude and the vertical cut-off rigidity of each of the cosmic ray intensity recording station are presented in table 4.1. The geomagnetic storm data are obtained from National Physical Laboratory (N.P.L.) New Delhi.

In order to avoid the overlapping of the points and smoothing out the variation in amplitudes of Fd's produce due to fluctuations in the recording systems of different stations, the stations are grouped according to the geomagnetic latitudes under the constraints outlined below.

1. The difference in geomagnetic latitude $\Delta\lambda$ of any two stations in a particular group is always less than 5°, i.e. $\Delta\lambda < 5°$ and,

2. The difference in cut-off rigidities $\triangle R$ of any two stations in a group is always been less than 2 GV i.e. $\triangle R < 2$ GV.

The percentage amplitudes of Fd's are computed by the expression

$$\triangle I = (I_o - I_m) \times 100 / I_o \qquad \ldots\ldots(2)$$

where I_o is the reference level intensity, defined as an average of four hours counting rate prior to and including the onset hour. I_m is the minimum value of intensity i.e. the lowest counting rate, during the depressed phase of the cosmic ray intensity for the event under consideration.

The onset time of Fd is defined as the hour from where the intensity begins to decrease definitely (Sandstrom 1965). The values of I_m and onset time are determined by the visual scanning of the time profiles of the pressure corrected hourly counting rates of the neutron monitors. (See tables 4.3 - 4.15).

For this purpose all the selected events are categorised accordingly as the events have pre-increase, pre-decrease or neither of the two.

In the case of events which do not have any pre-increase or pre-decrease, the onset time is assumed as the hour from where the intensity decreases continuously

Table 4.1

Geographic location, geomagnetic latitude and cut-off rigidity of the stations whose data have been used in the analysis

Stations	Height (m)	Geographic		Geomagnetic latitude (Deg.)	Cut-Off Rig. (GV)
		Latitute (Deg.)	longitude (Deg.)		
Alert	57	82.5N	62.5W	85.66N	0.00
Inuvik	21	68.35N	133.7W	70.4N	0.18
Goose Bay	46	53.27N	60.4 W	64.78N	0.52
Deep River	145	46.1 N	77.5 W	57.63N	1.02
Leeds	72	53.8 N	01.5 W	56.72N	2.2
Rome	60	41.91N	12.5 E	42.56N	6.32
Mt. Norikura	2770	36.11N	137.5E	25.5 N	11.39
Tokyo	20	35.75N	139.7E	25.32N	11.61
Ahmedabad	50	23.01N	72.6 E	13.68N	15.94

and reaches a minimum value. The essential condition which is to be satisfied in this case is that the reference level intensity I_o should always be greater than the intensity I of every successive hour during the depressed phase. If in any case $I_o \leq I$, the onset time is shifted towards the depressed phase so as to result $I_o > I$.

In second category, the events having pre-increase are considered for scanning, here the onset time of the pre-increase is assumed as the hour from where the intensity increase continuously until it attains a maximum value. Here also, the value of reference level intensity I_o is computed by the same process as in the previous category, specially keeping in view that in this case $I_o < I_i$ where I_i is the intensity of every successive hour during the pre-increase phase. For deciding the position of the onset time of the main decrease, the hour, where the intensity returns to a value approximately equal to the reference level intensity, is taken as the onset time for main decrease.

In the third category, the events having pre-decreases are considered for scanning. In this case also the reference level intensity I_o and onset time of pre-decrease are determined in the manner as in category second. However for this category of events $I_o > I_d$, where

I_d is the intensity of every successive hour during the pre-decrease phase.

The events selected for the analysis, and the associated 'Mangetic Storm' are presented in table 4.2.

In order to provide a direct view of the latitude dependence of the amplitude (ΔI) of Fd for the stations in a group and the mean geomagnetic latitude of the stations in a group are plotted. These curves are designated as amplitude-geomagnetic latitude curves and are discussed in detail in the following sections.

(3) LATITUDE DEPENDENCE OF FORBUSH DECREASES

To establish the latitude dependence of Fd's, curves are drawn taking geomagnetic latitude along x-axis and percentage of amplitude along y-axis. The curves are presented in the figs.4.1 and 4.2. It is very much evident from all curves that the mean amplitude of Fd increases with increase in geomagnetic latitude upto a latitude $\lambda \simeq 58°N$. Beyond $\lambda \simeq 58°N$ the amplitude - geomagnetic latitude curves become almost flat. As concern the dependence of the amplitude of Fd on the geomagnetic latitude and the position of the knee, the behaviour is more or less the same for all the events. The average behaviour of all the events exhibits the well

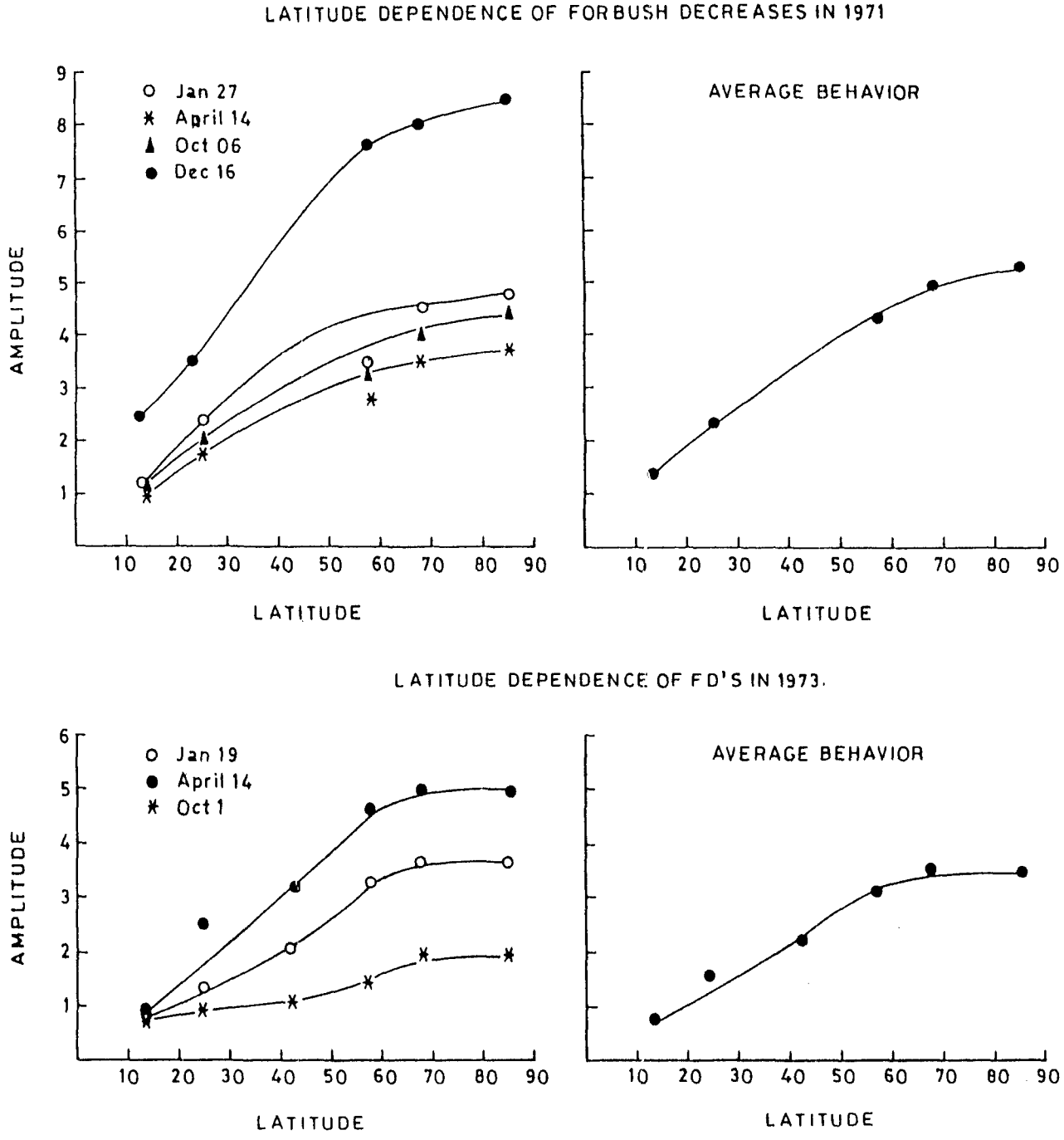
LATITUDE DEPENDENCE OF FORBUSH DECREASES IN 1971
AMPLITUDE
LATITUDE
O Jan 27
* April 14
▲ Oct 06
● Dec 16
AVERAGE BEHAVIOR
LATITUDE DEPENDENCE OF FD'S IN 1973.
AMPLITUDE
LATITUDE
O Jan 19
● April 14
* Oct 1
AVERAGE BEHAVIOR
LATITUDE

Fig. 4.1

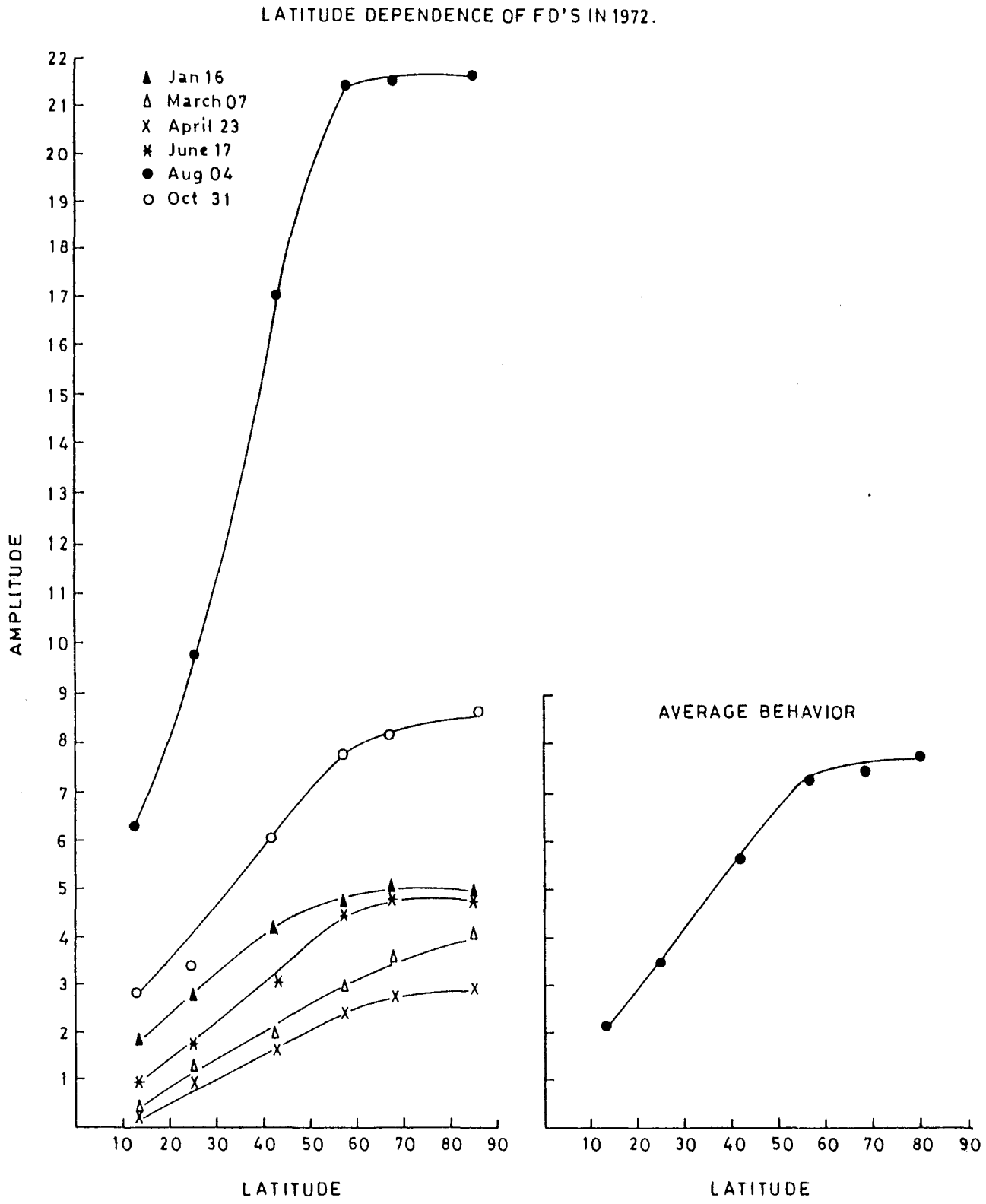
LATITUDE DEPENDENCE OF F D'S IN 1972.
Jan 16
March 07
April 23
June 17
Aug 04
Oct 31
AMPLITUDE
LATITUDE
AVERAGE BEHAVIOR
LATITUDE

Fig. 4.2

Table 4.2

Onset date and time for Forbush Decreases, associated with Magnetic Storm

FORBUSH DECREASE	ASSOCIATED M.S.		
ONSET DATE	ONSET DATE	ONSET TIME Hrs	Mts
1971 January 27	Januray 27	04	20
1971 April 14	April 14	12	45
1971 October 6	October 5	22	45
1971 December 16	December 16	19	06
1972 January 16	January 15	04	30
1972 March 7	March 6	21	08
1972 April 23	No Ms observed		
1972 June 17	June 17	06	23
1972 August 04	August 04	02	20
1972 October 31	October 31	16	55
1973 January 19	No Ms observed		
1973 April 14	April 14	12	45
1973 October 6	October 5	22	45

defined relationship between the amplitude of Fd and geomagnetic latitude and explicitly establishes the position of knee at 58°N and almost a flat curve beyond it.

(4) M.S. EFFECT ON LATITUDE DEPENDENCE OF FORBUSH DECREASES

The analysis of both the classesof event, i.e. associated with MS and not associated with MS, has been carried out separately for all the events. This is presented in fig.4.3-4.5. The average behaviour of the two classes of events has also been studied separately.

It is very much evident from these figures that there is no apparent difference in the morphological features between the two classes of events studied through this analysis. A continuous increase in amplitude with increase in geomagnetic latitude upto 58°N and beyond it, a steady amplitude is oberved almost in all the individual events of both classes as well as in the average behaviour of two classes.

(5) LATITUDE DEPENDENCE OF FD's AT SEA LEVEL STATIONS

The amplitude of Fd's - geomagnetic latitude curves, when sea level stations are grouped by excluding the mountain stations are presented in fig.4.6,47. It is

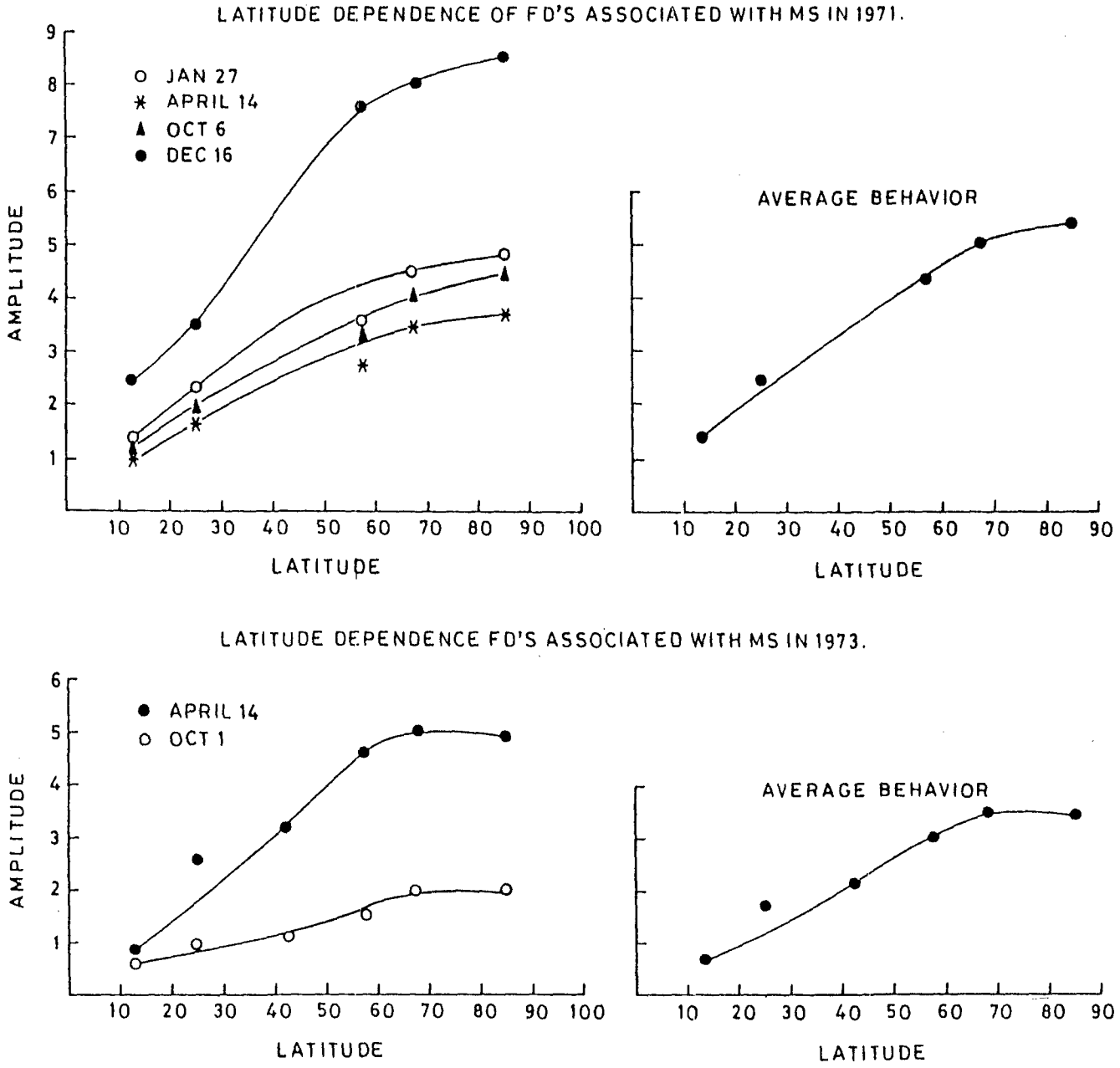
LATITUDE DEPENDENCE OF FD'S ASSOCIATED WITH MS IN 1971.
JAN 27
APRIL 14
OCT 6
DEC 16
AMPLITUDE
LATITUDE
AVERAGE BEHAVIOR
LATITUDE
LATITUDE DEPENDENCE FD'S ASSOCIATED WITH MS IN 1973.
APRIL 14
OCT 1
AMPLITUDE
LATITUDE
AVERAGE BEHAVIOR
LATITUDE

Fig. 4.3

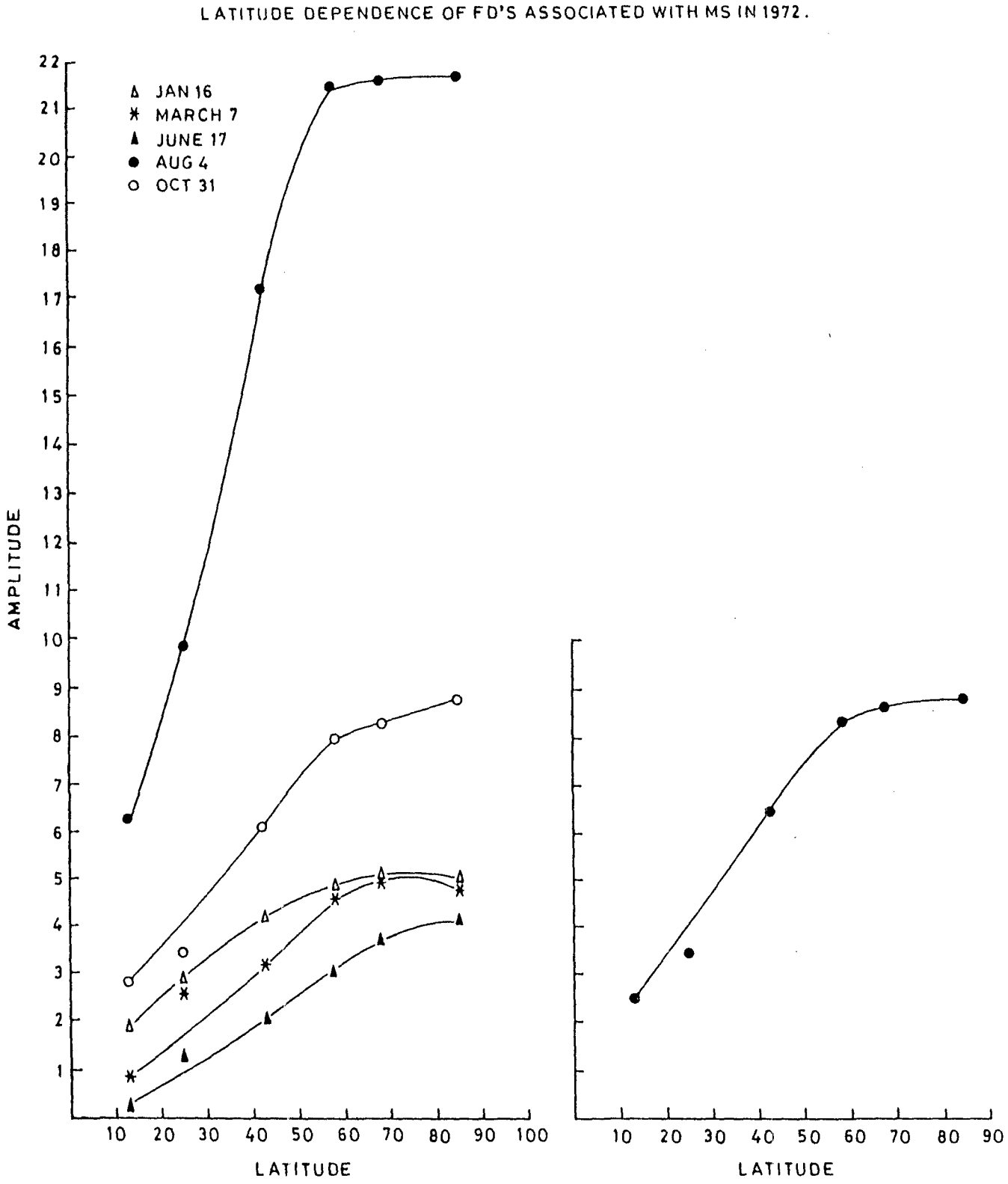
LATITUDE DEPENDENCE OF FD'S ASSOCIATED WITH MS IN 1972.
JAN 16
MARCH 7
JUNE 17
AUG 4
OCT 31
AMPLITUDE
LATITUDE
LATITUDE

Fig.4.4

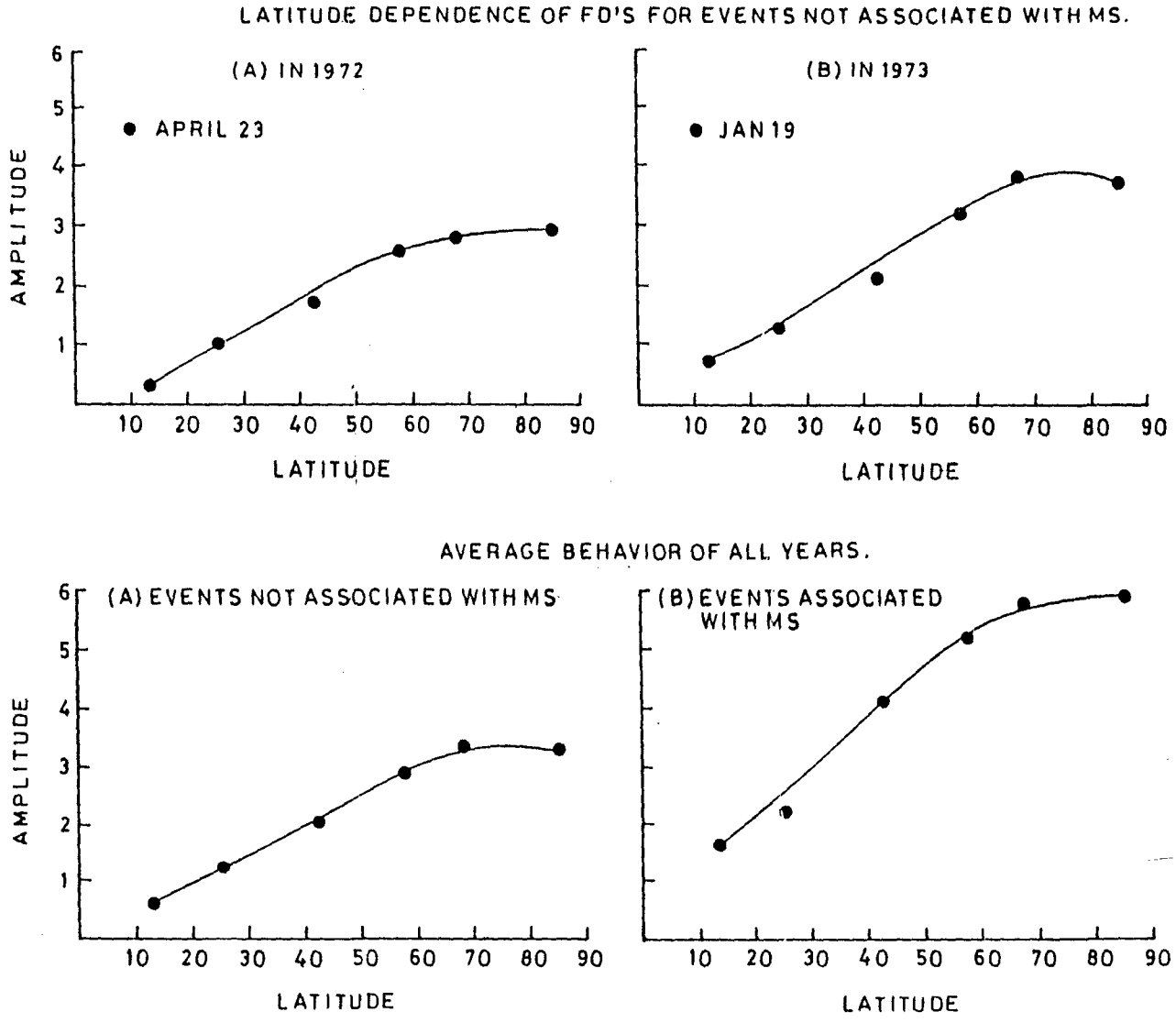
LATITUDE DEPENDENCE OF FD'S FOR EVENTS NOT ASSOCIATED WITH MS.
(A) IN 1972
APRIL 23
(B) IN 1973
JAN 19
AMPLITUDE
LATITUDE
AVERAGE BEHAVIOR OF ALL YEARS.
(A) EVENTS NOT ASSOCIATED WITH MS
(B) EVENTS ASSOCIATED WITH MS

Fig. 4.5

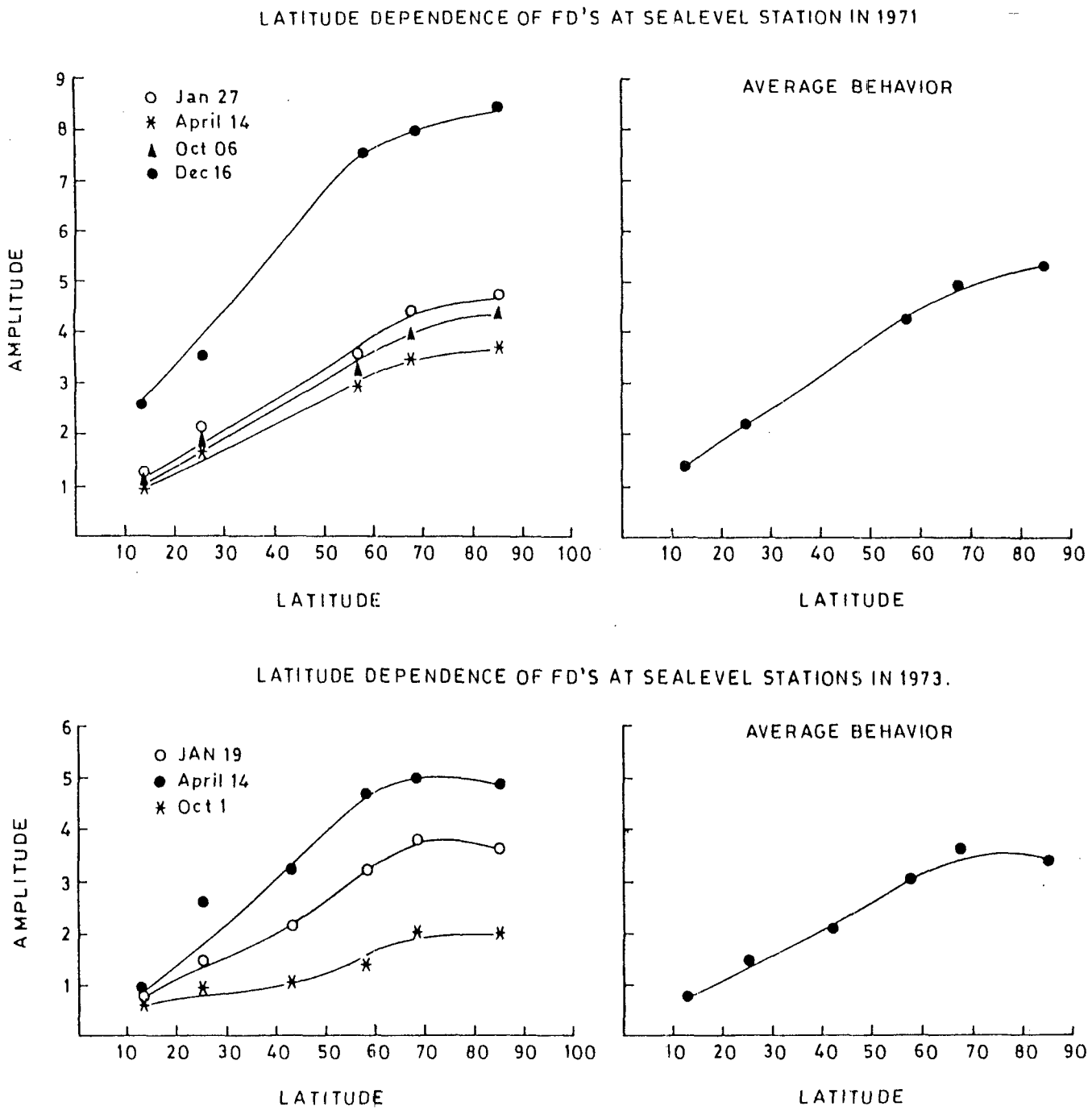
LATITUDE DEPENDENCE OF FD'S AT SEALEVEL STATION IN 1971
AMPLITUDE
Jan 27
April 14
Oct 06
Dec 16
LATITUDE
AVERAGE BEHAVIOR
LATITUDE
LATITUDE DEPENDENCE OF FD'S AT SEALEVEL STATIONS IN 1973.
AMPLITUDE
JAN 19
April 14
Oct 1
LATITUDE
AVERAGE BEHAVIOR
LATITUDE

Fig. 4.6

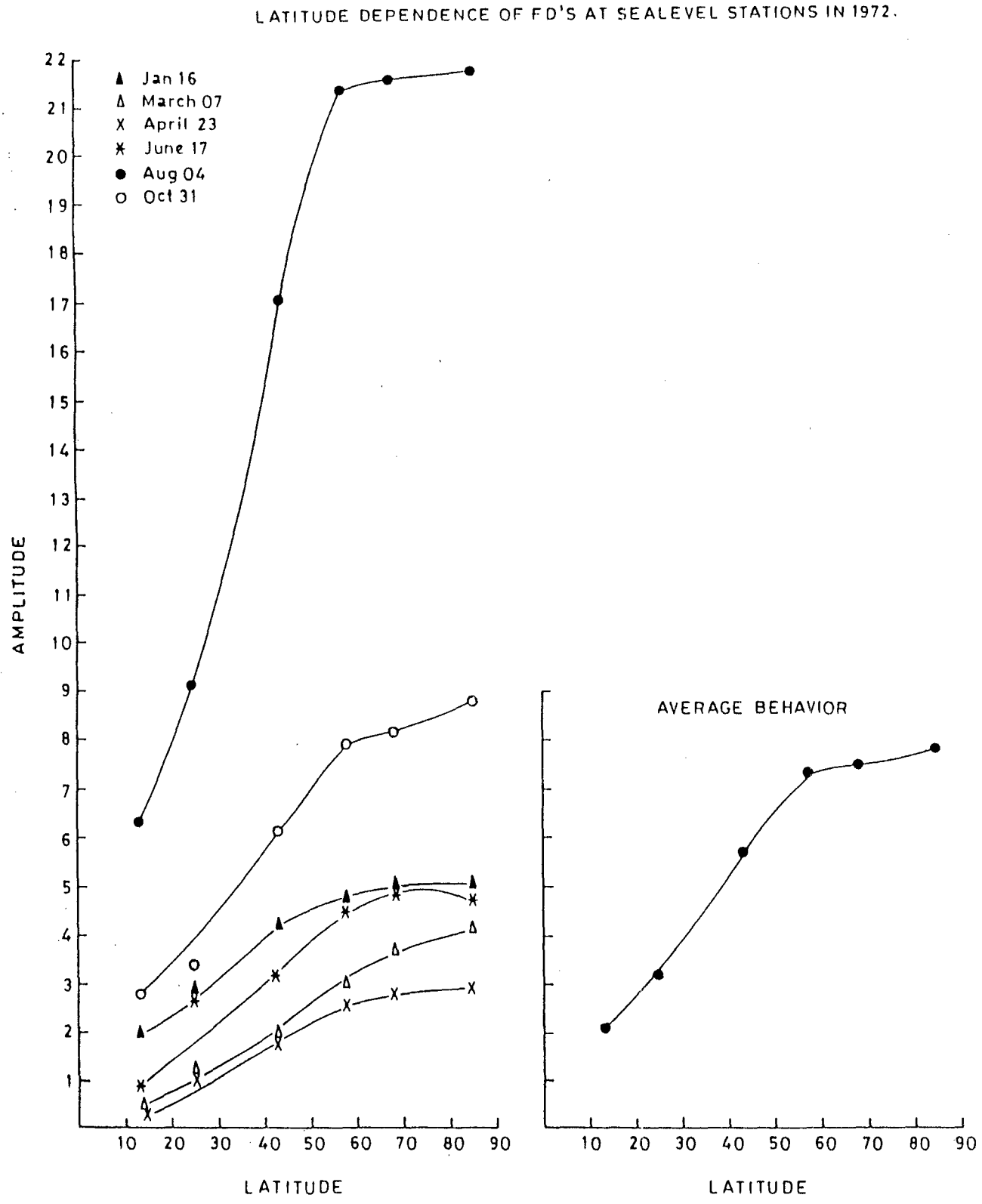
LATITUDE DEPENDENCE OF FD'S AT SEALEVEL STATIONS IN 1972.
Jan 16
March 07
April 23
June 17
Aug 04
Oct 31
AMPLITUDE
LATITUDE
AVERAGE BEHAVIOR
LATITUDE

Fig. 4.7

Table 4.3

Event on January 27 1971

Stations	Reference level intensity I_o					I_{min}	$\Delta I = \frac{I_o - I_m}{I_o} \times 100$	
	1	2	3	4	Mean		Amp ΔI	Mean
Alert	6760	6788	6787	6776	6772	6448	4.85	4.85
Inuvik	6519	6537	6532	6532	6530	6169	5.52	4.5
Goose Bay	6595	6594	6618	6593	6600	6367	3.53	
Deep River	6547	6551	6543	6532	6544	6318	3.45	3.48
Leeds	6368	6385	6354	6355	6365	6142	3.5	
Mt. Norikura	2541	2548	2566	2555	2552	2492	2.35	2.38
Tokyo	3459	3481	3472	3493	3476	3392	2.41	
Ahmedabad	4111	4121	4119	4114	4116	4070	1.2	1.2

Table 4.4

Event on April 14, 1971

Stations	Reference level intensity I_o					I_{min}	$\Delta I=\frac{I_o-I_m}{I_o}\times 100$	
	1	2	3	4	Mean		Amp ΔI	Mean
Alert	7005	6991	7013	7021	7007	6743	3.77	3.77
Inuvik	6708	6699	6695	6704	6701	6484	3.24	3.59
Coose Bay	6706	6718	6720	6707	6712	6447	3.95	
Deep River	6668	6679	6680	6686	6678	6500	2.67	2.83
Leeds	6506	6507	6527	6537	6519	6325	2.98	
Mt.Norikura	2594	2601	2595	2591	2595	2547	1.85	1.85
Ahmedabad	4155	4143	4153	4164	4153	4108	1.08	1.08

Table 4.5

Event on October 6, 1971

Stations	Reference level intensity I_o					I_{min}	$\Delta I=\frac{I_o-I_m}{I_o}\times 100$	
	1	2	3	4	Mean		Amp ΔI	Mean
Alert	7211	7221	7185	7191	7202	6875	4.54	4.54
Inuvik	6920	6912	6923	6900	6913	6613	4.34	4.17
Goose Bay	6996	6979	6978	6982	6983	6703	4.00	
Deep River	6870	6888	6875	6893	6881	6666	3.12	3.28
Leeds	6639	6675	6630	6634	6641	6416	3.43	
Mt.Norikura	2657	2646	2647	2656	2651	2577	2.79	1.96
Tokyo	3537	3518	3532	3522	3527	3487	1.13	
Ahmedabad	4113	4131	4148	4154	4136	4086	1.2	1.2

Table 4.6

Event on December 16, 1971

Stations	Reference level intensity I_o					I_{min}	$\Delta I=\frac{I_o-I_m}{I_o}\times 100$	
	1	2	3	4	Mean		Amp ΔI	Mean
Alert	7616	7606	7615	7620	7614	6963	8.55	8.55
Inuvik	6976	6982	6987	7013	6989	6389	8.58	8.04
Goose Bay	7079	7081	7077	7075	7078	6548	7.5	
Deep River	7079	7065	7074	7059	7069	6581	6.9	7.6
Leeds	6829	6796	6837	6850	6828	6261	8.3	
Mt.Norikura	2631	2622	2625	2625	2625	2520	4.00	3.51
Tokyo	3599	3624	3610	3599	3608	3499	3.02	
Ahmedabad	4154	4193	4177	4143	4166	4061	2.5	2.5

Table 4.7

Event on January 16, 1972

Stations	Reference level intensity I_o					I_{min}	$\Delta I = \frac{I_o - I_m}{I_o} \times 100$	
	1	2	3	4	Mean		Amp ΔI	Mean
Alert	7514	7465	7438	7454	7467	7090	5.045	5.045
Inuvik	6967	6963	6984	6972	6971	6607	5.22	5.13
Goose Bay	7016	7004	7004	7035	7014	6660	5.047	
Deep River	6960	6975	6942	6939	6954	6606	5.0	4.83
Leeds	6776	6760	6783	6788	6776	6460	4.66	
Rome	2991	3004	3011	3051	3014	2885	4.28	4.28
Mt.Norikura	2626	2630	2627	2637	2630	2548	3.12	2.84
Tokyo	3599	3610	3611	3593	3603	3511	2.55	
Ahmedabad	4176	4186	4196	4179	4182	4104	1.86	1.86

Table 4.8

Event on March 7, 1972

Stations	Reference level intensity I_o					I_{min}	$\Delta I=\frac{I_o-I_m}{I_o}\times 100$	
	1	2	3	4	Mean		Amp ΔI	Mean
Alert	7530	7534	7530	7514	7527	7204	4.29	4.29
Inuvik	7015	7035	7001	6979	7007	6756	3.58	3.75
Goose Bay	7102	7118	7128	7139	7121	6847	3.85	
Deep River	6912	7023	7035	7059	7007	6773	3.34	3.05
Leeds	6768	6825	6798	6839	6807	6619	2.76	
Rome	3004	2995	2992	2998	2997	2938	1.97	1.97
Mt.Norikura	2632	2638	2632	2637	2634	2602	1.21	1.35
Tokyo	3638	3597	3600	3619	3613	3559	1.49	
Ahmedabad	4185	4187	4171	4148	4172	4154	0.43	0.43

Table 4.9

Event on April 23, 1972

Stations	Reference level intensity I_o					I_{min}	$\Delta I=\frac{I_o-I_m}{I_o}\times 100$	
	1	2	3	4	Mean		Amp ΔI	Mean
Alert	7532	7526	7527	7554	7534	7309	2.98	2.98
Inuvik	7018	7005	6990	7003	7004	6817	2.67	2.88
Goose Bay	6978	6993	7020	7012	7000	6784	3.08	
Deep River	6965	6985	6994	7058	7000	6791	2.98	2.53
Leeds	6823	6824	6854	6834	6833	6691	2.07	
Rome	3004	2999	2988	2988	2994	2941	1.77	1.77
Mt.Norikura	2575	2592	2599	2609	2588	2593	1.12	1.08
Tokyo	3578	3588	3573	3562	3575	3538	1.03	
Ahmedabad	4154	4157	4171	4151	4158	4145	0.313	0.313

Table 4.10

Event on January 17, 1972

Stations	Reference level intensity I_o					I_{min}	$\Delta I=\frac{I_o-I_m}{I_o}\times 100$	
	1	2	3	4	Mean		Amp ΔI	Mean
Alert	7397	7422	7438	7426	7420	7060	4.85	4.85
Inuvik	6884	6898	6909	6033	6906	6550	5.15	5.02
Goose Bay	6964	6994	7015	7037	7002	6660	4.88	
Deep River	6906	6894	6901	6894	6898	6590	4.47	4.71
Leeds	6643	6683	6684	6716	6681	6349	4.96	
Rome	2945	2953	2942	2952	2948	2852	3.26	3.26
Mt.Norikura	2616	2613	2618	2615	2615	2538	2.94	2.66
Tokyo	3519	3524	3544	3545	3533	3449	2.38	
Ahmedabad	4101	4119	4119	4101	4110	4071	0.95	0.95

Table 4.11

Event on August 4,1972

Stations	Reference level intensity I_o					I_{min}	$\Delta I=\frac{I_o-I_m}{Io}\times 100$	
	1	2	3	4	Mean		Amp ΔI	Mean
Alert	7374	7393	7389	7397	7388	5780	21.76	21.76
Inuvik	6844	6801	6789	6786	6805	5368	21.1	21.5
Goose Bay	6922	6971	6959	6958	6952	5426	21.9	
Deep River	6808	6829	6847	6854	6834	5361	21.5	21.5
Rome	2937	2948	2941	2935	2940	2435	17.1	17.1
Mt.Norikura	2618	2608	2609	2618	2613	2337	10.5	9.8
Tokyo	3559	3525	3526	3527	3531	3210	9.16	
Ahmedabad	4158	4159	4144	4164	4156	3893	6.32	6.32

Table 4.12

Event on October 31, 1972

Stations	Reference level intensity I_o					I_{min}	$\Delta I = \frac{I_o - I_m}{I_o} \times 100$	
	1	2	3	4	Mean		Amp ΔI	Mean
Alert	7392	7430	7410	7435	7416	6749	8.99	8.99
Inuvik	6864	6881	6854	6851	6862	6282	8.45	8.2
Goose Bay	6895	6944	6931	6908	6919	6375	7.86	
Deep River	6960	6066	6945	6944	6953	6389	8.11	7.99
Leeds	6672	6683	6683	6740	6691	6166	7.88	
Rome	2968	2991	2985	2972	2979	2797	6.1	6.1
Mt.Norikura	2612	2606	2598	2621	2609	2522	3.34	3.35
Tokyo	3540	3549	3539	3541	3542	3423	3.36	
Ahmedabad	4126	4166	4156	4130	4144	4029	2.78	2.78

Table 4.13

Event on January 19, 1973

Stations	Reference level intensity I_o					I_{min}	$\Delta I=\frac{I_o-I_m}{I_o}\times 100$	
	1	2	3	4	Mean		Amp ΔI	Mean
Alert	7515	7528	7531	7528	7525	7260	3.52	3.52
Inuvik	7001	7012	7018	7007	7009	6725	4.05	3.98
Goose Bay	7076	7091	7079	7078	7081	6803	3.9	
Deep River	7064	7071	7070	7071	7069	6820	3.52	3.37
Leeds	6845	6846	6848	6861	6850	6630	3.22	
Rome	2982	2987	2997	2980	2986	2923	2.11	2.11
Mt.Norikura	2528	2535	2534	2525	2530	2501	1.15	1.35
Tokyo	3554	3563	3562	3564	3560	3505	1.54	
Ahmedbabd	4153	4171	4139	4154	4154	4121	0.794	0.794

Table 4.15

Event on October 1, 1973

Stations	Reference level intensity I_o					I_{min}	$\Delta I=\frac{I_o-I_m}{I_o}\times 100$	
	1	2	3	4	Mean		Amp ΔI	Mean
Alert	7540	7513	7522	7542	7529	7380	1.98	1.98
Inuvik	7039	7023	7032	7031	7031	6870	2.28	2.08
Gosse Bay	7075	7064	7064	6068	6067	6934	1.88	
Deep River	7009	7015	7032	7028	7021	6920	1.44	1.49
Leeds	6808	6798	6813	6801	6805	6701	1.53	
Rome	2978	2978	2975	2976	2976	2944	1.07	1.07
Mt.Norikura	2636	2637	2637	2632	2635	2600	1.32	0.94
Tokyo	3549	3553	3546	3556	3551	3531	0.56	
Ahmedabad	4167	4179	4194	4197	4184	4153	0.73	0.73

Table 4.16
Dependence of Fd magnitude at ~15 GV station and ~ 1 GV station.

Events	Amplitude at 58°N (~1GV) b	Amplitude at 13°N (~15GV) a	% change b-a/a	Mean
1971				
January 27	4.4	1.2	2.66	
April 14	3.3	1	2.3	2.35
October 6	3.7	1.1	2.36	
December 16	7.7	2.5	2.08	
1972				
January 16	4.9	1.8	1.7	
June 17	4.4	1.0	3.4	2.3
August 04	21.5	6.3	2.4	
October 31	7.7	2.8	1.7	
1973				
January 19	3.3	0.9	2.6	
April 14	4.5	1.0	3.5	2.5
October 1	1.5	0.6	1.5	

evident from these curves that there is no conspicuous difference in the morphological features of the events for the two cases i.e. (1) when sea leval and mountain stations are grouped together or (2) when sea level stations are grouped alone. However in case (2) the behaviour of events towards the latitude dependence becomes more impressive. Due to lack of sufficient data of mountain stations it can't be able to study the latitude dependence of Fd's on mountain stations.

(6) CONCLUSIONS

. The broad conclusions of the present study may be summarised as follows:

1. The amplitude ΔI of the Fd has a clear dependence on geomagnetic latitude.
2. The amplitude ΔI of Fd increases with increase in geomagnetic latitude upto a latitude $\lambda \approx 58°N$. Beyond $\lambda \approx 58°N$ the amplitude-geomagnetic latitude curves become almost flat thus establishes the position of knee at a latitude $\lambda \approx 58°N$.
3. The comparitive study of the amplitude of Fd at a high latitude sea level station from one event to another reveals some understanding about the comparitive change in the strength of the interplanetary magnetic disturbance which cause them.

4. The resemblence of altitude dependence for both the classes of events makes it obvious that the Fd's are not directly related to geomagnetic phenomenon.

5. The magnitude of Fd is approximately 2 to 2.5 times as large at a station with vertical cut-off rigidity $\sim$1GV, than at equatorial stations with cut-off rigidity $\sim$15 GV. This result seems to be in agreement with the findings of (Lockwood, 1971).

These result will be useful for developing an understanding about the features of IMF and developing models to explain Fd's.

****

References

1. Agrawal, S.P., Ananth, A.G. and Rao, U.R. (1972) Cand. J. Phys. **50**, 1323.
2. Alfven, H. (1954) Tellus, **6** 232.
3. Bachel et al. (1960) Nuovo cimento **16** 292.
4. Barouch, E. and Burlaga, L.F. (1975) J. Geo phys. Res. **80** 449.
5. Barnden, L.R. (1973) Proc. 13th Intl. Conf. Cosmic rays, Denever, **2** 1277.
6. Badruddin, Yadav, R.S. and Yadav, N.R. (1986) Solar phys. **105** 413.
7. Burlaga, L.F. Sittler, E., Mariani, F. and Schwenn, R. (1981) J. Geo phys. Res. **86** 6673.
8. Chapman, S. (1964) Solar plasma Geomagn. and Aurora, Gordon and Breach Sci. Publ. Inc. London.
9. Chapman, S., and Ferraro V.C.A. (1929) Monthly Notices, Roy. Astron. Soc. **89** 470.
10. Cocconi, G., Goldn, T., Griesen, X., Hayakawa, S. (1958) Nuovo cimento **8** 161.
11. Dorman, L.I., (1963) Prog. Ele. part. and cosmic ray phys. **VIII** (Ed. J.G. Wilson, North Holland).
12. Fenton, A.G. et al. (1959) Can. J. Phys. **37** 970.
13. forbush, S.E., (1938) Phy. Rev. **54** 975.
14. Iucci, N., Parisi, M., Storini, M., and Villoresi, G. (1984) Nuovo cimento **7c** 467.

15. Iucci, N., Pinter, S., Storini, M., Parisi, M., and Villoresi, G. (1986) Nuovo cimento **9c** 39.

16. Kumar, S., Yadav, R.S., (1981 a) Proc. 17th ICRC Paris, **10** 226.

17. Kumar, S., et al. (1981 b) Proc. 17th ICRC, Paris, **10** 242.

18. Lockwood, J.A. (1958) Phy. Rev. **112** 1750.

19. Lockwood, J.A. (1971) Space. Sci. Rev. **12** 658.

20. Lockwood, J.A., Webber, W.R. and Jokipii, J.R. (1986) J. Geo phys. Res. **91** 2851.

21. Mc-Cracken, K.G., Rao, U.R. and Bukata, R.P. (1966) Phys. Rev. Lett. **17** 928.

22. Morrison, P (1956) Phy. Rev. **101** 1397.

23. Parker, E.N. (1963) Interplanetary Dynamical process (Interscience New York).

24. Piddington, J.H. (1958) Phy. Rev. **112** 589.

25. Rao, U.R., Ananth, A.G. and Agrawal, S.P. (1972) Planet space Sci. **20** 1799.

26. Reorder, J.G., Santochi, O.R., Anderson, J.C., Cardoson J.M., and Manzano, J.R. (1960) Nuovo cimento **18** 131.

27. Shah, G.N., Naul, C.L. Razdon, H. and Bemalkhedkar, M.M. (1978) J Geo Phy. Res. **83** 3740.

28. Sandstrom A.E. (1965) Cosmic ray Phy. (North Holland Amsterdam) 201.

29. Sandstrom, A.E. and Forbush, S.E. (1958) J Geo Phy. Res. **63** 875.

30. Simpson, J.A. (1954) Phys. Rev. **94** 426.

31. Thomas, B.T. and Gall, R. (1984) J. Geo. Phys. Res. **89** 2991.

32. Venkatesan, D. (1987) Phys. Scripta **T18** 39.

33. Venkatesan, D., Shukla, A.K., and Afrawal, S.P. (1982) Solar Phys. **81** 375.

34. Webber, W.R. (1962 a) Prog. in elementary particles and cosmic ray Phys. **6** 75.

35. Webber, W.R. (1962 b) Prog. in elementary particles and cosmic ray Phys. **6** 77.

36. Webber, W.R. and Lockwood, J.A., (1987) Astrophy. J. **317** 534.

37. Yadav, R.S. Badruddin, Yadav, N.R., and Agrawal, S.P. (1983) Proce. 18th ICRC, Bangalore **4** 227.

38. Yadav, R.S. Yadav, N.R. and Badruddin (1987) Proce. of 20th ICRC, Moscow **4** 83.

39. Zhang, G., and Burlaga, L.F. (1988) J Geo. Phys. Res. **93** 2511.

****